

An Electrophysiological Analysis of Synaptic Transmission at the *Drosophila* Larval Neuromuscular Junction

Dissertation zur Erlangung des
naturwissenschaftlichen Doktorgrades
der Bayerischen Julius-Maximilians-Universität Würzburg

vorgelegt von

Daniel Bucher
Urbana, Illinois

Würzburg, 2008



Eingereicht am:

Mitglieder der Promotionskommission:

Vorsitzender : Prof Dr. Müller

Gutachter : Prof Dr. Buchner.....

Gutachter : Prof Dr. Nagel

Tag des Promotionskolloquiums:

Doktorurkunde ausgehändigt am:

for Frances, Rose, Russ, and Tony who helped make this possible,
my parents for their unfaltering love and support,
and lastly, for the people who make this all worthwhile...

Table of Contents

1 Abstract	1
Zusammenfassung	3
2 Introduction	
2.1 The <i>Drosophila</i> larval neuromuscular junction	5
2.1.1 Morphology and physiology of the muscle 6 & 7 synapse	5
2.1.2 Synaptic transmission at the <i>Drosophila</i> neuromuscular junction	9
2.2 Null mutants characterized at the <i>Drosophila</i> neuromuscular junction	13
2.2.1 Sap-47 ¹⁵⁶	13
2.2.2 Synapsin ⁹⁷	15
2.2.3 Sap-47 ¹⁵⁶ Synapsin ⁹⁷ double mutants	16
2.2.4 Serine-Arginine protein kinase 3	17
2.2.5 <i>Löchrig</i>	19
2.3 Expression of light activated proteins at the <i>Drosophila</i> neuromuscular junction	21
2.3.1 Channelrhodopsin-2	21
2.3.2 Photoactivated adenylate cyclase	22
3 Materials and Methods	
3.1 The setup	24
3.1.1 The slab	24
3.1.2 Faraday cage	25
3.1.3 Peltier element	25
3.1.4 Optics and manipulators	25
3.1.5 Microelectrodes	26
3.1.6 Amplifier(s)	28
3.1.7 Acquisition	30
3.1.8 Analysis	32
3.2 Recording at the <i>Drosophila</i> neuromuscular junction	33
3.2.1 Solutions	33
3.2.2 Dissection	33
3.2.3 Recording techniques and criteria	34
3.3 Immunocytochemistry at the <i>Drosophila</i> neuromuscular junction	35

4 Results	
4.1 Sap-47 ¹⁵⁶	36
4.2 Synapsin ⁹⁷	41
4.3 Sap-47 ¹⁵⁶ Syn ⁹⁷ double mutants	43
4.4 Serine-Arginine protein kinase 3	45
4.5 <i>Löchrig</i>	48
4.6 Channelrhodopsin-2	51
4.7 Photoactivated adenylate cyclase	53
5 Discussion	
5.1 The potential Sap-47 ¹⁵⁶ phenotype	61
5.2 Null mutant data	63
5.3 A possible <i>Löchrig</i> phenotype	65
5.4 Heterologous expression of Channelrhodopsin-2 and PAC at the neuromuscular junction	66
6 References	68
Appendix A: Fortran code for analysis of eEJP decay	84
Appendix B: <i>Cirriculum Vitae</i>	89
Appendix C: Publication list	93

1. Abstract

In this thesis, synaptic transmission was studied electrophysiologically at an invertebrate model synapse, the neuromuscular junction of the *Drosophila* 3rd instar wandering larvae.

In the first part, synaptic function is characterized at the neuromuscular junction in fly lines which are null mutants for the synaptic proteins “the synapse associated protein of 47 kDa” (*Sap-47*¹⁵⁶), Synapsin (*Syn*⁹⁷), the corresponding double mutant (*Sap-47*¹⁵⁶, *Syn*⁹⁷), a null mutant for an as yet uncharacterized *Drosophila* SR protein kinase, the Serine-Arginine protein kinase 3 (SRPK3), and the *Löchrig* (*Loe*) mutant which shows a strong neurodegenerative phenotype. Intracellular voltage recordings from larval body wall muscles 6 and 7 were performed to measure amplitude and frequency of spontaneous single vesicle fusion events (miniature excitatory junction potentials or mEJPs). Evoked excitatory junction potentials (eEJPs) at different frequencies and calcium concentrations were also measured to see if synaptic transmission was altered in mutants which lacked these synaptic proteins. In addition, structure and morphology of presynaptic boutons at the larval neuromuscular junction were examined immunohistochemically using monoclonal antibodies against different synaptic vesicle proteins (SAP-47, CSP, and Synapsin) as well as the active zone protein Bruchpilot. Synaptic physiology and morphology was found to be similar in all null mutant lines. However, *Löchrig* mutants displayed an elongated bouton morphology, a significant shift towards larger events in mEJP amplitude frequency histograms, and increased synaptic facilitation during a 10 Hz tetanus. These deficits suggest that *Loe* mutants may have a defect in some aspect of synaptic vesicle recycling.

The second part of this thesis involved the electrophysiological characterization of heterologously expressed light activated proteins at the *Drosophila* neuromuscular junction. Channelrhodopsin-2 (ChR2), a light gated ion channel, and a photoactivated adenylate cyclase (PAC) were expressed in larval motor neurons using the UAS-Gal4 system. Single EJPs could be recorded from muscles 15, 16, and 17 when larva expressing ChR2 were illuminated with short (100 ms) light pulses, whereas long light pulses (10 seconds) resulted in trains of EJPs with a frequency of around 25 Hz. Larva expressing PAC in preparations where motor neurons were cut from the ventral ganglion displayed a significant

increase in mEJP frequency after a 1 minute exposure to blue light. Evoked responses in low (.2 mM) calcium were also significantly increased when PAC was stimulated with blue light. When motor nerves were left intact, PAC stimulation resulted in light evoked EJPs in muscles 6 and 7 in a manner consistent with RP3 motor neuron activity. ChR2 and PAC are therefore useful and reliable tools for manipulating neuronal activity *in vivo*.

1. Zusammenfassung

Thema dieser Arbeit war die elektrophysiologische Untersuchung synaptischer Transmission, untersucht an einer Modellsynapse in Invertebraten, der neuromuskulären Synapse von *Drosophila*-Larven des dritten Larvalstadiums.

Im ersten Teil dieser Arbeit, wurde die synaptische Funktion an der neuromuskulären Synapse von Nullmutanten für verschiedene synaptische Proteine charakterisiert (das synapse associated protein of 47 kDa (*Sap-47*¹⁵⁶), Synapsin (*Syn*⁹⁷), eine bis dahin uncharakterisierte *Drosophila* SR-Proteinkinase (SRPK3), und eine Mutante mit einem starken neurodegenerativen Phänotyp (*Loe*). Intrazelluläre Ableitungen wurden von Muskel 6 und 7 des Hautmuskelschlauches durchgeführt, um die Amplitude und Frequenz der spontanen Freisetzung von Neurotransmitter aus einzelnen synaptischen Vesikeln (miniature excitatory junction potentials oder mEJPs) zu messen. Außerdem wurden Evoked excitatory junction potentials (eEJPs) bei verschiedenen Frequenzen und verschiedenen Kalziumkonzentrationen gemessen, um zu erforschen, ob die synaptische Transmission in den genannten Mutanten verändert ist. Zusätzlich wurde die Struktur und die Morphology der präsynaptischen Boutons immunhistochemisch untersucht. Dabei wurden monoklonal Antikörper gegen verschiedene Proteine der synaptischen Vesikel (SAP-47, CSP und Synapsin) und gegen das Aktive Zone Protein Bruchpilot benutzt. Die synaptische Physiologie war in den genannten Nullmutanten für synaptische Proteine nicht verändert, im Vergleich zu den wildtypischen Kontrollen, während Löchrig-Mutanten Defekte der synaptischen Übertragung zeigten, die im Einklang standen mit einem Defekt des Recyclings synaptischer Vesikel.

Der zweite Teil dieser Arbeit beinhaltet die elektrophysiologische Charakterisierung von heterolog exprimierten Licht-aktivierbaren Proteinen an der neuromuskulären Synapse von *Drosophila*. Channelrhodopsin-2 (ChR2), ein Licht gesteuerter Ionenkanal und eine Licht-aktivierbare Adenylatcyclase (PAC) wurden mit Hilfe des UAS-Gal4-Systems an der larvalen, neuromuskulären Synapse exprimiert. Wenn ChR2-exprimierende Larven mit kurzen (100ms) Lichtpulsen beleuchtet wurden, konnten einzelne EJPs von den Muskeln 15, 16 und 17 abgeleitet werden. Längere Lichtpulse

(10 Sekunden) führten zu einer Serie von EJPs mit einer Frequenz von ca. 25 Hz. Larven, die PAC exprimierten zeigten, in Präparationen in denen die Motoneurone vom Ventralganglion gelöst wurden, nach einminütiger Belichtung mit Blaulicht einen signifikanten Anstieg der mEJP-Frequenz. Auch die EJPs waren in einer Umgebung mit geringer Kalziumkonzentration (0,2 mM) signifikant erhöht, wenn PAC durch Blaulicht stimuliert wurde. Wurden die Motoneurone intakt gelassen, führte die Stimulation der PAC durch Blaulicht zu EJPs in den Muskeln 6 und 7, die im Einklang standen mit RP3 Motoneuronaktivität. Beide Proteine (ChR2 und PAC) erwiesen sich daher als nützliche, zuverlässige Werkzeuge, um die neurale Aktivität *in vivo* zu manipulieren.

2. Introduction

2.1 The *Drosophila* larval neuromuscular junction

In a review, Akira Chiba once compared the popularity of the *Drosophila* neuromuscular synapse to the art of Bonsai:

“A Bonsai garden's minimalistic style typically allows only one or two dwarf trees, a few blossoming grasses, and a small rock. They supposedly depict something far more complex and large, the real universe. The popularity of Bonsai, despite the profundity it represents, lies in its simplicity and accessibility.”

Given the complexity of mammalian central synapses, sometimes a more minimalistic system is a welcome change. The *Drosophila* larval neuromuscular junction (figure 2-1) is an ideal model synapse because of its simplicity, accessibility to various electrophysiological recording and imaging techniques, and the genetic malleability which is intrinsic to *Drosophila*.

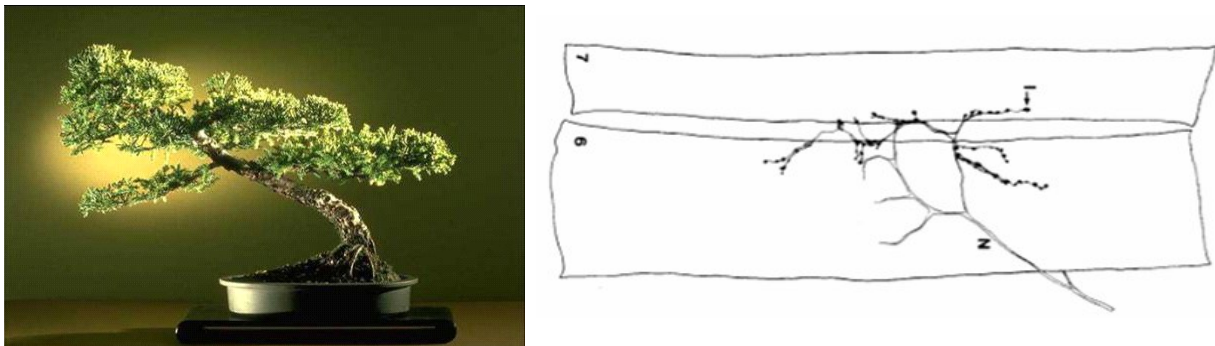


Figure 2-1. The *Drosophila* neuromuscular junction, the Bonsai model synapse (Budnik et al., 1990).

2.1.1 Morphology and physiology of the muscle 6 & 7 synapse

A *Drosophila* larva can be divided into six head, ten abdominal, and three thoracic segments, with each hemisegment demonstrating a bilateral symmetry (Cohen and Juergens, 1991). The abdominal segments A1-A7 contain thirty muscle fibers which develop according to a redundant genetic program into a well characterized pattern (Crossley, 1978). Each muscle fiber is a multinucleated cell that results from the fusion of about a dozen myoblasts and has been assigned a corresponding number so it can be easily identified by its position, orientation, and size. The musculature is innervated by a set of approximately thirty-four motor neurons, which leave the ventral ganglion in six subgroups of nerves: the four segmental nerves (SNa-d), the intersegmental nerve (ISN) and the transverse nerve (TN) (figure 2-2) (Hoang and Chiba, 2001).

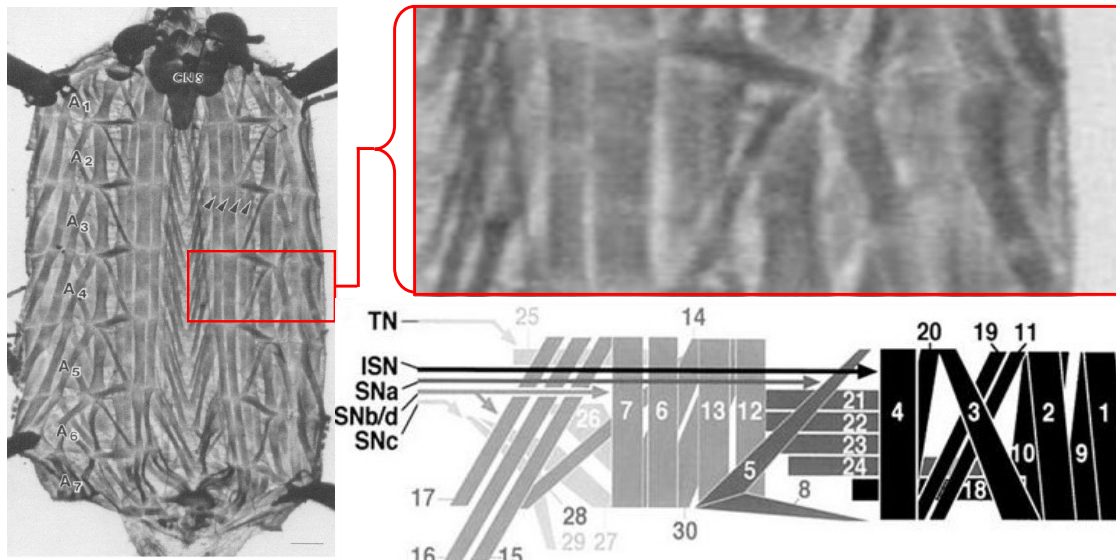


Figure 2-2. A *Drosophila* 3rd instar larva “fillet” which shows the mirror symmetry of the hemisegments as well as the numbering scheme of the muscle fibers (Budnick et al., 1990, Hoang and Chiba, 2001).

Motor neurons form presynaptic contact points (or boutons) on muscle fibers. Each presynaptic bouton contains synapses, where digital action potential signals are converted to an analog chemical signal (the release of neurotransmitter). At the *Drosophila* neuromuscular junction, the neurotransmitter is the amino acid glutamate (Jan and Jan, 1976). When glutamate is released into the synaptic cleft, it activates postsynaptic receptors and causes a depolarization in the muscle fiber. Experiments using a heterologously expressed postsynaptic calcium sensor suggest that boutons display a distal to proximal activity gradient, in that boutons farther from the point of innervation seem to be more active (Guerrero et al., 2005).

Motor neuron axons terminate on their target muscle(s) with remarkable precision in a stereotyped morphology which has been shown to be highly conserved in larvae reared under similar conditions (Johansen et al., 1989, Kurdyak et al., 1994). Motor neurons innervate their target muscles following a principle of synaptic exclusion, such that only one motor neuron axon of a given bouton type will innervate a muscle fiber. Presynaptic boutons were classified by size and appearance into four groups (Johansen et al., 1989, Jia et al., 1993). Each muscle can be innervated by the four types of presynaptic boutons and the type of bouton that forms is thought to be determined by cell-autonomous factors (figure 2-3) (Hoang and Chiba, 2001).

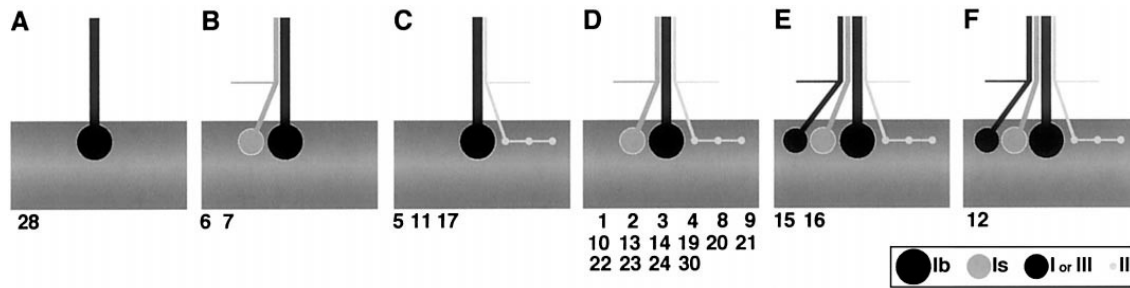


Figure 2-3. A figure illustrating synaptic exclusion. Only one motor neuron of each bouton type innervates a given muscle fiber. A-F depict which muscles (indicated by the numbers below) are innervated by which bouton types (see text) (Hoang and Chiba, 2001).

Type Ib (big) boutons are present on all muscle cells and have large (3-6 μm in diameter) round terminals and is glutamatergic. They are surrounded by a pronounced subsynaptic reticulum, which is formed by the muscle cell membrane.

Type Is (small) endings are present on almost all muscles fibers and have smaller (2-4 μm) glutamatergic terminals with a less pronounced subsynaptic reticulum.

Type II boutons are very small (1-2 μm) glutamatergic endings present on most muscle fibers.

Type III terminals are medium sized (2-3 μm) and have an oval shape. They are found solely on longitudinal muscle number 12 and have been found to co-release insulin in addition to glutamate (Gorczyca et al., 1993).

Interestingly, different bouton types display not only differences in morphology but physiology as well. More than thirty years ago the first recordings were performed at the *Drosophila* muscles 6 and 7 synapse (Jan and Jan, 1976) and although recordings are performed in other muscle fibers, it remains the standard today. Longitudinal muscle fibers 6 and 7 are located ventromedially and run the length of the larva. They are bilaterally symmetrical and are electrically coupled to muscle fibers in neighboring hemisegments (Ueda and Kidokoro, 1996).

The muscle 6 and 7 synapse is innervated by two motor neurons, the MN6/7 (also RP3 or axon 1) which gives rise to type Ib boutons and the MNSNb/d (or axon 2) which has type Is boutons (figure 2-4 top). Experiments measuring activity at 10 Hz showed that Ib boutons from the RP3 motor neuron tend to facilitate whereas type Is boutons show synaptic depression (figure 2-4 bottom) (Lnenicka and Keshishian, 2000). An evoked excitatory junction potentials (EJP) at the muscle 6 and 7 synapse is the combined response of the MN6/7 and MNSNb/d motor neurons. The contributions of Ib boutons to an EJP is thought to be smaller than the response from the Is boutons. For this reason (and given how the motor neurons respond to 10 Hz stimulation) Ib boutons have low release probability synapses (P_r) whereas Is boutons have high P_r synapses (Millar et al., 2002).

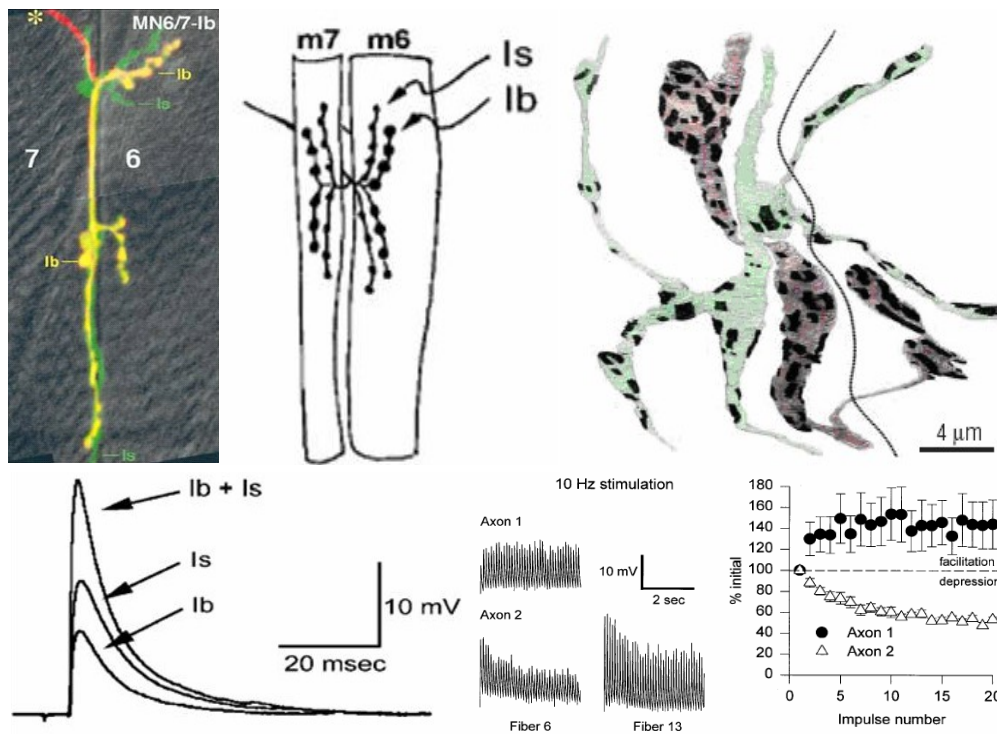


Figure 2-4. Morphology and physiology of the muscle 6 & 7 synapse. Above: florescent labeling, a simplified diagram, and a 3-D reconstruction from serial EM sections of two different motor nerves which innervate muscles 6 & 7. Below: Electrophysiological properties of the motor nerves which innervate muscles 6 & 7 (Hoang and Chiba, 2001, Ball et al., 2002, Stewart et al., 1994, Lnenicka and Keshishian, 2000).

2.1.2 Synaptic transmission at the *Drosophila* neuromuscular junction

Synaptic transmission occurs when calcium enters through voltage sensitive presynaptic calcium channels. Resting intracellular calcium ($[Ca^{2+}]_i$) is thought to be around 22 to 23 nM at the *Drosophila* neuromuscular junction and in cultured central neurons (Berke and Wu, 2000, Macleod et al., 2002). Presynaptic calcium channels were first discovered in the temperature sensitive mutant *cacophony* (*cac*^{TS2}), which codes for the primary α 1 subunit of a calcium channel (Kawasaki et al., 2000, Dellinger et al., 2000)

Presynaptic terminals contain electron-dense specializations known as active zones. Active zones of in most *Drosophila* synapses look like T shaped structures at the EM level and have been shown to be important for synaptic transmission, particularly calcium channel clustering and coordinated vesicle release (Kittel et al., 2006). The nc82 antibody stains active zones by recognizing the Bruchpilot protein, a homolog to mammalian ELKS/CAST/ERC (Wagh et al., 2006). When active zones are imaged with stimulated emission depletion microscopy (STED, a technique which overcomes the limits imposed by diffraction in standard confocal laser scanning microscopy), Bruchpilot appears to have a donut shaped structure (figure 2-5). In *Bruchpilot* (*brp*) null mutants T-bars were absent, presynaptic calcium channels were reduced in density, evoked EJPs were decreased, and short-term plasticity was altered (Kittel et al., 2006).

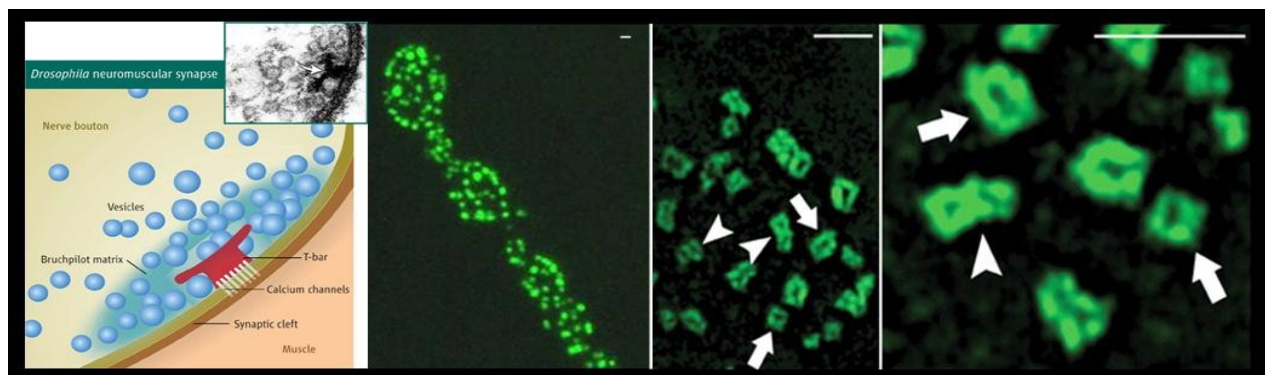


Figure 2-5. Active zones are thought to be important in coordinating the release of synaptic vesicles (left) and look like T shaped structures in EM sections (left panel, top right corner). Synaptic active zones are recognized in *Drosophila* using the nc82 antibody which recognizes Bruchpilot (middle). STED imaging (right) shows that the punctate staining pattern of nc82 actually has a donut appearance at higher magnification, scale bar 1 μ m, (Atwood, 2006, Kittel et al., 2006).

A defining feature of a chemical synapse is the collection of vesicles which are present at a presynaptic terminal. Since synaptic vesicles must be present in order for an action potential to be transmitted to a neighboring cell, different vesicle pools have evolved to ensure synaptic transmission can take place. These pools can be divided into three types: the readily releasable pool (vesicles docked, primed, and ready for release), the recycling pool, and the reserve pool. The muscle 6 and 7 synapse in *Drosophila* is thought to have around 80,000 synaptic vesicles (Rizzoli and Betz, 2005), 80% of which are thought to be in the reserve pool (70,000 vesicles) while 14 to 19% make up the recycling pool (approximately 14,000) vesicles. The readily releasable pool is thought to make up just under 1/2 % of the total vesicle complement (around 300 vesicles) however it may contribute to up to twenty percent of baseline synaptic transmission at 10 Hz (Verstreken et al., 2002). This could be accomplished by functioning as “kiss and run” vesicles, however there is some disagreement as to whether this mechanism exists (Dickman et al., 2002) at the *Drosophila* neuromuscular junction.

In order for a synaptic vesicle to release its neurotransmitter into the synaptic cleft it must undergo exocytosis and this requires the coordinated activity of several proteins (figure 2-6 A & D). Exocytosis can be thought to occur in three steps: priming, fusion, and disassembly. Synaptic active zones contain proteins which are referred to as t-SNAREs (for target soluble N-ethylmaleimide sensitive factor attachment receptors) that interact with specific proteins on the synaptic vesicle, called v-SNAREs (vesicle-SNARE) (reviewed by Richmond and Broadie, 2002). At most synapses, including the *Drosophila* neuromuscular junction, the v-SNARE is Synaptobrevin and the t-SNAREs are Syntaxin and SNAP-25 (soluble N-ethylmaleimide sensitive factor attachment protein 25 kDa). A protein called Unc-13 (which was initially isolated from a screen of *C. elegans* mutants which appeared uncoordinated) is thought to prime the complex in preparation for fusion. Primed vesicles can be thought of as molecular mouse traps. The binding of calcium to Synaptotagmin, a synaptic vesicle protein which interacts with Syntaxin causes intertwined α -helical bundles within the SNARE complex to contract, bringing the two lipid bilayers into direct opposition and causing them to mix. This results in a fusion pore which, depending on the type of fusion event, allows for either a gradual or instantaneous release of transmitter. After fusion the SNARE complex must disassemble and rewind in order to prepare for subsequent rounds of exocytosis. This process occurs via ATP hydrolysis by the ATPase NSF (N-ethylmaleimide sensitive factor).

A prerequisite for sustained synaptic transmission is that vesicles must be recycled. When a synaptic vesicle fuses with the membrane, it presumably becomes continuous with the lipid bilayer of the neuron. Retrieval of membrane occurs through a process known as endocytosis. At *Drosophila* neuromuscular boutons, imaging experiments using styryl dyes (which label cycling synaptic vesicles) suggest that endocytosis occurs at the periphery (Kuromi and Kidokoro, 2003). Dozens of proteins have been identified and implicated in this process (figure 2-6 C) however bulk retrieval of membrane is thought to be mediated by clathrin lattices with rates of replenishment around 1,000 vesicles per second (Broadie, 2004, Delgado et al., 2000).

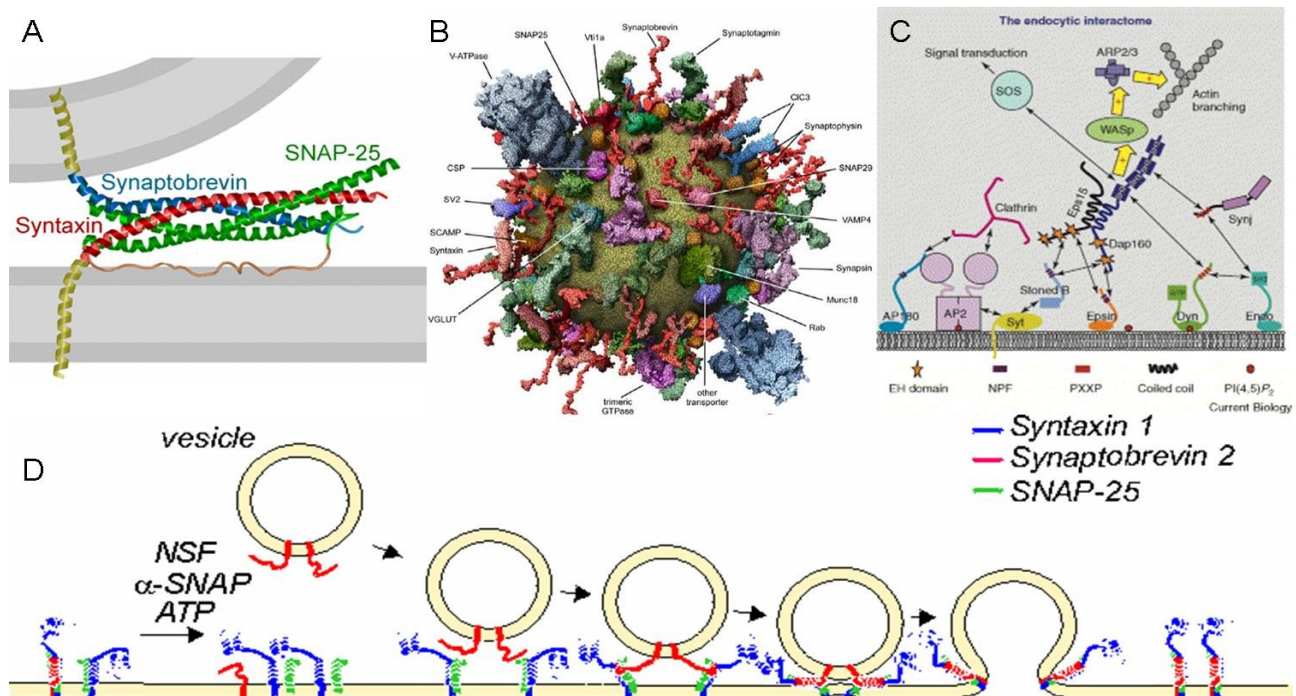


Figure 2-6. Proteins involved in exocytosis and endocytosis. A. Target and vesicle SNAREs interact to form the fusion apparatus. B. The complement of proteins on a synaptic vesicle (Takamori et al., 2006). C. Proteins thought to be involved in endocytosis at the *Drosophila* neuromuscular junction (Broadie, 2004). D. Synaptic vesicle docking, priming, and fusion (modified from www.mpibpc.mpg.de/groups/jahn).

When an action potential triggers the synchronized release of synaptic vesicles, molecules of neurotransmitter enter the synaptic cleft and begin to diffuse in all directions. Directly across from the site of neurotransmitter release are billions of postsynaptic receptors, which activate and open in the

presence of neurotransmitter. At the *Drosophila* neuromuscular junction, the amino acid glutamate functions as a neurotransmitter and ionotropic glutamate receptors are expressed postsynaptically. When glutamate molecules bind, they open and allow calcium and sodium to flow down their electrochemical gradients, thereby depolarizing the muscle fiber. Five glutamate receptor subunits are thought to be expressed at the *Drosophila* neuromuscular junction, DGluRIIA (Schuster et al., 1991), DGluRIIB (Petersen et al., 1997), and three obligatory subunits DGluRIII, DGluRIID, and DGluRIIE (Marrus et al., 2004, Qin et al., 2005). Glutamate receptors at the neuromuscular junction are thought to be heterotetramers which consist of three obligate subunits (DGluRIID, DGluRIIE, and DGluRIII) and either a DGluRIIA or IIB subunit. Interestingly, channel properties seem to be dictated by the IIA and IIB subunits (figure 2-7 A). IIB channels close rapidly in response to glutamate while IIA channels remain open longer. These alternative responses can be explained by differences in gating kinetics such as activation, inactivation, and desensitization (figure 2-7 B) (Heckmann and Dudel, 1997). The number of IIA and IIB channels at the postsynapse play an important role in shaping the postsynaptic response and it is thought that subunit number and composition in receptive fields may be altered in order to modulate synaptic plasticity at the *Drosophila* neuromuscular junction (DiAntonio et al., 1999, Petersen et al., 1997, Trussell and Fischbach, 1989).

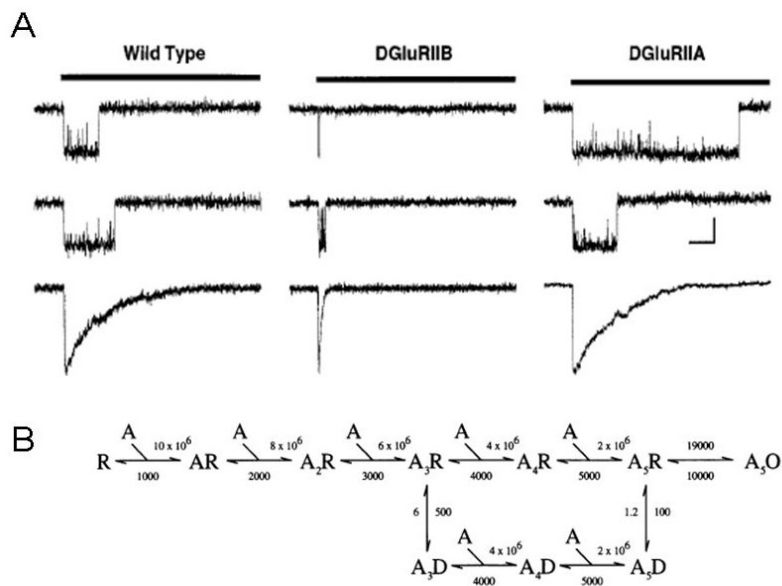


Figure 2-7. A. Outside out patches of larval muscle fibers from wild type, DGluRIIA, and DGluRIIB null mutants, scale bar 10 msec, 5 pA. Lower traces show average responses to rapidly applied 10mM glutamate normalized to peak current amplitude (DiAntonio et al., 1999). B. Gating kinetics of postsynaptic glutamate receptors (Heckmann and Dudel, 1997).

2.2 Null mutants characterized at the *Drosophila* neuromuscular junction

2.2.1 Sap-47¹⁵⁶

One of the first mutants which was characterized during my thesis work was a null mutant for the synapse-associated protein of 47 kDa (Sap-47). The SAP-47 protein was first isolated because it contained the antigenic epitope for a monoclonal antibody from a hybridoma library that was generated by immunizing mice with homogenized *Drosophila* heads (Hofbauer, 1991). Monoclonal antibody nc46 was found to stain most synapses in the *Drosophila* central nervous system and its antigen SAP-47, appeared to be conserved in insects, fish, mouse, and man. It however displays almost no sequence homology to any known proteins (Reichmuth et al., 1995, Doerks et al., 2002).

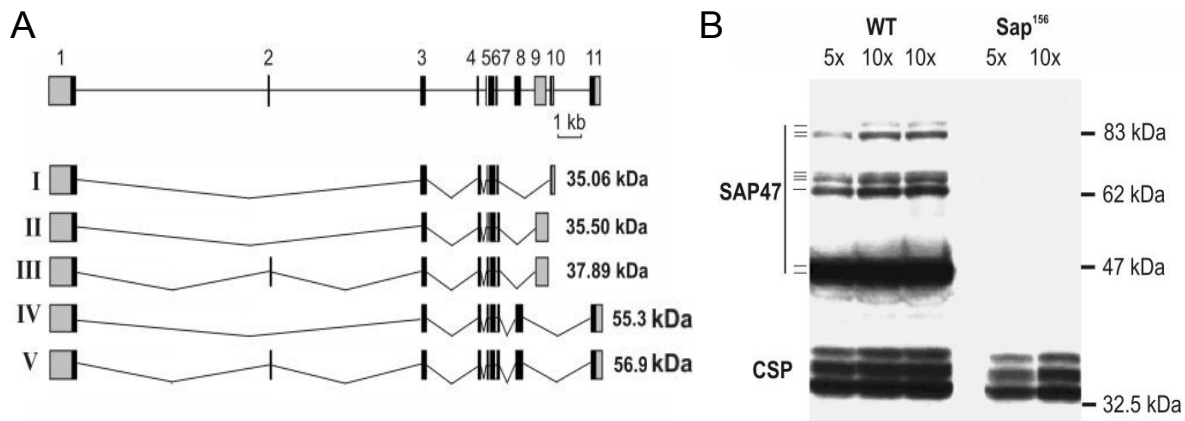


Figure 2-8. A. Exon-intron structure of the five proposed splice isoforms of the *Sap-47*¹⁵⁶ gene. B. Western blot analysis of (WT, *w*¹¹¹⁸) and *Sap-47*¹⁵⁶ null mutant, Cysteine String Protein was used as a loading control (Funk et al, 2004).

The *Sap-47* gene is located at 89A8-B3 on chromosome 3R and was initially found to code for 2 polypeptides of approximately 350 amino acids, which have a predicted molecular mass of 35 kDa but migrate at 47 kDa on Western blots because of secondary and tertiary structures. Subsequent study of available cDNA, expressed sequence tags, and putative transcripts revealed 11 exons and 10 introns which are thought to code for at least 9 protein isoforms of the SAP-47 protein (figure 2-8 A) (fly base access number CG8884, <http://flybase.bio.indiana.edu>). The deletion mutant *Sap-47*¹⁵⁶ (Funk et al., 2004) is fully viable and fertile. This mutant suffers a ~1.7 kb chromosomal deletion that removes the first exon and part of the first intron and is therefore considered a null mutant (figure 2-8 B).

Except for a tripeptide repeat which loosely resembles the M-domain of the yeast SRH1 protein and other conspicuous di and tripeptide repeats, there were few initial clues as to the possible function of SAP-47. Later work revealed a novel domain termed BSD (for BTTF2-like transcription factors, synapse-associated, DOS2-like proteins) that consisted of 60 amino acids which were predicted to form three α helices and had conserved C-terminal tryptophan and phenylalanine residues. Unfortunately this offered little insight as to the “fitness related function of the protein” (Doerks et al., 2002).

Observations that nc46 had a similar staining pattern to ab49 (which recognizes the Cysteine String Protein) was some of the first evidence which suggested that SAP-47 might be associated with synaptic vesicles (Mastrogiacomo et al., 1994, Zinsmaier et al., 1990, 1994). Further evidence which confirmed this came from electron microscopic immuno-gold labeling of the larval nerve muscle synapse with nc46 (Reisch, 2000, Saumweber et al., in preparation). Of 1631 gold particles in sections from 18 different presynaptic terminals, 87.5 % were found to be within 30 nm of a synaptic vesicle. Only 8.5 % of the gold particles were not found within this distance (the 4 % of gold particles which were detected outside boutons were considered unspecific background).

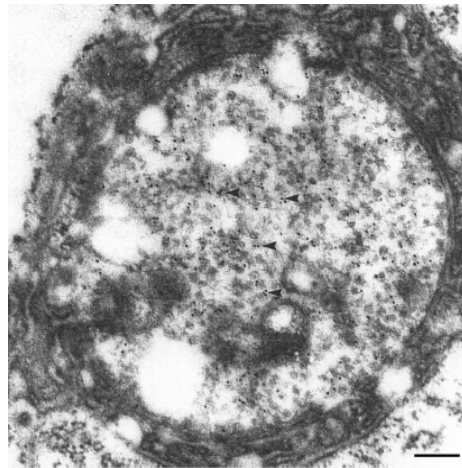


Figure 2-9. SAP-47 is closely associated with synaptic vesicles. An EM section showing immuno-gold labeled SAP-47, scale bar 200 nm (Reisch, 2000).

SAP-47 is most likely not integral to the synaptic vesicle membrane, as SAP-47 was found in the soluble fraction of brain homogenate and glycerol density gradient centrifugation clearly separates SAP-47 from known integral synaptic vesicle membrane proteins such as CSP (Arnold et al., 2004, Umbach et al., 1994). Thus, SAP-47 is associated with synaptic vesicles (figure 2-9) but is not an integral part of the synaptic vesicle protein complement. The presence of the SAP-47 protein at synapses and its association with synaptic vesicles suggests that perhaps synaptic transmission might be affected so *Sap-47*¹⁵⁶ null mutants were characterized at the *Drosophila* neuromuscular junction.

2.2.2 Synapsin⁹⁷

Synapsin, or Protein I as it was initially called (Ueda and Greengard, 1977, Kennedy et al., 1983), was one of the first synaptic vesicle associated proteins to be discovered (Südhof and Jahn 1991). In *Drosophila*, one Synapsin gene is differently spliced and edited at the RNA level to give rise to various isoforms (figure 2-10 A) (fly base access number FBgn0004575, <http://flybase.bio.indiana.edu>) (Klagges et al., 1996, Godenschwege et al., 2004, Diegelman et al., 2006). *Drosophila* Synapsin contains three conserved domains (A, C, and E) and is present in most presynaptic terminals (figure 2-10 B).

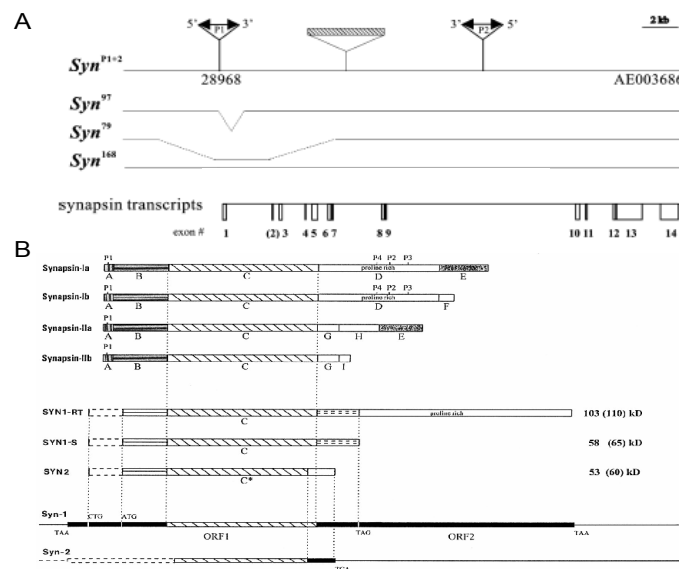


Figure 2-10. A. Genomic organization of wild type and Synapsin null mutants as well as p-element insertion sights.

B. Domain structures of vertebrate and *Drosophila* Synapsins (Klagges et al., 1996, Godenschwege et al., 2004).

Synapsin is thought to be involved in the regulation of neurotransmitter release, specifically in vesicle mobilization between reserve and actively releasing synaptic vesicle pools at various frequencies (Chi, et al., 2003). Models suggest that Synapsin anchors reserve pool vesicles to the cytoskeleton. Phosphorylation of Synapsin via PKA is thought to result in a conformational change in the protein, which allows vesicles to detach from the cytoskeleton and enter the cycling pool of vesicles (Ceccaldi et al., 1995).

The mammalian genome contains three Synapsin genes which due to alternative splicing code for several different isoforms. Single, double, and triple knock-out mice have been shown to have a variety of defects in synaptic function such as decreased post-tetanic potentiation, increased paired pulsed facilitation, reduced synaptic depression, and decreased inhibitory post synaptic potentials (Li et al., 1995, Rosahl et al., 1995, Feng et al., 2002). In cultured hippocampal neurons, the total recycling vesicle pools appear significantly reduced, however endocytosis and synaptic vesicle repriming kinetics appear normal (Ryan et al., 1996). Even though the physiological defects of Synapsin deletion are still being debated, flies which lack Synapsin appear to be impaired in learning and memory as well as other complex behaviors. This suggests that vesicle cycling may be important for certain aspects of cellular information processing. We therefore examined synaptic transmission in *Synapsin*⁹⁷ null mutants at the *Drosophila* neuromuscular junction.

2.2.3 Sap-47¹⁵⁶ Synapsin⁹⁷ double mutants

In order to investigate a possible interaction between SAP-47 and Synapsin, S. Becker, N. Funk, and T. Nuwal each recombined the Sap-47¹⁵⁶ and Synapsin⁹⁷ null mutants. In all instances a third gene (black pearl) was affected so no homozygous animals were obtained however transheterozygotes of the three recombinations were viable and fertile (*SapSyn*^{SB}, *SapSyn*^{NF}, *SapSyn*^{TN}). Additional *SapSyn* double mutants were generated by Viera Albertova (*SapSyn*^{VA}) which were homozygous viable after extensive back crossing with CS wild type flies. Since these double mutant lines all lack both SAP-47 and Synapsin proteins, they were examined for electrophysiological defects at the *Drosophila* neuromuscular junction.

2.2.4 Serine-Arginine protein kinase 3

A search for potential interaction partners with the active zone protein Bruchpilot (BRP) resulted in the discovery of an uncharacterized serine-threonine kinase (Nieratschker, 2004, Nieratschker et al., 2008 in preparation). Using the P-element line $SRPK3^{P1}$ a null mutant was generated and it was shown that deletion of the kinase gene locus resulted in BRP aggregates in larval motor neuron axons. The kinase was named Serine-Arginine protein kinase 3 (SRPK3) (fly base access number CG11489, <http://flybase.bio.indiana.edu>). The *SRPK3* gene has two transcription start sites and is thought to give rise to at least four and possibly five isoforms (RC, RB, RE, RF, and potentially RD) (figure 2-11).

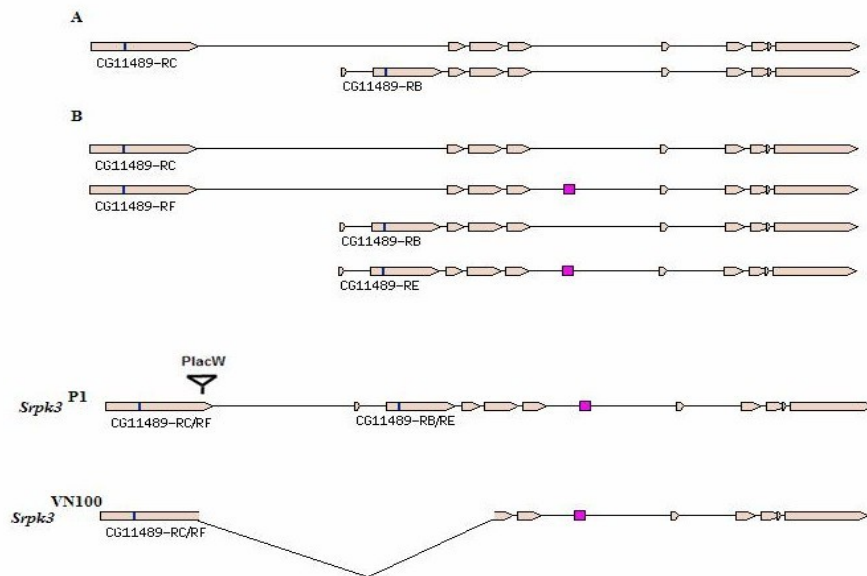


Figure 2-11. The *SRPK3* gene has two transcription start sites (A) and alternative splicing gives rise to at least four isoforms (B). The line $SRPK3^{P1}$ lacks isoforms 1 and 2 (RC), $SRPK3^{VN100}$ is the null mutant (image modified from fly base).

Protein aggregates in neuron axons generally reflects disruption of axonal transport however deletion of *SRPK3* did not appear to disrupt fast axonal transport in general. Larval motor neuron axons stained with ab49 (which labels the Cysteine String Protein) or an anti-Synaptotagmin antibody; two proteins which have been shown to accumulate in axonal transport mutants (Zinsmaier et al., 1994, Hurd and Saxton, 1996), did not show aggregates in the axons of *SRPK3* null mutants suggesting that the observed effect of *SRPK3* is specific for Bruchpilot (figure 2-12).

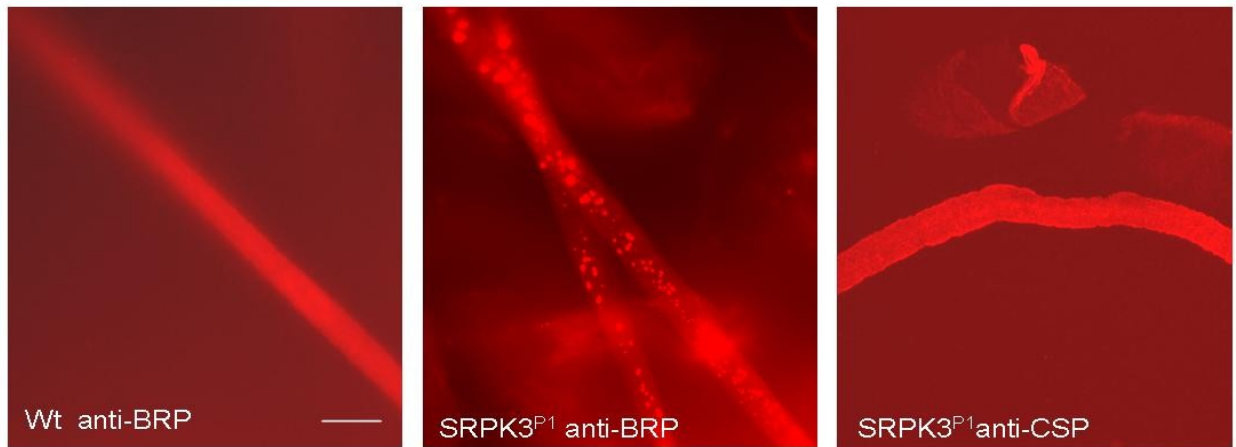


Figure 2-12. Aggregates of the Bruchpilot protein as seen in larval motor neuron axons of SRPK3 null mutants compared to wild type, scale bar is 10 μ m. Axonal transport of CSP and Synaptotagmin appeared normal (Synaptotagmin data not shown) (Nieratschker et al., 2008 in preparation).

Over-expressed GFP-labeled SRPK3 was found to co-localize with BRP at the active zone (figure 2-13). Since SRPK3 is a kinase it was hypothesized that SRPK3 may regulate BRP in some way. Interestingly, SRPK3 null mutants display similar behavioral defects in adult flies to BRP-RNAi-knock-down flies (Wagh et al., 2006, Bloch, 2007, Nieratschker et al., in preparation). Since BRP null mutants display defects in synaptic transmission (Kittel et al., 2006), we characterized SRPK3 null (and overexpression) mutants at the *Drosophila* neuromuscular junction.

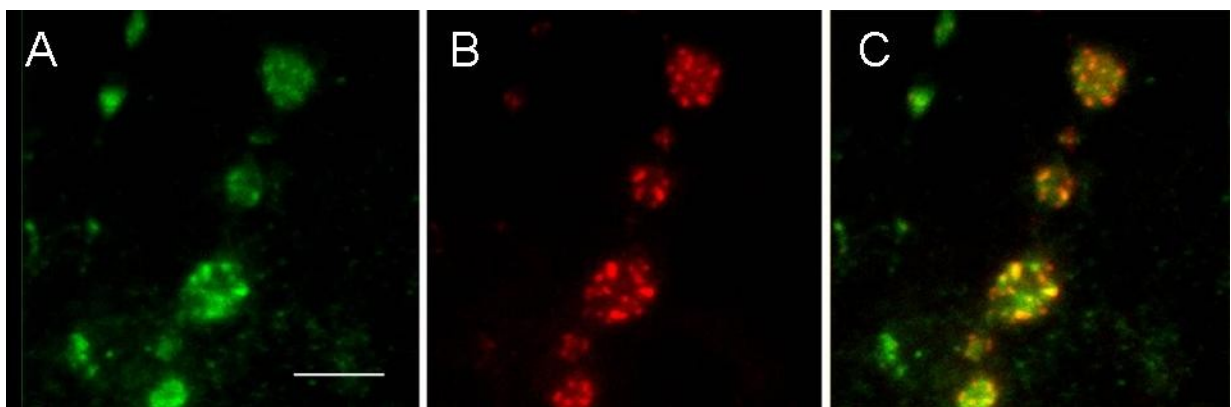


Figure 2-13. Over-expressed SRPK3-GFP (A) co-localizes with Bruchpilot (B) at active zones (overlay C) and may therefore regulate synaptic transmission, scale bar is 5 μ m (Neiratschker et al., 2008 in preparation).

2.2.5 Löchrig

The *Löchrig* (*Loe*) mutant received its name because it accurately describes in German the appearance of this fly's brain, full of holes (figure 2-15). *Löchrig* was isolated from a collection of p-element insertion lines which were aged and then screened histologically for signs of neurodegeneration (Deak et al., 1997). *Loe* flies were found to have a mutation that affects a specific isoform of the γ subunit of AMP activated protein kinase (AMPK) (Tschäpe et al., 2002). AMPK plays an important role in cellular energy homeostasis, acting as a metabolic sensor and master switch. Activation of AMPK via AMP signals that cellular energy levels need to be increased so anabolic, energy consuming pathways are inhibited and catabolic, energy generating pathways are stimulated (figure 2-14 C).

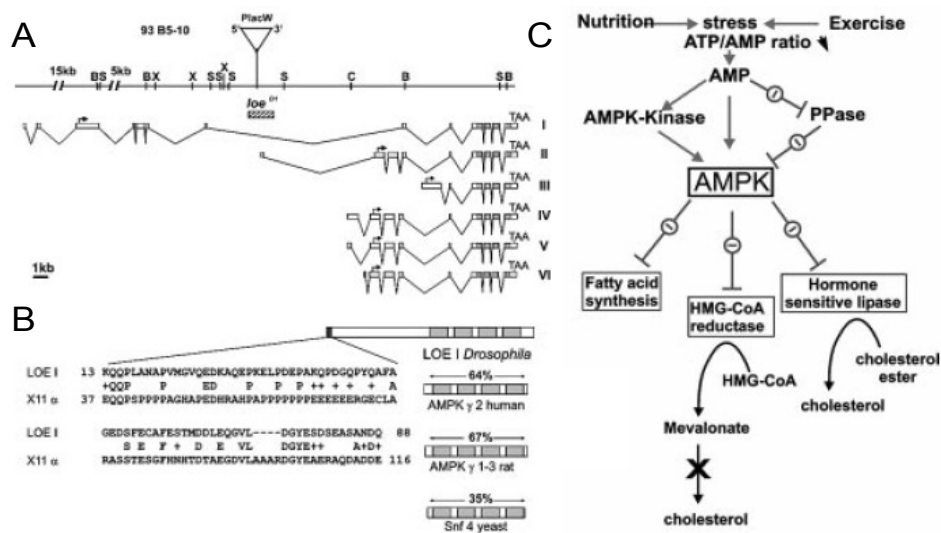


Figure 2-14. A. The *Loe* gene locus and Exon intron structure of the *Loe* I to *Loe* VI isoforms as well as insertion site of the PLAC-W p-element. B. Homology comparison of AMPK γ C- terminus. C. The role of AMPK in cellular energy homeostasis (Tschäpe et al, 2002).

Löchrig flies exhibit pronounced, age dependent, neurodegeneration, as well as low levels of cholesterol ester; the storage form of cholesterol in *Drosophila*. In humans, 25% of our body's cholesterol is relegated to 2% of our body mass, in our brains (Dietschy and Turley, 2001). Cholesterol plays an important role in the physical properties of the lipid bilayer and also contributes to membrane compartmentalization by forming lipid raft microdomains (Simons and Ikonen, 1997).

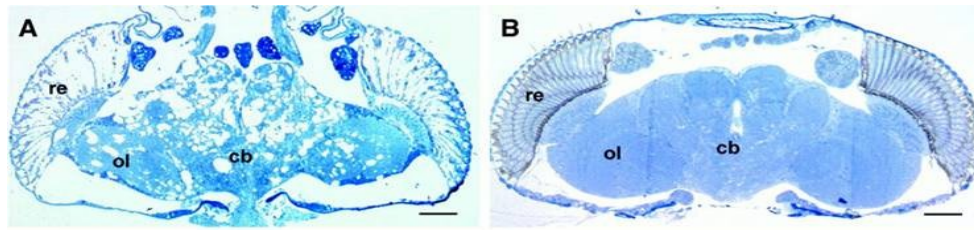


Figure 2-15. Horizontal plastic sections from 10 day old *Loe* (A) and wild type (B) flies stained with toluidine blue. re, retina; cb, central part of the brain; ol, optic lobes, scale bar 50 μm , (Tschäpe et al., 2002).

Recently, the role of lipids in synaptic function has become an area of interest (Rohrbough and Broadie, 2005) since cholesterol plays an important role in cell membrane curvature and fluidity and is the primary component of lipid rafts. At the synapse, the rate of membrane turnover is very rapid. Vesicles are continuously fusing with the presynaptic membrane to release neurotransmitter and then needing to be recycled and refilled (except of course for kiss and run vesicles, providing they exist). Getting the correct complement of vesicle proteins onto a synaptic vesicle in a timely fashion is an entropic wonder and it has been suggested that lipid rafts may somehow contribute to this process (figure 2-16 A). To suggest that a disruption of synaptic vesicle cycling may lead to wide spread neurodegeneration may seem far fetched however *Loe* mutants display a morphological phenotype at the *Drosophila* neuromuscular junction. The periphery of presynaptic boutons in *Loe* flies appear fused and more drawn out compared to normal, round, wild type boutons (figure 2-16 B). Interestingly, it is at the bouton periphery where vesicle recycling is thought to occur so synaptic transmission was characterized in *Loe* at the *Drosophila* neuromuscular junction.

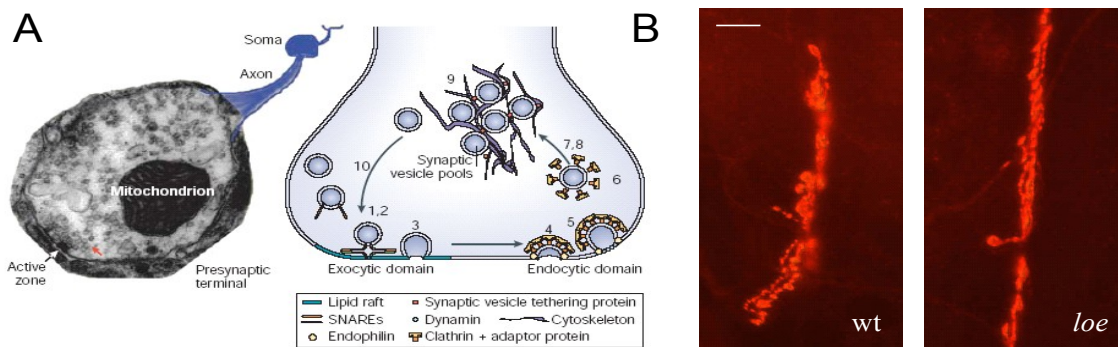


Figure 2-16. A. A potential role for lipids at the synapse (Rohrbough and Broadie 2005). B. *Loe* mutants display an altered bouton morphology at the *Drosophila* neuromuscular junction when compared to wild type flies, scale bar 20 μm .

2.3 Expression of light activated proteins at the *Drosophila* neuromuscular junction

2.3.1 Channelrhodopsin-2

Channelrhodopsin-2 (ChR2 or Chop) protein was cloned from the photosensitive green algae *Chlamydomonas reinhardtii* (figure 2-17 A) (Nagel et al., 2003). It displays homology to microbial-type rhodopsins, however it is unique in that even though it displays the seven-transmembrane α helices (a typical characteristic of G protein-coupled receptors) ChR2 is in fact a light-gated cation-selective ion channel (figure 2-17 B). ChR2 shows a maximal absorbance at 460 nm and opens rapidly after exposure to light (figure 2-17 C). Continuous exposure of the channel to light causes it to shift to a smaller steady-state conductance (figure 2-17 D).

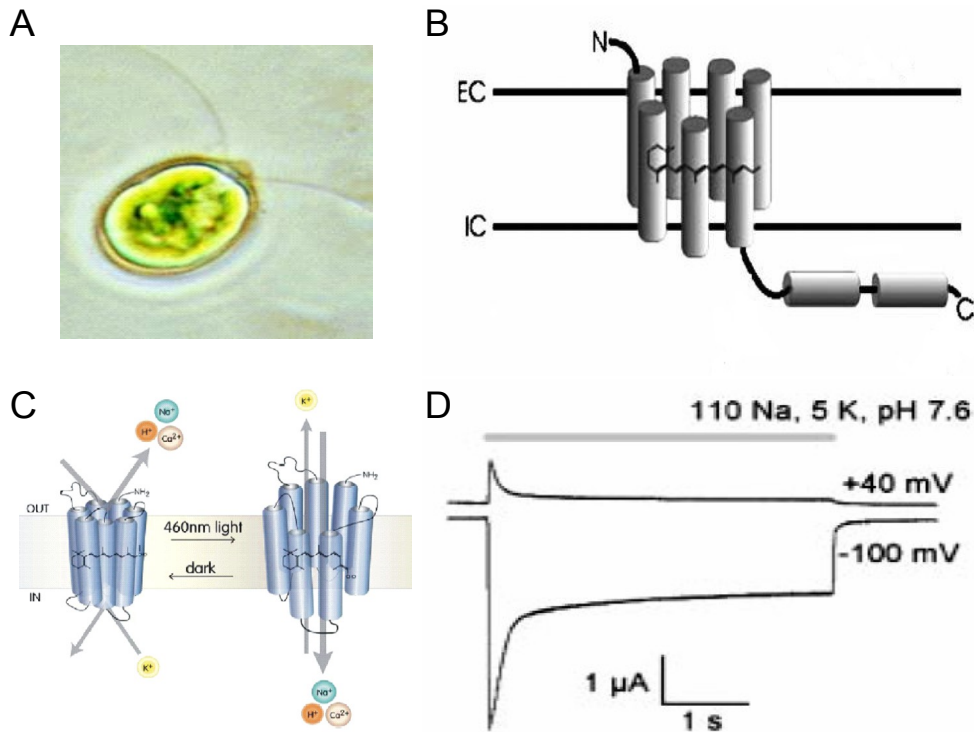


Figure 2-17. A. *Chlamydomonas reinhardtii* (from Protist image data base). B. The predicted seven transmembrane structure of a ChR2 subunit (Nagel et al., 2003). C. A diagram of Channelrhodopsin-2 (Flannery and Greenberg, 2006). D. Two electrode voltage clamp recording showing Channelrhodopsin-2 kinetics after exposure to light in *Xenopus* Oocytes (Nagel et al., 2003).

Naturally occurring light activated proteins are excellent tools for noninvasively manipulating the excitability of neurons (Boyden et al., 2005). Using the Gal-4 UAS system (Brand and Perrimon, 1993) we can express a UAS-ChR2 construct at the *Drosophila* neuromuscular junction with the motor neuron specific promoter D-42 (Parkes et al., 1998) in order to evaluate the effectiveness of ChR2 as a optophysiologic tool for manipulating neuronal activity.

2.3.2 Photoactivated adenylate cyclase

The variety of different functions cAMP carries out at the synapse are remarkable in their diversity. Cyclic AMP was shown to play a role in developmental processes by inducing changes in gene expression via the cAMP responsive element binding protein (CREB) (Hoeffler et al., 1988). Cyclic AMP also acts at ion channels and through various second messenger pathways to acutely modulate various aspects of synaptic function. A large amount of work has been done at the *Drosophila* neuromuscular junction to illustrate the many ways cAMP can regulate various aspects of synaptic function. Previous work showed impaired synaptic transmission in *dunce* and *rutabaga* flies (which have mutations in phosphodiesterase or adenylate cyclase activity respectively) (Zhong and Wu, 1991). Increases in intracellular cAMP were found to activate protein kinase A (PKA) (Schwartz and Greenberg, 1987), which has a variety of effects at the *Drosophila* neuromuscular junction. PKA activity has been shown to modulate the frequency of spontaneous vesicle fusion events via two independent pathways (Yoshihara et al., 1999). It has also been implicated in hypertonicity induced vesicle release (Suzuki et al., 2002, Suzuki et al., 2002) and the trafficking of synaptic vesicles from the reserve pool to the cycling pool via phosphorylation of Synapsin (Ceccaldi et al., 1995). Signaling through presynaptic metabotropic glutamate receptors (G α s) (figure 2-18 B) causes an elevation of cAMP and deletion of this pathway results in impaired synaptic transmission (Hou et al., 2003). Stimulation of G α s acts through PKA dependent and independent (Wolfgang et al., 1996) pathways and has been suggested to be important in regulating synaptic strength pre and postsynaptically (Zhang et al., 1999, Renden and Brodie, 2002). At the *Drosophila* neuromuscular junction, cAMP can also potentiate synaptic transmission by acting through non PKA-dependent mechanisms such as the activation of presynaptic cyclic nucleotide gated channels (Cheung et al., 2006)

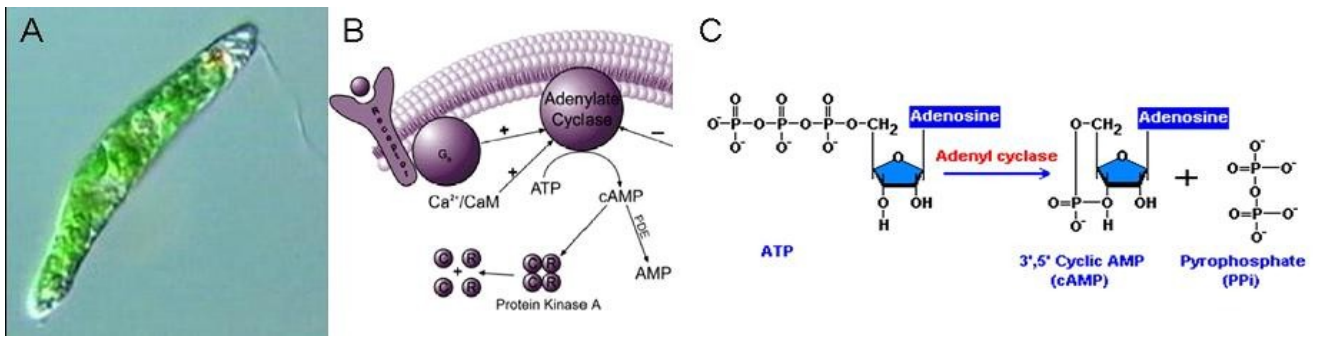


Figure 2-18. A. *Euglina gracilis* (from the Protist image data base). B. The G α s signal transduction pathway (modified from Calbiochem). C. Adenylate cyclase converts ATP to cAMP and pyrophosphate.

Using the Gal-4 UAS system we can heterologously express a photo-activated adenylate cyclase (PAC) which was originally cloned from the eye spot of the protozoan *Euglina gracilis* (figure 2-18 A) (Iseki et al., 2002) in larval motor neurons. Application of blue light causes a rapid increase in the level of intracellular cAMP, therefore we used PAC to characterize the various functions cAMP has at the synapse.

3. Materials and Methods

3.1 The setup

An electrophysiology “rig” consists of several independent components working together so one can measure bioelectric signals of different magnitudes from various sources, from the opening of a single ion channel to the simultaneous opening of billions. Components can vary depending on the task at hand and have been divided into eight parts for the sake of discussion (figure 3-1).

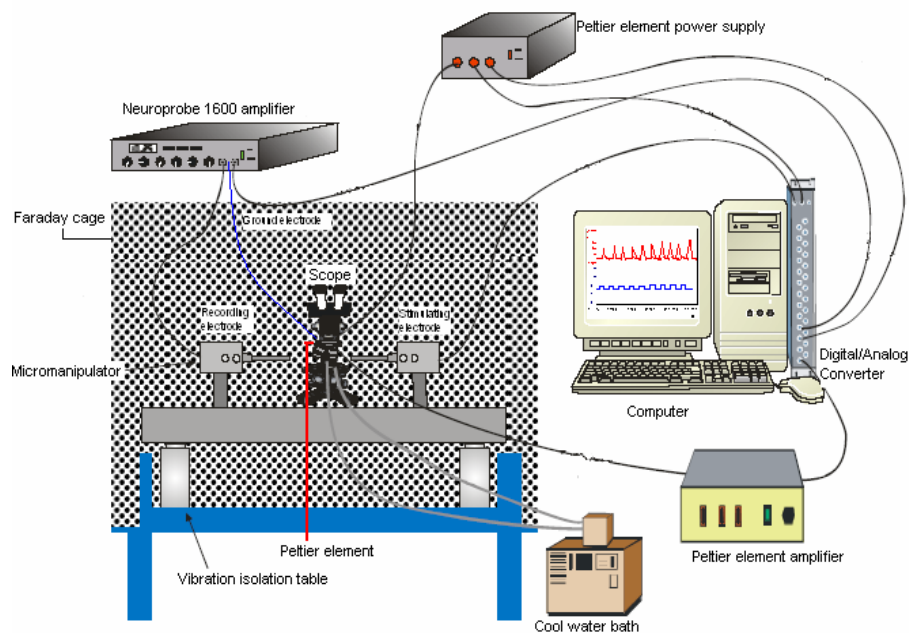


Figure 3-1. A schematic of our electrophysiology set up “Lucille” (figure by Christian Leibold) and it's different parts (the slab, Faraday cage, Peltier element, microscope and manipulators, amplifier, and the computer with data acquisition processor).

3.1.1 The slab

Given the delicate nature of bioelectric systems, steps must be taken to ensure that an electrophysiology setup is protected from periodic vibrations and sudden movements. A poorly isolated system can result in noise as well as unstable baselines (because of undesired electrode movement in the preparation after placement). Fortunately, unwanted vibrations can be easily eliminated by placing a heavy slab table on pneumatic supports.

3.1.2 Faraday cage

Given the small size of the electrical signals at the *Drosophila* neuromuscular junction, a Faraday cage is required. It is simply an enclosure formed by a conducting material to prevent stray electrical fields from overhead lighting and other electronic devices from disturbing the measurements. All metal objects in the Faraday cage should be connected to a central ground (being careful to avoid ground loops). Improper grounding can result in electrical noise which increases the magnitude of the baseline signal. Periodic noise can also occur in poorly isolated cages. This generally results from the 50 Hz duty cycle of AC current however residual 50 Hz noise can be eliminated by using a line frequency filter.

3.1.3 Peltier element

Although most experiments performed in this thesis were done at room temperature, the temperature of the preparation could be regulated by using a Peltier element. This device gets its name from the effect which occurs when a current is passed through two dissimilar metals that are connected at two points (Peltier junctions). The current drives a transfer of heat from one junction to another such that one heats up and the other cools down, the so-called Peltier effect (for Jean Charles Athanase Peltier who re-discovered the effect in 1834). The temperature of one junction can be quickly and precisely regulated by adjusting the current delivered, providing the heat from the second junction is removed by using a circulating water bath.

3.1.4 Optics and manipulators

Given the size of the *Drosophila* larva neuromuscular junction preparation, some magnification is required in order to find the appropriate motor nerves and ensure accurate electrode placement. For these recordings we used a modified Leitz Dialux 20 fixed stage microscope and 2 Leitz manipulators for positioning the recording and stimulating electrodes. Generally electrodes were positioned over the preparation using a low power (L 10/0.22) objective. Then a higher power (L 32/0.40) objective was used to find the motor nerve which innervated the desired muscle hemisegment.

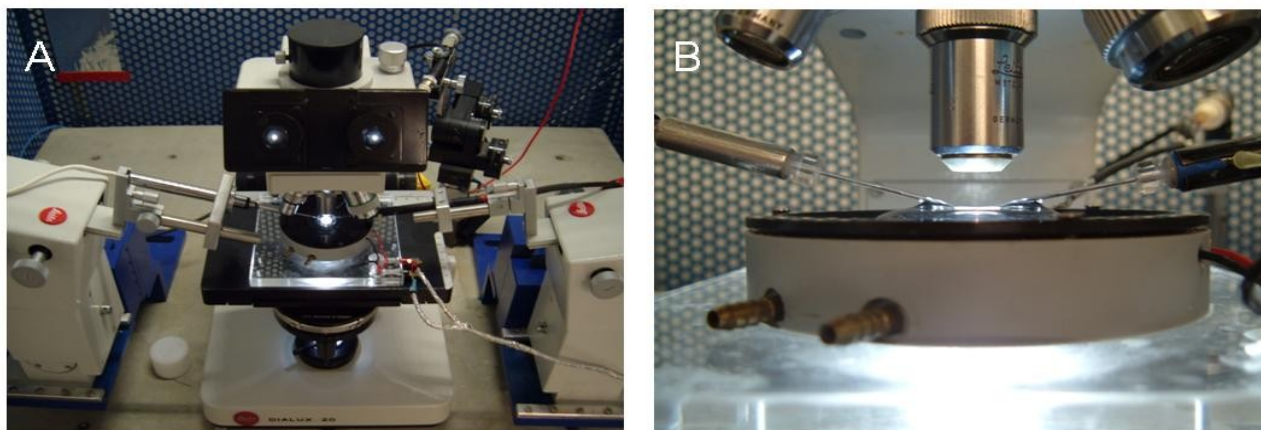


Figure 3-2. A. The many parts of Lucille: Peltier element (center of stage), micromanipulators (left and right), microscope (center), vibration table (below), and Faraday cage (background). B. A close up of the recording chamber (Peltier element), stimulating electrode (right), recording electrode (left), and reference (background).

3.1.5 Microelectrodes

A microelectrode is an essential component in any electrophysiological recording. They must be handled carefully and maintained properly in order to ensure accurate, low noise recordings. A microelectrode consists of four separate components: the electrode holder, the wire, in this case a silver / silver chloride (Ag/AgCl), the conducting solution (3M KCl for recording electrodes, HL3.1 for stimulating electrodes) and the glass (or in this case borosilicate) pipette. Pipette holders are plastic housings which connect the Ag/AgCl wire to the amplifier via a BNC cable. Electrode holders generally have a copper pin which makes contact with the Ag/AgCl wire. In the case of extremely choppy baselines (or no baseline at all) one should make sure that the copper pin is making a solid contact with the Ag/AgCl wire and that no KCl salt has accumulated at the contact point. Electrodes should be regularly disassembled and washed in ddH₂O to prevent accumulation of KCl salts. When breaking in a new wire, it should be sanded gently with a fine grade sand paper and then coated with chloride. This can be accomplished by putting the wire in 0.1M HCl and then passing a small positive current from the electrode into the bath or by soaking the electrode in bleach overnight. Silver / silver chloride electrodes are reversible but exhaustible (figure 3-3 B) therefore chloride should be re-applied fairly regularly (every couple months), particularly when large offsets are observed when the recording pipette is placed in the bath.

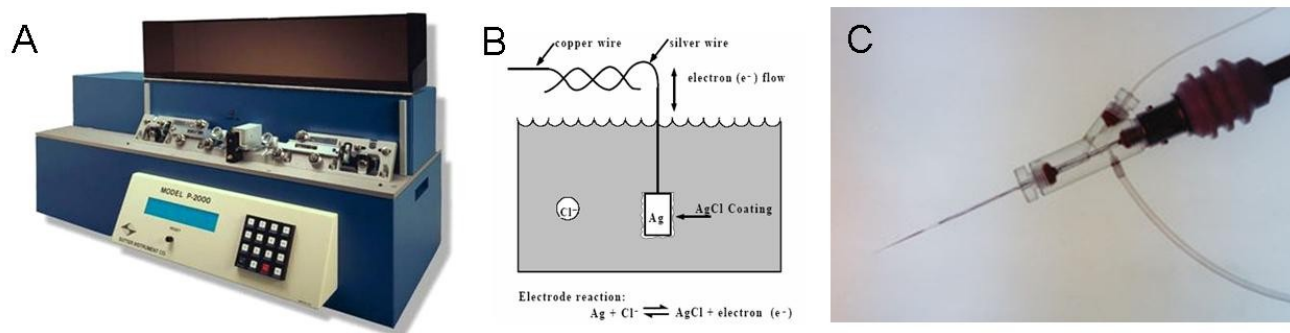


Figure 3-3. A. The Sutter P-2000 laser pipette puller (modified from The Pipette Cookbook, www.sutter.com). B. The electrochemistry of a silver / silver chloride (Ag/AgCl) (modified from the Axon guide). C. A micropipette and electrode holder (modified from www.drugdiscoveryonline.com).

Pipettes were pulled on a Sutter Instruments P-2000 automatic pipette puller. (figure 3-3 A) This device allows the manipulator to adjust parameters such as heat intensity, initial-pull strength, hard-pull threshold velocity, and inter-pull durations to fashion micropipettes into the desired form. Settings were continuously modified depending on the value determined by the ramp test (which can vary because of humidity, ambient temperature, and other factors). Pipettes were pulled within the following values: Heat: 240 – 280, Velocity: 40 – 80, Delay: 180 – 240, Pressure: 100 – 150. For questions regarding settings, one should consult the Sutter Instruments Pipette Cookbook (www.sutter.com).

Stimulating pipettes were broken back to an inner diameter of approximately 10 μm and fire polished so they could accommodate the motor nerve without damaging it but not such that there would be space between the pipette and the nerve (figure 3-4 A). A 50 cc syringe was connected to the electrode holder so positive and negative pressure could be applied to draw the motor nerve axon into the stimulating pipette.

Recording electrodes were filled with 3M KCl, making sure that no bubbles were at the tip of the electrode and that the AgCl wire making was as close to the end of the electrode as possible. Recording electrodes were then submerged in a bath of HL3.1 ringers to a depth approximately

equivalent to where the recordings would take place. Any voltage offset was zeroed and then the electrode resistance was measured. Only microelectrodes which had tip resistances between 10-20 M Ω were used. Before any measurements were taken, capacitance was compensated to offset any charging or discharging of the pipette in the solution (figure 3-4 B); this was done using a Hewlett Packard 54600A oscilloscope.

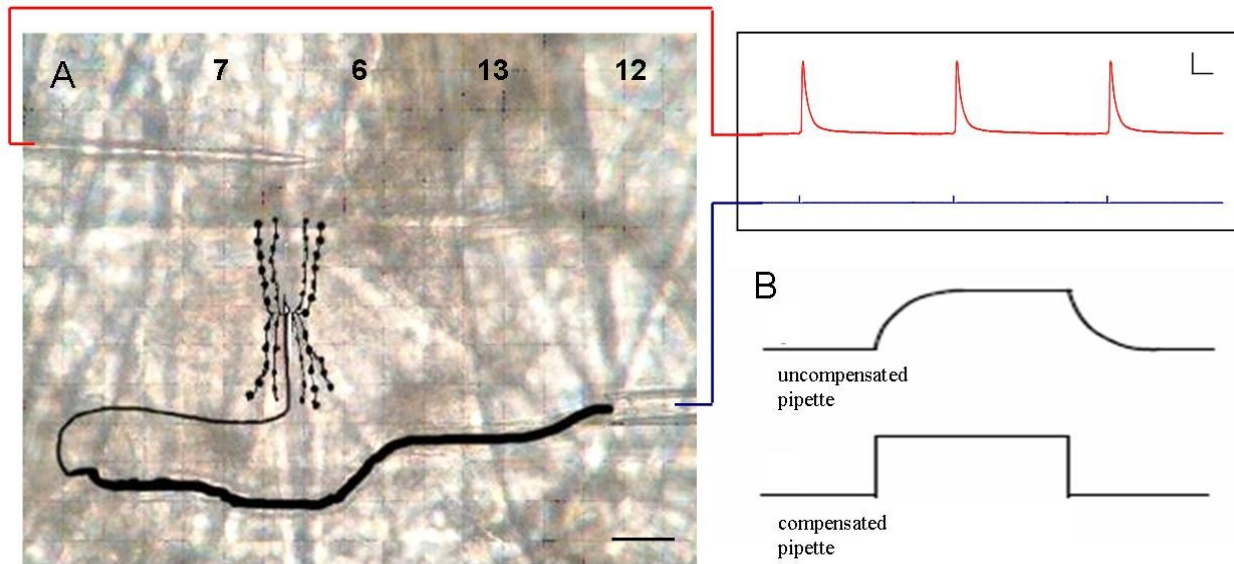


Figure 3-4. A. A microscope's view of the preparation. Stimulation of the motor nerves which innervate muscles 6 and 7 (black) is given via a stimulating pipette (bottom right, blue line). The change in membrane potential in the muscle fiber is measured with the recording electrode (top left, red line) scale bar is 50 μ M. B. Before performing any measurements, the capacitance of the recording electrode must be compensated.

3.1.6 Amplifier(s)

Most of the recordings for this thesis were done using an A-M Systems Neuroprobe 1600 amplifier (figure 3-5). The Neuroprobe 1600 consists of a high-input-impedance electrometer amplifier combined with current injection and balance circuitry (and therefore capable of simultaneous stimulation and recording through the same electrode). It has a digital panel meter which displays membrane potential, signal conditioning filters, and an internally-generated square wave current source for capacitance compensation and measuring electrode resistance.



Neuroprobe 1600



NPI TEC-05X

Figure 3-5. Neuroprobe 1600 from A-M Systems (Carlsborg, Wa) and the TEC-05X from NPI (Tamms, Germany).

The other amplifier is the considerably more sophisticated TEC-05X from NPI electronics (figure 3-5). The TEC-05X is a classical two electrode amplifier in that one headstage is strictly used for voltage measurements and the other for current injection. The TEC-05X is capable of performing recordings in current clamp, bridge, and voltage clamp modes. Current clamp recordings involve injecting a specific amount of current and then observing the resulting change in membrane potential. They can be thought of as simulating the current produced by synaptic inputs. Bridge recordings, on the other hand, utilize special compensation circuitry in the operational amplifier to compensate for the voltage drop across the recording pipette in a measurement. By generating a signal that is proportional to the product of the micropipette current and resistance, the signal can then be subtracted from the amplifier output and in this way, measurements of membrane voltage can be made (figure 3-6 A). The bridge mode gets its name from “the bridge balance technique” which in earlier times used a Wheatstone bridge (an array of resistors which can be used to measure an unknown resistance by balancing two legs of a bridge circuit) to compensate for the voltage change due to the recording pipette. The two electrode voltage clamp (TEVC) was first developed by Kenneth “Kacy” Cole in the 1940’s and was used by Alan Hodgkin and Andrew Huxley to determine the ionic basis of the action potential (despite Kacy’s invaluable contribution to the research for which Hodgkin and Huxley would later win the Nobel prize, his third of the prize would be given to Sir John Eccles). In TEVC recordings, one electrode (ME1) is used to measure the potential difference across the cell membrane. This electrode is connected to an operational amplifier which compares the signal to an arbitrary command voltage. Any difference between the command and measured voltage is immediately compensated by injecting current into the cell with the second electrode (ME2). The amount of current injected directly reflects the amount of current entering or leaving the cell (figure 3-6 B).

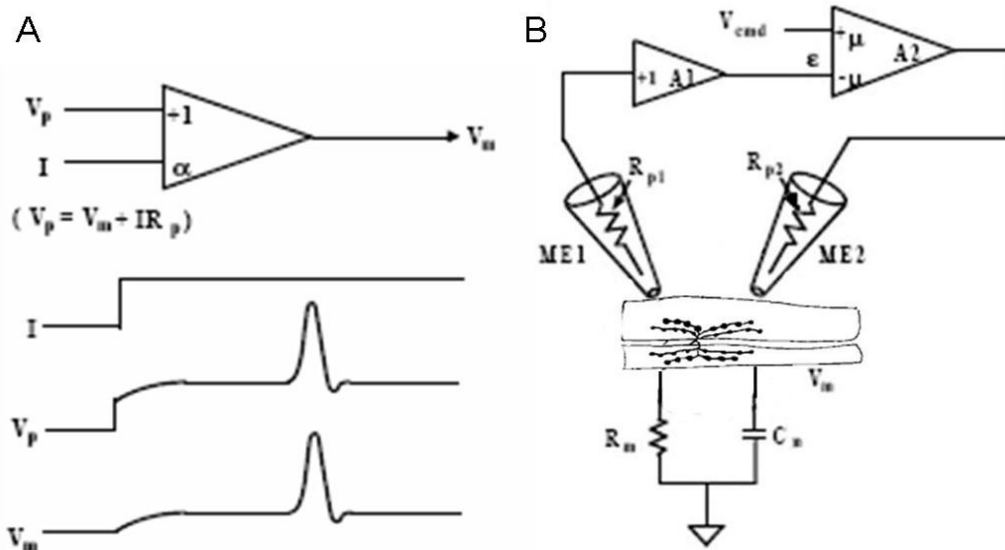


Figure 3-6. A. Compensating for pipette resistance using the bridge balance technique (modified from Axon guide). B. Schematic of the two electrode voltage clamp at the *Drosophila* neuromuscular junction (modified from Axon guide).

3.1.7 Acquisition

Signal acquisition was accomplished by using a data acquisition processor (DAP) 3200/315a from Microstar labs. The DAP is a complete microcomputer which occupies an expansion slot in a PC. It has an Intel i486 microprocessor with 4Mb of DRAM onboard memory, direct memory access controllers (DMA), digital to analog and analog to digital converters, and first-in first-out (FIFO) buffers to facilitate high speed data transfer (at rates up to 909K samples per second).

The DAP communicates with the computer via DAPL command prompt. DAPL differs from scripting and object-oriented languages in that it is not procedural or conditional. Instead DAPL commands specify configurations and relatively few immediate actions. This is accomplished by communicating tasks with buffered structures referred to as pipes. Pipes retain data using FIFO buffers in the DAP card until the required task(s) are performed. The DAPL programming structure also employs a “scheduling fairness” command, so that tasks which require more CPU do not exclude other tasks. Interactions with the DAP can also be accomplished using the graphical user interface based DAP Tools.

3.1.8 Analysis

Signals were generated and data was stored using DASylab, a modular programming environment optimized for data acquisition, process control, and system analysis. It utilizes the graphical interface provided by Microsoft Windows to create a workspace where modules with different functions can be connected to form virtual instruments. Individual module functions include A/D and D/A converters, signal generators, chart recorders, analog meters, digital filters, pre/post triggers, a variety of mathematical and statistical functions, as well as the ability to export data to other Microsoft applications. DASylab's remarkable versatility is only limited by the creativity (and proficiency) of the user. Recording worksheets were based on earlier designs from Dr.'s Christian Leibold and Dietmar Reisch (figure 3-7). Data was acquired at 10 kHz (two orders of magnitude greater than what would be predicted by the Nyquist–Shannon sampling theorem) using an RE Electronics computer with a 731MHz Pentium III processor and 256 MB RAM. When necessary, data was filtered at 1 or 5 kHz using a Bessel filter.

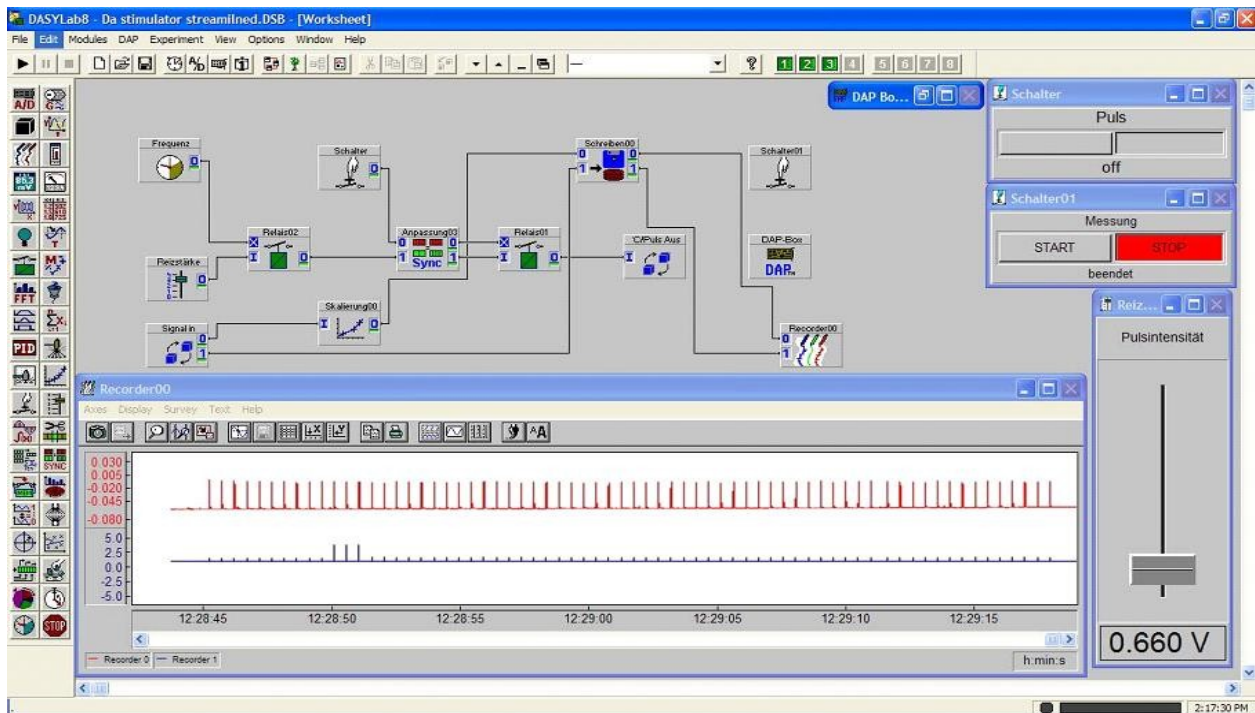


Figure 3-7. The DASylab virtual acquisition system. Pictured is a worksheet used for evoking and recording EJPs.

Data was initially analyzed by hand, using the cursor function in DASylab. However automated analysis was implemented in the interest of efficiency. For mEJPs, 1 minute bins of membrane voltage were analyzed with Mini Analysis (Synapsoft) (figure 3-8), using the following settings (obtained from Christoph Schuster's group): Threshold: 0.5; Period to search a local maximum: 35000 μ s; Time before a peak to search for baseline: 30000 μ s; Period to search a decay time: 35000 μ s; Fraction of peak to find a decay time: 0.1; Period to average a baseline: 4500 μ s; Area threshold: 3; Number of points to average for a peak: 5; Direction of peak: Positive. For EJPs, 60 consecutive EJPs evoked at 0.5 or 1 Hz were analyzed using a Fortran program. Values determined by the Fortran script were confirmed first by hand using the cursor function in DASylab and later with Mini Analysis. Average EJP amplitude values predicted by the script differed from Mini Analysis results by less than +/- 0.17 mV. Code used for the Fortran based analysis is listed in Appendix 1.

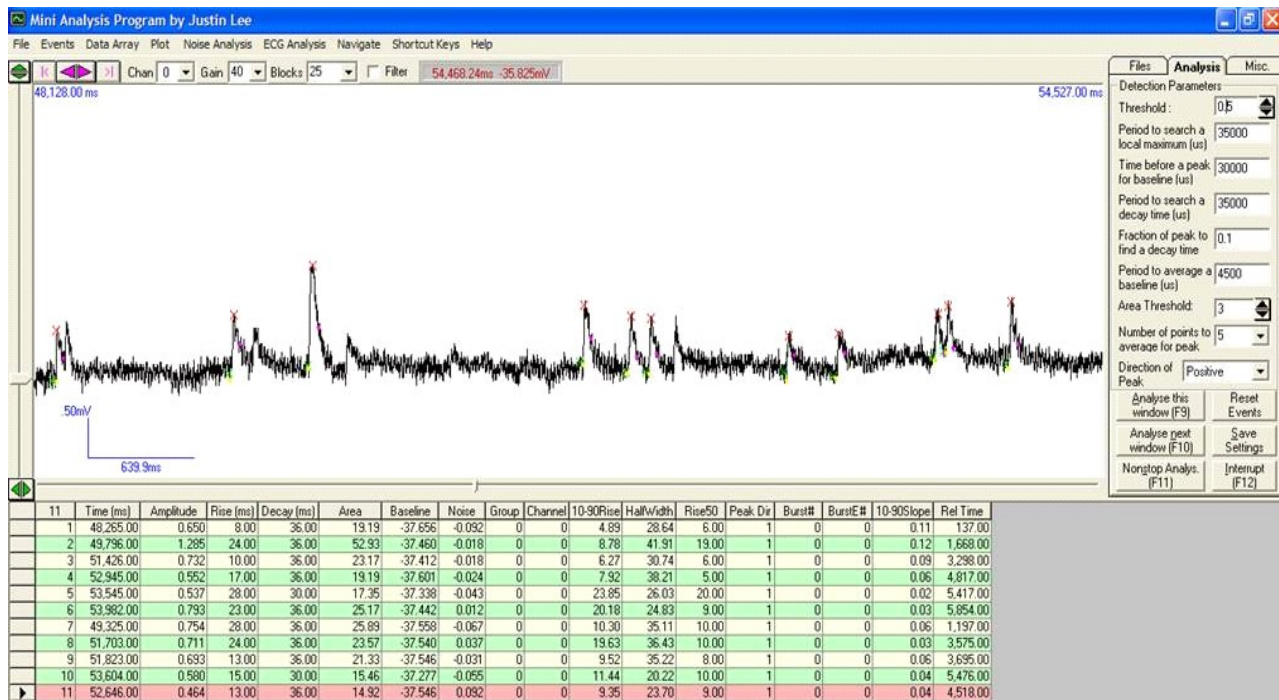


Figure 3-8. Mini Analysis was used for automated analysis of mEJPs.

3.2 Recording at the *Drosophila* neuromuscular junction

3.2.1 Solutions

Recordings were performed on third instar wandering larvae which were reared on cornmeal medium at 18 or 25 °C. Larvae were rinsed and dissected in hemolymph like ringers 3.1 without calcium (Stewart et al., 1994). After dissection the preparation was rinsed with HL3 ringers with 1mM calcium.

	Standard (mM)	HL3 (mM)	HL6 (mM)
CaCl ₂	1.8	1.0	0.5
MgCl ₂	4.0	20.0	15.0
KCl	2.0	5.0	24.8
NaCl	128.0	70.0	23.7
NaHCO ₃	—	10.0	10.0
Isothionic acid (Na ⁺)	—	—	20.0
BES	—	—	5.0
HEPES	5.0	10.0	—
Sucrose	35.5	115	—
Trehalose · 2H ₂ O	—	5.0	80.0
L-Alanine	—	—	5.7
L-Arginine · HCl	—	—	2.0
Glycine	—	—	14.5
L-Histidine	—	—	11.0
L-Methionine	—	—	1.7
L-Proline	—	—	13.0
L-Serine	—	—	2.3
L-Threonine	—	—	2.5
L-Tyrosine	—	—	1.4
L-Valine	—	—	1.0
Trolox*	—	—	1.0
TPEN*	—	—	0.0001
pH	7.3	7.3	7.2
Osmolality	300	343	341

Figure 3-9. Components of Standard, HL3, and HL6 ringers (Macleod et al., 2002).

3.2.2 Dissection

For measurements, a larva was pinned on the recording chamber using dissecting needles and an incision was made between the dorsal trachea. The gut and fat body were removed being careful not to damage the muscle fibers and motor nerves. Then the motor nerve fibers were severed at the ventral ganglion using a pair of micro dissection scissors and the brain was removed. In some preparations the motor nerves and ventral ganglion were left intact. Recordings were typically made in muscles 6 and 7 from segments A3 and A4. Occasionally recordings were performed in hemisegments A2 and A5 and also in muscle(s) 12, 13, 15, 16, and 17.

3.2.3 Recording techniques and criteria

If muscles in the appropriate hemisegment appeared healthy, then the stimulating and recording electrodes were positioned. In preliminary recordings a high frequency stimulus was given to the motor nerve unit to elicit a contraction to make sure the recording electrode would be properly placed. This practice was discontinued in subsequent recordings because it seemed to predispose the muscle fiber to contractions. One can easily tell when they are stimulating in one hemisegment and recording in another because of the decreased eEJP amplitude and the protracted rise and decay time constants (τ). Contractions are a major disadvantage of the *Drosophila* neuromuscular junction preparation. When a muscle fiber contracts with the recording electrode in it, it is usually best to replace the electrode and move to a different muscle fiber or contralateral hemisegment. Insertion of the recording electrode in the muscle fiber can be accomplished by simply pressing the capacitance override (or buzz) button on the amplifier which causes a feedback loop and the electrode begins to vibrate. Position of the recording electrode in relation to the presynaptic boutons is not important because of the high input resistance of the muscle fibers, which makes them effectively isopotential. (Wong et al., 1999).

Since there are two motor nerves which innervate muscles 6 and 7, it is important to be sure both are firing. Given the all or nothing nature of the action potential, it is required that nerve muscle “units” respond in a similar manner. A small current pulse should elicit an action potential in one of the two motor neurons. Further increasing the stimulus strength should lead to recruitment of both motor neurons. Typically one increases the stimulus strength by another 50 % once responses from both motor nerves have been obtained. In some preparations, signals from the two motor nerves do not summate exactly. Recordings which show improper temporal summation can be easily recognized and should be discarded because they lead to an underestimation of the evoked EJP amplitude.

Reports of EJP in the literature are variable, ranging from 20 to 75 mV in amplitude and between 100 and 250 ms in duration (Lnenicka and Keshishian, 2000, Verstreken et al., 2002). EJPs recorded on Lucille were around 35 mV in amplitude and lasted about 150 ms. Only muscle fibers which had resting potentials lower than -50 mV and input resistances less than 5 M Ω were used. Evoked EJPs were elicited with 0.1 ms pulses.

3.3 Immunohistochemistry at the *Drosophila* neuromuscular junction

3rd instar wandering larvae were dissected in HL3.1 (70 mM NaCl, 10 mM NaHCO₃, 115 mM Sucrose, 5 mM Trehalose, 5 mM KCl, 20 mM MgCl₂, 10 mM HEPES, pH 7.4). Larvae were pinned down and cut open between the dorsal trachea. The gut and fat body were removed in order to expose the muscles and nervous system. Preparations were fixed in 4% paraformaldehyde pH 7.4 for 1.5 hours on ice. Fixative was prepared as follows: 2 g paraformaldehyde and 25 ml H₂O were mixed for 5 minutes at 60°C. 100 µl of 1N NaHO was added and the solution was allowed to cool to room temperature. 20 ml of 2X PEM buffer (200 mM PIPES, 4 mM EGTA, 1 mM MgSO₄, pH 7.0) were added and the pH was checked. If pH was between 7.0 and 7.2 then another 5 ml of 2X PEM buffer was added. After fixation larval filets were washed 3 times for 15 minutes in PBST at room temperature. Unspecific bindings was blocked by incubating with blocking solution (2 % BSA, 5 % Normal Horse serum 0.2 % Triton in PBST) for 1 hour at room temperature. Incubation with the primary antibody was typically performed over night at 4°C. All primary antibodies used (nc82, nc46, 3C11) were diluted 1:100. Before incubation with the secondary antibody, unbound primary antibody was removed by washing with PBST (3 X 45 minutes) at room temperature. Incubation with secondary antibodies (goat α-mouse IgG Cy3, goat α-rabbit IgG Alexa488, or HRP-Cy3) was performed at room temperature in the dark for 1 h. Secondary antibodies were diluted 1:1000 in PBST. Then unbound secondary antibody was removed by washing in PBST for 4X 1h in the dark. In instances when a second primary was used (in serial antibody stains) preparations were blocked a second time for 1 hour at room temperature then washed and the second primary antibody was added. Preparations were embedded in Vectashield and Scans were performed on a Leica confocal laser scanning microscope and images were processed with Image J.

4. Results

4.1 *Sap-47*¹⁵⁶

*Sap-47*¹⁵⁶ null mutants were examined for morphologic as well as physiologic differences at the *Drosophila* larval neuromuscular junction. The monoclonal antibody nc82 which labels the active zone protein Bruchpilot was used to examine active zone number and distribution in *Sap-47*¹⁵⁶ null mutants and wild type (figure 4-1 A & B). Given the large number of anti mouse primary antibodies in the Buchner lab, we also attempted to develop a serial immunohistochemical staining protocol (in collaboration with Wiebke Hammers) so one could use multiple mouse monoclonal antibodies. The idea was to perform one round of staining with primary and secondary antibodies and then block and repeat with a second primary mouse monoclonal antibody. Different blocking protocols were used and in some instances appeared to work (figure 4-1 C & D) however repeated attempts with the same protocol did not yield reproducible results.

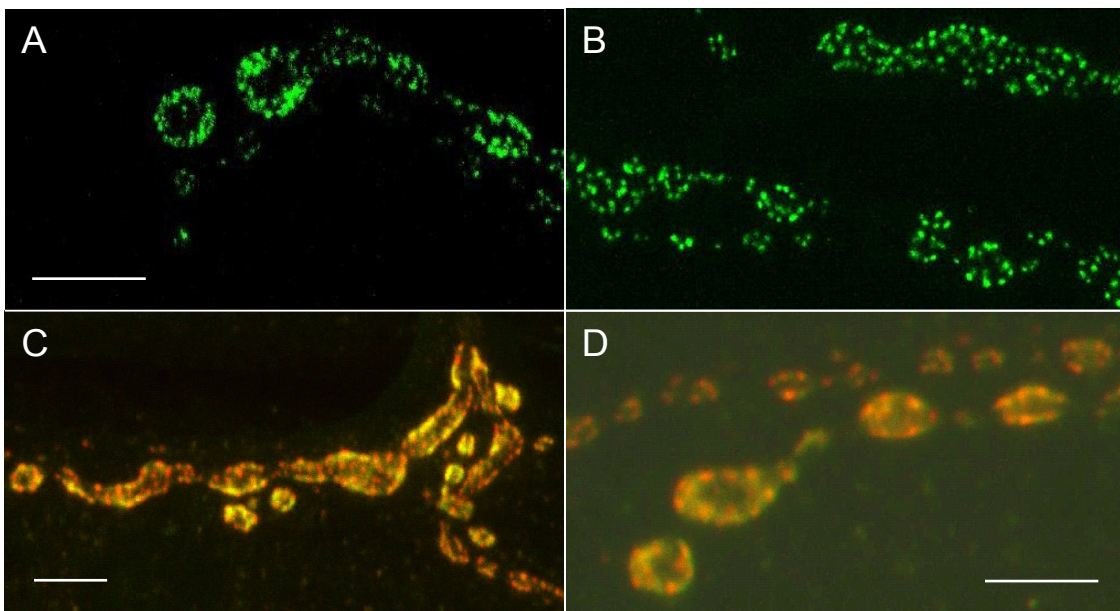


Figure 4-1. Active zone number and distribution was examined using nc82 stains in wild type (A) and *Sap-47*¹⁵⁶ null mutants (B). An example of a serial antibody stain that worked with nc46 (anti- SAP-47, alexa-488) and nc82 (anti-bruchpilot, cy-3) (C & D). Scale bars are 5 μ m in A, B, D, and 10 μ m in C.

Measurements to examine synaptic function were also performed at the larval neuromuscular junction. Evoked synaptic transmission was measured in wild type and *Sap-47*¹⁵⁶ null mutants under a variety of conditions. The parameters which were analyzed initially were amplitude (which was calculated by subtracting the membrane voltage at the peak of the EJP response from baseline) and EJP decay rate (which was the time it took the voltage signal to decay to 50% (time to decay or TD₅₀). After several rounds of experiments, it appeared as though *Sap-47*¹⁵⁶ null mutants might display a significantly decreased TD₅₀ (figure 4-2).

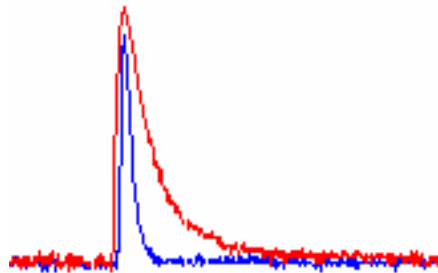


Figure 4-2. A possible preliminary synaptic phenotype in *Sap-47*¹⁵⁶ null mutant flies (red wild type, blue *Sap-47*¹⁵⁶).

In the literature, the duration of an EJP signal is 120 - 200 ms (Verstreken et al., 2002) however the duration of this decay can be affected by various electronic and physiologic parameters. Recording pipette size and resistance, depth of electrode penetration in the preparation, number of ion channels open on the muscle fiber (membrane resistance), and temporal summation of the signal from the two motor nerves are just some of the factors which could influence the duration of the EJP. Several experiments were performed which attempted to control for potential variability of the EJP signal. Recordings were made in the same muscle and hemisegment (muscle 6, hemisegments A3 or A4) and only units which showed perfect temporal summation were used. Fibers which displayed dramatic differences in input resistance (typical input resistances were around 5 M Ω) were not used for this analysis. The result of these experiments showed that in fact, there was no significant difference in EJP decay time in *Sap-47*¹⁵⁶ and wild type (wild type = 27.9 ± 3.3 ms and *Sap-47*¹⁵⁶ = 24.2 ± 3.5 ms; n = 11 and 12 respectively; P > 0.05).

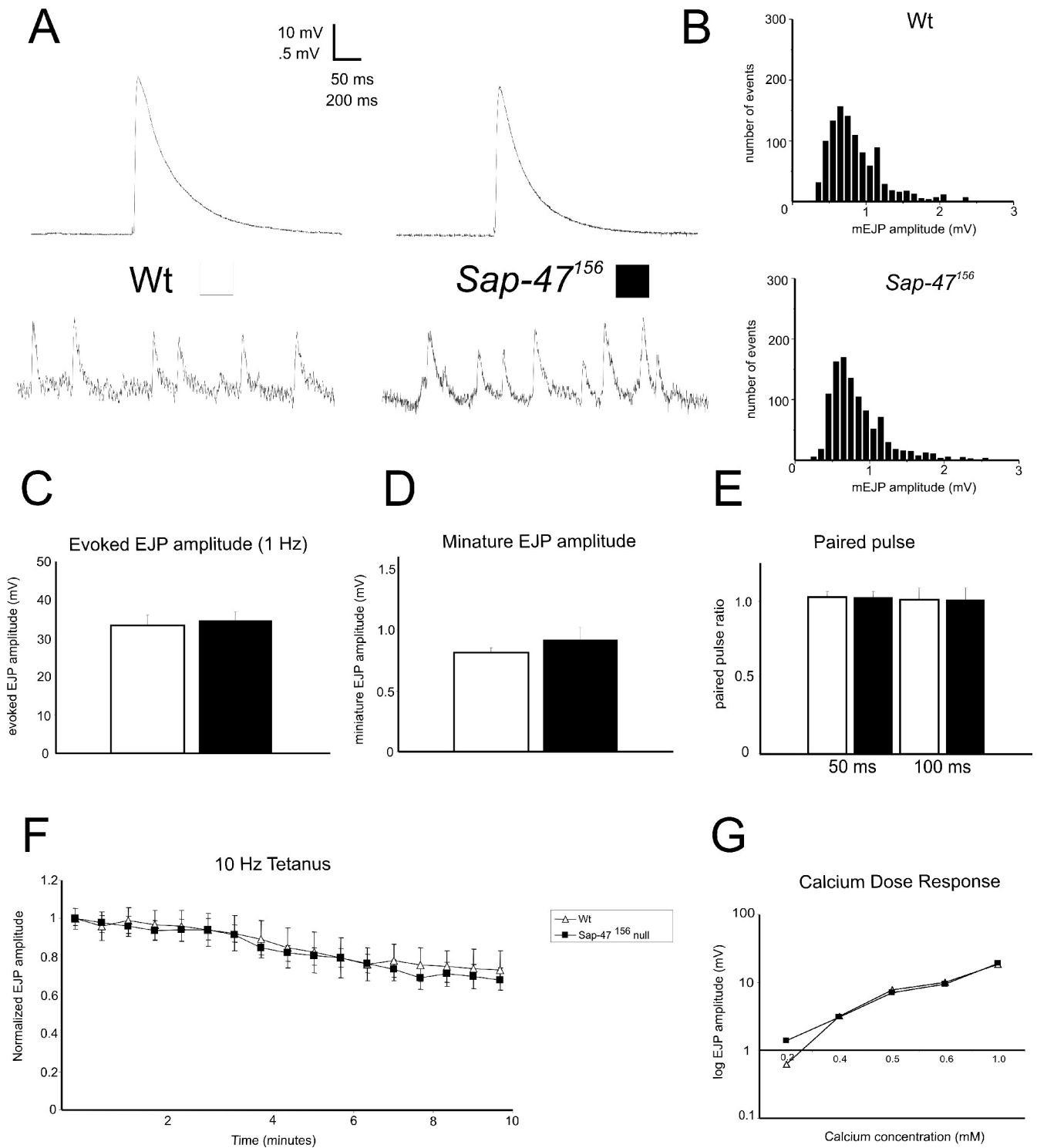


Figure 4-3. Electrophysiological characterization of *Sap-47*¹⁵⁶ null mutants. Evoked and miniature EJPs had similar amplitudes in wild type and *Sap-47*¹⁵⁶ null mutants (A, C, D). Miniature EJP amplitude frequency histograms (B), paired pulse (E), 10 Hz tetanus (F), and calcium dose response experiments (G) also appeared similar in wild type and *Sap-47*¹⁵⁶ null mutants.

The amplitudes of evoked EJPs at 1 Hz were also analyzed but no significant difference was observed (figure 4-3 A & C) (wild type = 34.8 ± 2.2 mV and *Sap-47*¹⁵⁶ = 33.4 ± 2.6 mV; n = 14, 13; p > 0.05). Further experiments were performed where the motor nerve was stimulated at a lower frequency. The thought was that a longer interval between evoked responses might allow the synapse to recuperate more completely. If the *Sap-47*¹⁵⁶ protein was involved in transporting vesicles between reserve and releasable pools, or to active zones, then a longer pause between stimulations might result in a difference in evoked EJP amplitude. Experiments at 0.05 Hz were conducted, however, no difference was observed (wild type = 22.2 ± 0.5 mV and *Sap-47*¹⁵⁶ = 23.9 ± 1.3 mV; n = 4).

Spontaneous miniature EJPs were analyzed in wild type and *Sap-47*¹⁵⁶ null mutants and the mean mEJP amplitude was found to be similar (figure 4-3 A & D) (wild type = 0.81 ± 0.04 mV and *Sap-47*¹⁵⁶ flies = 0.92 ± 0.1 mV; n = 11, 9; p > 0.05). A histogram comparing event amplitude (abscissa) and frequency (ordinate) was also made (figure 4-3 B). One can see that both amplitude event frequencies appear similar for wild type and *Sap-47*¹⁵⁶ flies and both display the expected Poisson distribution (Fatt and Katz, 1952, del Castillo and Katz, 1954). Quantal content was calculated by dividing mean evoked EJP amplitudes by mean miniature EJP amplitude and then correcting for non-linear summation (Martin, 1955). No significant difference between *Sap-47*¹⁵⁶ and wild type was found (116.2 ± 18 vesicles and 153.6 ± 28 vesicles; n = 10; p > 0.05).

High frequency synaptic transmission was examined in wild type and *Sap-47*¹⁵⁶ null mutant flies. In these experiments, the motor nerve unit was stimulated at 10 Hz for a duration of 10 minutes. Frequencies greater than 10 Hz were generally not used because the resulting calcium influx through postsynaptic receptors in the muscle cell caused the preparation to twitch. If the SAP-47 protein played an essential role in transporting vesicles between reserve pools or trafficking synaptic vesicles to active zones, one would likely see an effect on the amplitude of the evoked response in these experiments. Also, if the SAP-47 protein was involved in some aspect of synaptic vesicle recycling, one would likely see an effect with these experiments because of the high rates of vesicle turnover (assuming 50 to 100 vesicles released per action potential at 10 Hz for 600 seconds is 300,000 to 600,000 vesicles). If some aspect of synaptic vesicle fusion, transport, or recycling was compromised, one might expect to see a decrease in the evoked EJP amplitude over time. As one can see, the *Sap-47*¹⁵⁶ null mutant resembles

wild type in its response to a prolonged 10 Hz stimulus (figure 4-3 F) (wild type $n = 7$ and *Sap-47*¹⁵⁶ $n = 5$; $p > 0.05$).

Calcium plays an essential role as the electrochemical transducer at the synapse. Depolarization of the presynaptic terminal causes voltage-gated calcium channels to open, which allows calcium to enter into the cell at a rate which is dependent on the chemical driving force for calcium and the resting membrane potential of the cell. The amount of calcium that enters the cell directly determines the number of synaptic vesicles which will release their contents. By altering the amount of calcium in the extracellular bathing solution, one can effectively measure how many calcium ions are required for the release of one vesicle. If the SAP-47 protein functions as a calcium sensor or regulates synaptic vesicle exocytosis, one would expect to see an effect on the slope of calcium dose response curve. The calcium dose response curve for wild type and *Sap-47*¹⁵⁶ null mutants are effectively identical (figure 4-3 G) ($n = 2$).

Synaptic plasticity is thought to be important for learning and memory. A common experiment to test for a very basic form of synaptic plasticity is paired pulse experiments. By giving the motor nerve unit two consecutive pulses at 50 or 100 millisecond time intervals, one can test if the evoked EJPs get larger (facilitate) or smaller (depress). Whether or not a synapse facilitates or depresses is thought to be affected by the release probability P_r of a synapse (the probability that a synaptic vesicle docked at an active zone will release). After successive rounds of stimulation, typically intracellular calcium rises in the synaptic terminal. At a low release probability synapse, this activity dependent increase in intracellular calcium results in more vesicles releasing per action potential and therefore a facilitation of the synaptic signal. At a high release probability synapse, after successive rounds of stimulation, the level of intracellular calcium increases however the number of vesicles docked and ready for release at active zones is reduced because of activity and therefore the signal depresses (Millar et al., 2002). Interestingly, muscles 6 and 7 in *Drosophila* larvae are innervated by two physiologically and morphologically distinct motor neurons termed MN6/7-Ib (or RP3) and MNSNb/d-Is (Hoang and Chiba, 2001). The RP3 motor neuron has been shown to facilitate in response to 10 Hz stimulation while the MNSNb/d-Is motor neuron depresses (Lnenicka and Keshishian, 2000). Paired pulse experiments at the *Drosophila* muscle 6/7 synapse typically do not show any facilitation or depression (Ueda and Wu, 2006). The paired pulse ratio can be calculated by dividing the amplitude of the EJP

from the second pulse by the amplitude of the EJP from the first pulse. No marked difference in paired pulse facilitation or depression in wild type and *Sap-47*¹⁵⁶ null mutants was detected (figure 4-3 E) (n = 3). The preliminary characterization of *Sap-47*¹⁵⁶ is included in a manuscript by Saumweber et al.

4.2 Synapsin

Expression patterns of SAP-47 and Synapsin were examined at the *Drosophila* neuromuscular junction muscle 6 and 7 synapse immunohistochemically using the monoclonal antibody 3C11 (which recognizes Synapsin) and an anti-GFP antibody that recognized a UAS-SAP-47-GFP construct which was expressed in motor neurons using the Gal-4 D-42 driver. It is evident that the staining patterns for Synapsin and SAP-47 show a considerable overlap (figure 4-4).

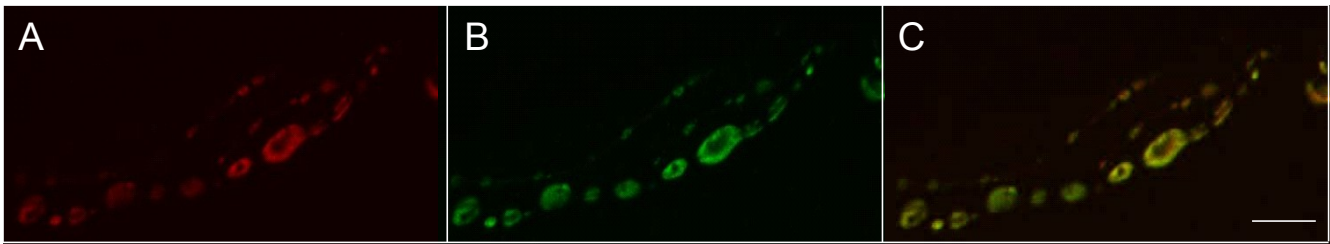


Figure 4-4. Monoclonal antibody stains of the *Drosophila* neuromuscular junction showing co-localization of SAP-47 and Synapsin. 3C11 and Cy-3 labeled Synapsin (A), a UAS-SAP-47-GFP construct (generated by Natalja Funk) driven with Gal-4 D-42 is labeled with an anti-GFP antibody and Alexa-488 (B) and the overlay which shows a similar expression pattern for SAP-47 and Synapsin (C), scale bar 5 μ m.

Synaptic transmission was measured in wild type and Synapsin null mutants (*Syn*⁹⁷) at the *Drosophila* neuromuscular junction. Evoked EJP amplitudes were not found to be significantly different (figure 4-5 A & B) (wild type = 33.1 ± 3 mV and *Syn*⁹⁷ = 34.3 ± 4.7 mV, n = 4). Miniature EJP amplitude (figure 4-5 C) (wild type = 0.86 ± 0.05 mV and *Syn*⁹⁷ = 0.91 ± 0.02 mV, n = 4) and quantal content (figure 4-5 D) (wild type = 154 ± 28 vesicles and *Syn*⁹⁷ = 127 ± 28 vesicles, n = 4) were also not found to significantly differ in wild type and *Syn*⁹⁷ mutants. High frequency (10 Hz) synaptic transmission in *Syn*⁹⁷ larvae was also similar to wild type (4-5 E) (n = 3).

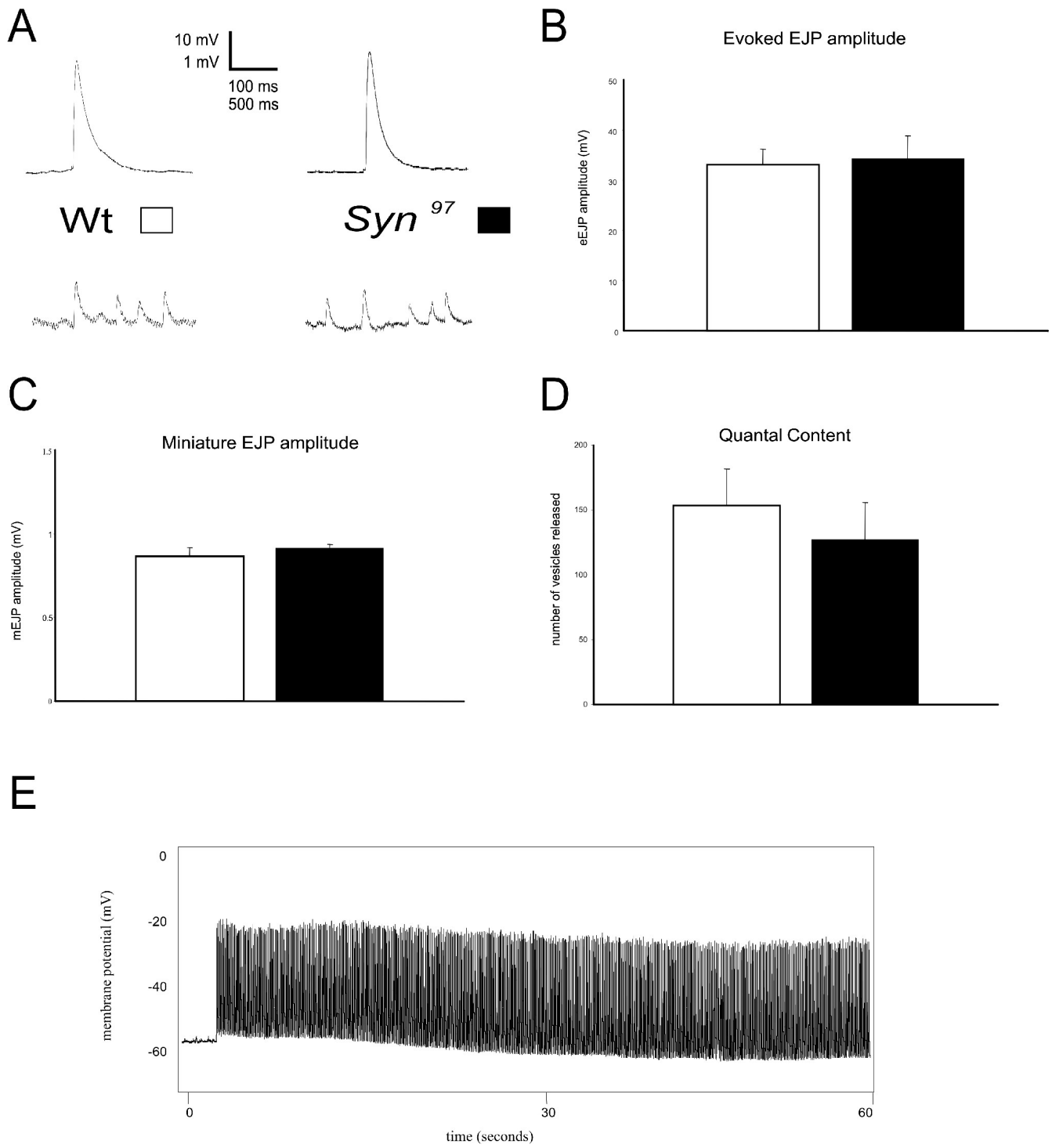


Figure 4-5. Electrophysiological characterization of *Syn*⁹⁷ null mutants. Evoked EJPs (A & B), mEJPs (A & C), quantal content (D), and 10 Hz synaptic transmission (E) appears normal in Synapsin null mutants.

4.3 Sap-47¹⁵⁶ Syn⁹⁷ double mutants

Synaptic transmission was analyzed in wild type and Sap-47¹⁵⁶ Syn⁹⁷ double mutant flies at the larval neuromuscular junction. Evoked EJPs appeared similar in wild type and *SapSyn^{SB} /SapSyn^{NF}* null mutant flies (figure 4-6 A & B) (wild type = 33.1 ± 3 mV and *SapSyn^{SB} /SapSyn^{NF}* = 34.2 ± 5.1 mV, n = 5; p > 0.05). Miniature EJP amplitude (figure 4-6 A & C) (wild type = 0.86 ± 0.05 mV and *SapSyn^{SB} /SapSyn^{NF}* = 0.90 ± 0.05 mV, n = 3) and quantal content (figure 4-6 D) (wild type = 154 ± 28 vesicles and *SapSyn^{SB} /SapSyn^{NF}* = 142 ± 28 vesicles, n = 3) are also similar. Experiments were also performed where the motor nerve was stimulated with a 10 Hz tetanus for 5 to 10 minutes (figure 4-6 E), however however high frequency synaptic transmission appeared normal. Evoked and miniature EJPs, as well as 10 Hz tetanus experiments, in *SapSyn^{VA}* and *SapSyn^{TN}* also appear normal (data not shown) suggesting that SAP-47 and Synapsin do not appear to be important for synaptic transmission under these experimental conditions.

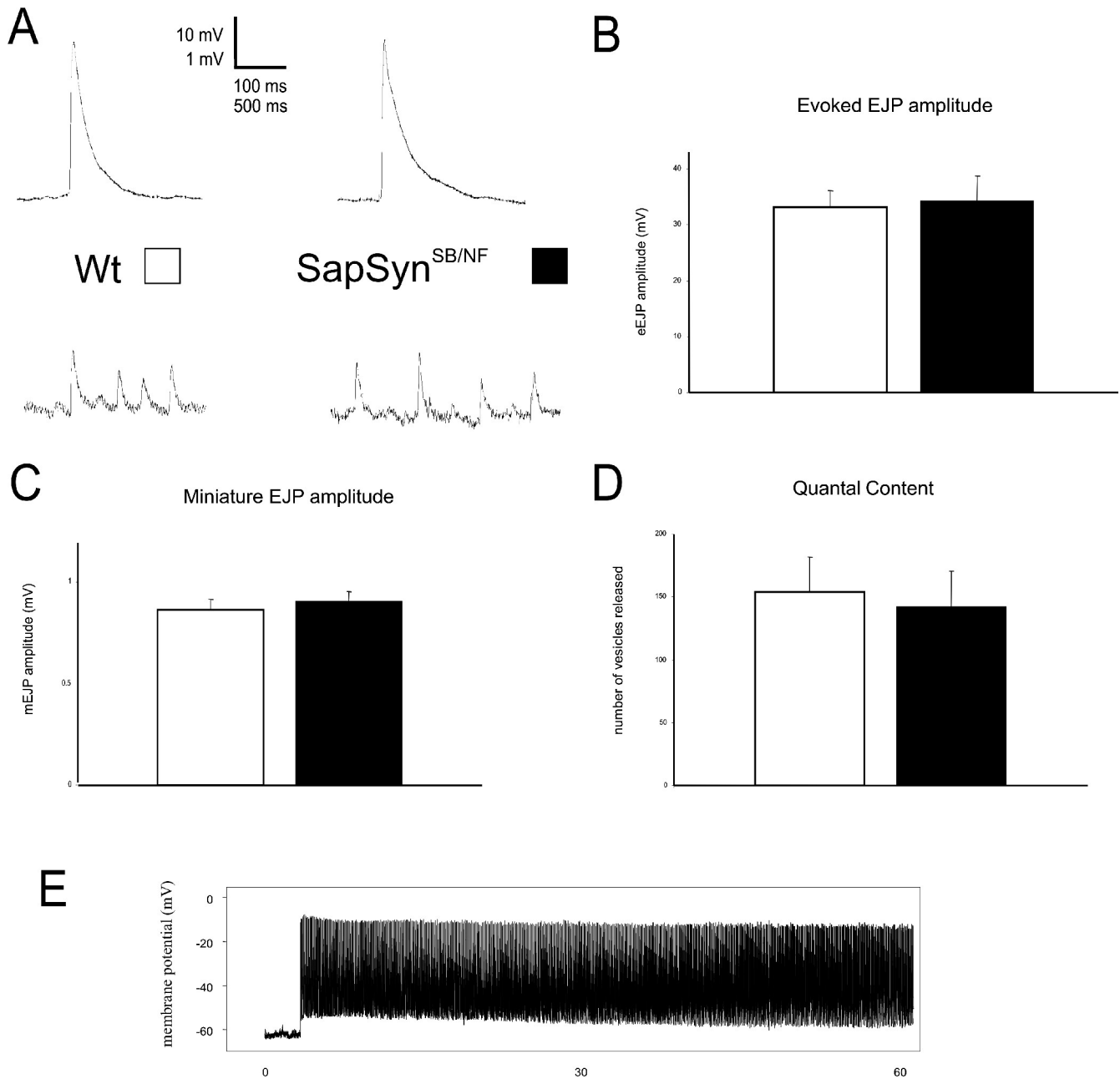


Figure 4-6. Electrophysiological characterization of *Sap-47¹⁵⁶ Syn⁹⁷* double mutants. Evoked EJPs (A & B), mEJPs (A & C), quantal content (D), and 10 Hz synaptic transmission (E) appears normal in *SapSyn^{SB}/SapSyn^{NF}* double mutants.

4.4 Serine-Arginine protein kinase 3

Since the SRPK3 line is not cantonized, measurements were compared with w^{1118} larvae as controls. Evoked EJP responses w^{1118} and SRPK3_{null} larvae did not display significantly different amplitudes (figure 4-7 A & E) ($w^{1118} = 34.2 \pm 4.0$ mV and SRPK3_{null} = 33.8 ± 3.7 mV; $n = 9, 7$; $p > 0.05$). Spontaneous single vesicle fusion events (mEJPs) had similar mean amplitudes, frequencies, and amplitude frequency distributions (figure 4-7 A, B, C, D) ($w^{1118} = 0.92 \pm .1$ mV and SRPK3_{null} = 0.92 ± 0.07 mV; $n = 8$; $p > 0.05$; $w^{1118} = 1.5 \pm 0.2$ Hz and SRPK3_{null} = 1.4 ± 0.2 Hz; $n = 8$; $p > 0.05$). Not surprisingly, quantal content was also not significantly different (figure 4-7 F) ($w^{1118} = 116 \pm 19$ vesicles and SRPK3_{null} = 119 ± 27 vesicles; $n = 8$; $p > 0.05$) suggesting that synaptic transmission in SRPK3_{null} mutants is normal under these conditions at the neuromuscular junction. This data is included in a manuscript by Nieratschker et al.

Synaptic transmission was also characterized in larva which over-expressed SRPK3 using a pan-neuronal ELAV driver line. Experiments were performed in 0.5, and 1 mM calcium however no difference in evoked response amplitude was observed at these concentrations in w^{1118} and SRPK3_{overexpression} larvae (figure 4-8 A & C) ($w^{1118} = 31.3 \pm 3.6$ mV and SRPK3_{overexpression} = 30.8 ± 2.8 mV; $n = 6$; $p > 0.05$). Minature EJPs showed similar mean amplitudes (figure 4-8 B) ($w^{1118} = 0.85 \pm 0.07$ mV and SRPK3_{overexpression} = 0.86 ± 0.15 mV; $n = 6$; $p > 0.05$) and quantal content (figure 4-8 D) ($w^{1118} = 107 \pm 19$ vesicles and SRPK3_{overexpression} = 109 ± 22 vesicles; $n = 6$; $p > 0.05$).

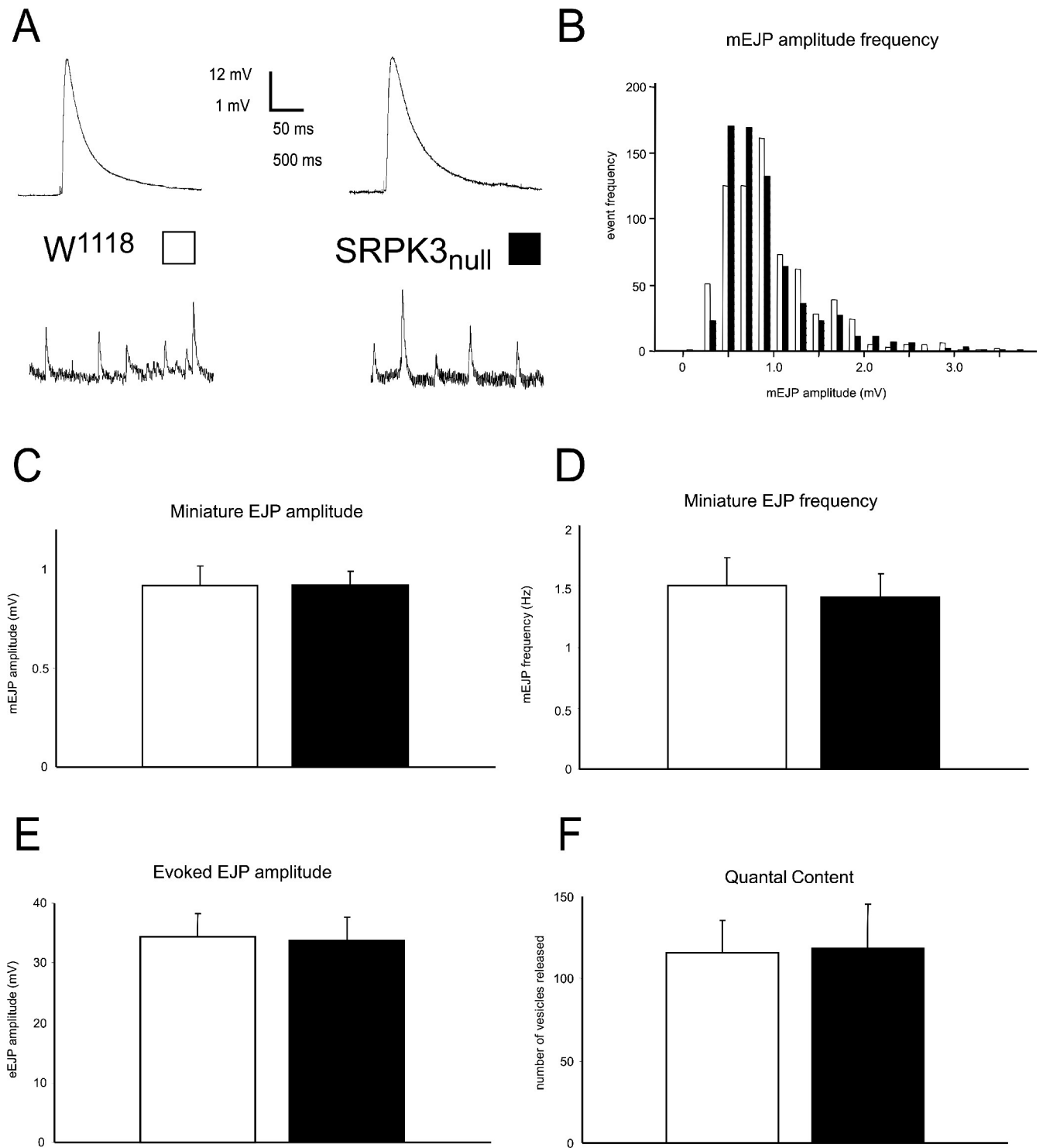


Figure 4-7. Electrophysiological characterization of w^{1118} and $SRPK3_{null}$ larva. Miniature EJP amplitude, frequency, and amplitude frequency distribution are similar in w^{1118} and $SRPK3_{null}$ larva (A, B, C, D). Evoked responses (E) and quantal content (F) are also not significantly different.

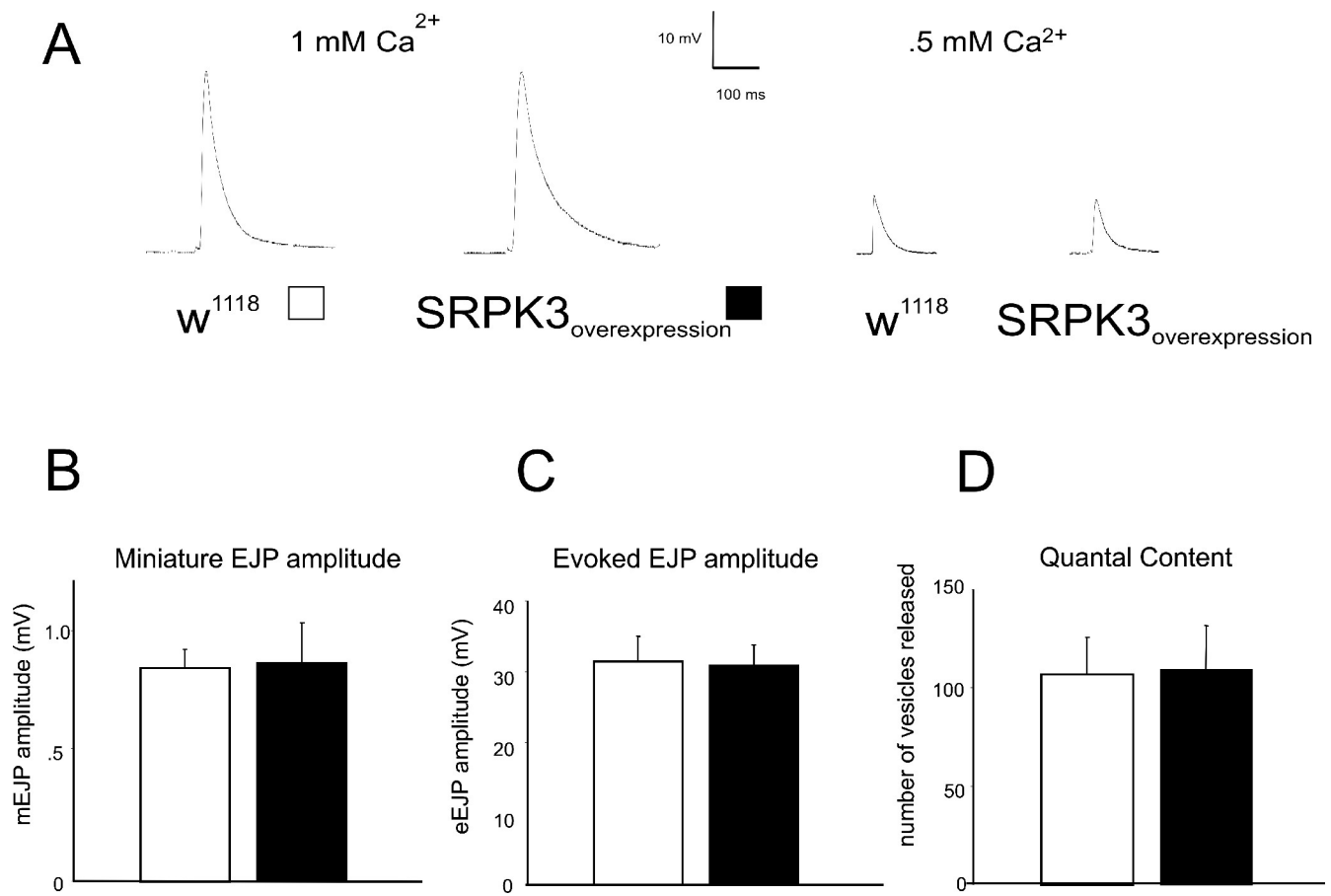


Figure 4-8. Electrophysiological characterization of w¹¹¹⁸ and SRPK3_{overexpression} larva. Evoked responses at 1 Hz were similar for w¹¹¹⁸ and SRPK3_{overexpression} larva in 1 and .5 mM calcium (A & C). Miniature EJP amplitude (B) and quantal content (D) were also not significantly different.

4.5 *Löchrig*

The morphology of presynaptic boutons which innervate muscles 6 and 7 was further investigated immunohistochemically in *Löchrig* mutants. Interestingly, the staining pattern of the presynaptic vesicle protein SAP-47 (nc46), as well as active zone number and distribution (nc82) (figure 4-9 A & D) appeared normal in *Loe* mutants. Stains of the neuronal membrane with an α -horseradish peroxidase antibody (which recognizes a Na-K ATPase) appeared different from wild type (figure 4-9 B & E). Boutons were fused and often had a drawn out appearance.

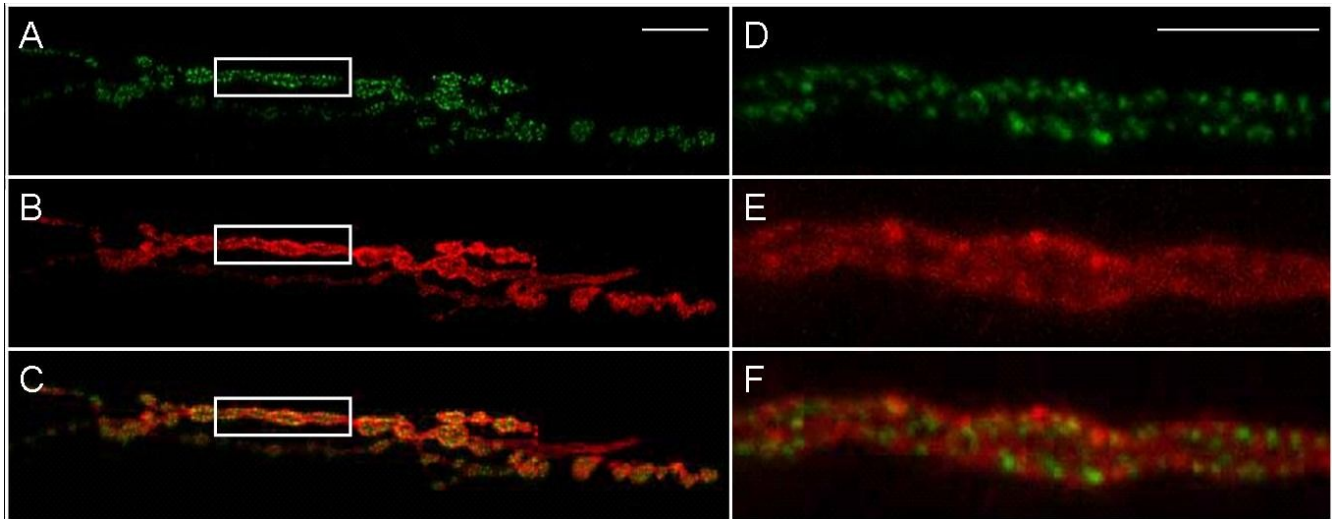


Figure 4-9. Morphological characterization of *Löchrig* presynaptic boutons. Stains with nc82 and Alexa 488 (A & D) and horseradish peroxidase-Cy3 (B & E), overlay (C & F), scale bars are 10 μ m in A, B, C and 5 μ m in D, E, F.

To determine if this difference in morphology resulted in, or reflected a defect in some aspect of synaptic function, synaptic transmission was measured at the neuromuscular junction. Evoked responses appeared similar to wild type (figure 4-10 A & C) (wild type = 25.2 ± 4.3 mV and *Loe* = 24.3 ± 2.3 mV, n = 4). Miniature EJP frequency was also found to be similar (figure 4-10 D) (wild type = 1.9 ± 0.8 Hz and *Loe* = 2.1 ± 0.9 mV, n = 9; $p > 0.05$) however the mean amplitude of miniature EJP responses was noticeably (although not significantly) larger in *Loe* mutants (figure 4-10 E) (wild type = 0.73 ± 0.16 mV and *Loe* = 0.97 ± 0.27 mV, n = 10; $p > 0.05$). When mEJP amplitude frequency histograms are plotted for wild type and *Loe* flies (figure 4-10 B), one sees a significant rightward shift

($p < 0.05$) in the distribution of *Löchrig* mutants, suggesting an increased frequency of larger mEJP events. Since intravesicular glutamate concentration is thought to be uniform in synaptic vesicles at the larval neuromuscular junction (Karunanithi et al., 2002) this suggests that the larger observed response could be due to larger synaptic vesicles. *Loe* flies were capable of maintaining a 10 Hz stimulus however showed an increase in normalized response amplitude ($n = 3$) when compared to wild type flies (figure 4-10 F). This evidence further supports the idea that *Löchrig* mutants may have larger than normal synaptic vesicles suggesting perhaps that vesicle recycling is impaired.

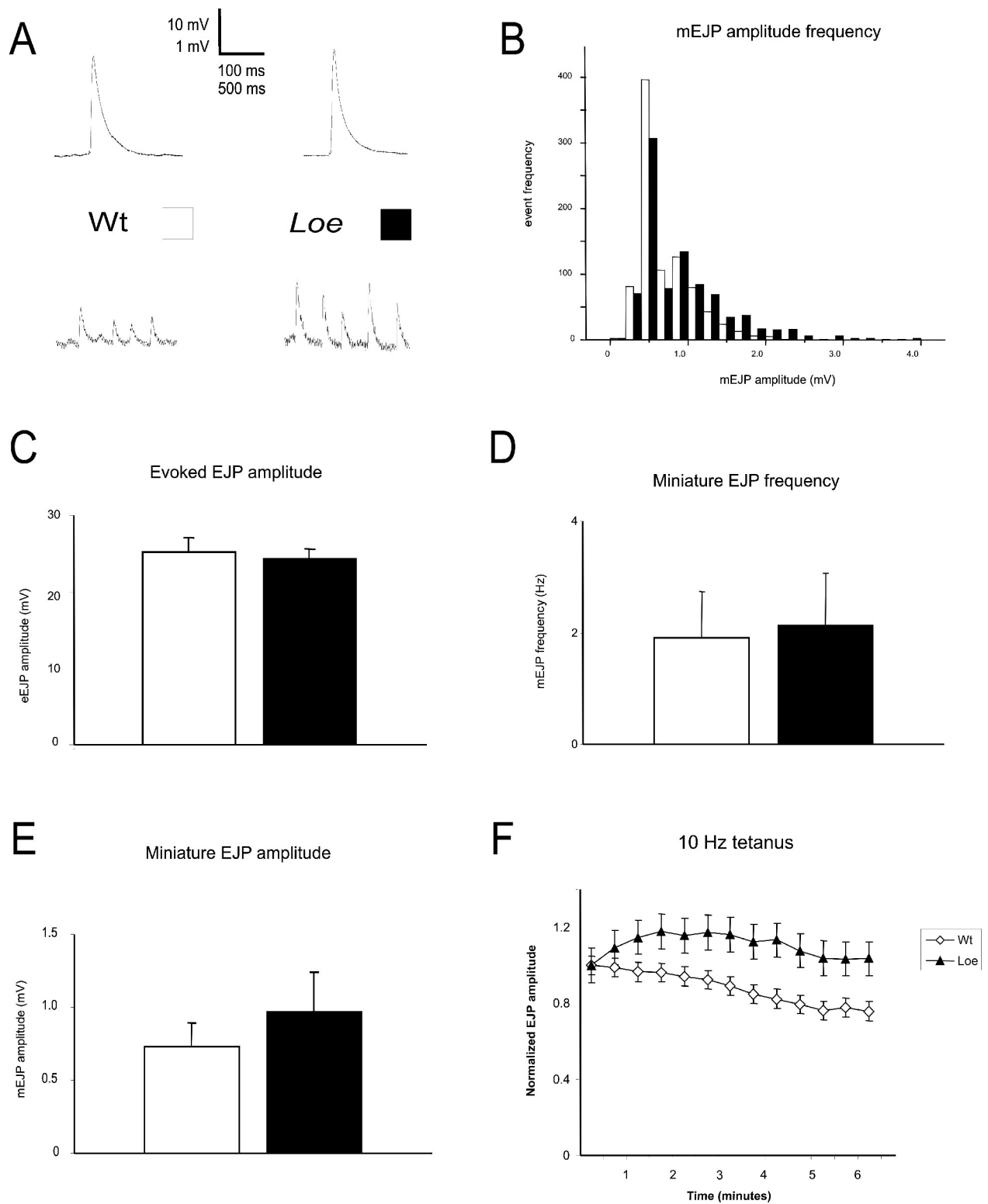


Figure 4-10. Electrophysiological characterization of *Löchrig* mutants. Evoked EJP amplitude (A & C) and mEJP frequency (D) are similar in wild type and *Loe* mutants. Miniature EJP amplitudes are not significantly different in wild type and *Loe* (E) however amplitude frequency histograms show a significant rightward shift in *Löchrig* mutants (B). 10 Hz experiments appear to facilitate more in *Loe* than in wild type (F).

4.6 Channelrhodopsin-2

Experiments looking at Channelrhodopsin-2 function were performed with the motor nerves left intact (still attached to the ventral ganglion). We expressed ChR2 in a subset of motor neurons using the Gal-4 promoter D-42. Recordings from larva expressing channelrhodopsin-2 were complicated because larva typically show light induced contractions (Schroll et al., 2006). Contraction of the larval muscle during a recording generally breaks the electrode and tears the muscle fiber leaving it unusable (see 3.2.3 Recording techniques and criteria) therefore a “tickling the dragons tail” approach was employed for recordings. Generally responses from single motor neurons were not sufficient to evoke contractions. For this reason, recordings were performed in muscles 15, 16, and 17, where single responses were frequently encountered. The observed mean resting potential was - 45.4 mV and the light evoked EJP amplitude was 5.8 ± 1.2 mV ($n = 7$) (Schroll et al., 2006). Light pulses of 100 milliseconds were sufficient to elicit single responses while longer light pulses resulted in sustained responses which had an average response frequency of 25 Hz. In stable preparations, repeated exposure of short or long light pulses evoked reproducible responses. Therefore, ChR2 can be used to manipulate neuronal activity in genetically defined subpopulations of neurons with relatively high temporal fidelity. These findings are part of a paper by Schroll et al., 2006 which demonstrates that ChR2 can be used to modulate aversive/appetitive learning by activating dopaminergic or octopaminergic and tyraminergetic neurons in *Drosophila* larva.

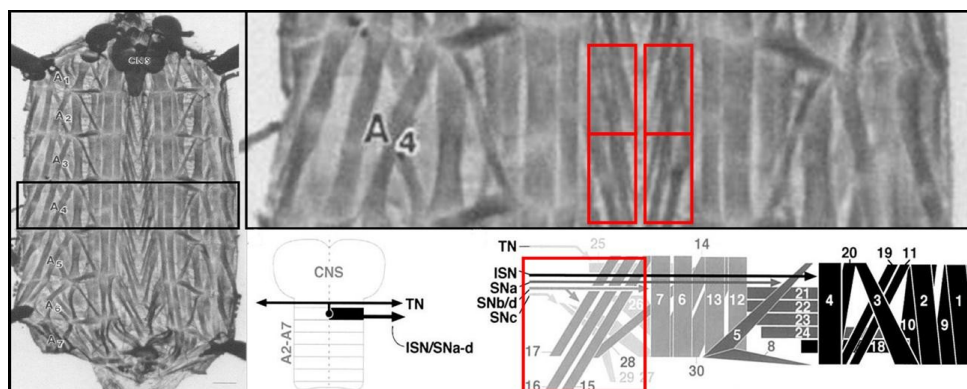


Figure 4-11. A prepared larva (Budnik and Wu 1990) with a close up of abdominal hemisegments A4. Recordings took place in muscle fibers 15, 16, and 17 which are outlined by the red boxes. The inlay on the bottom right shows the muscle fiber numbering scheme (Hoang and Chiba, 2001).

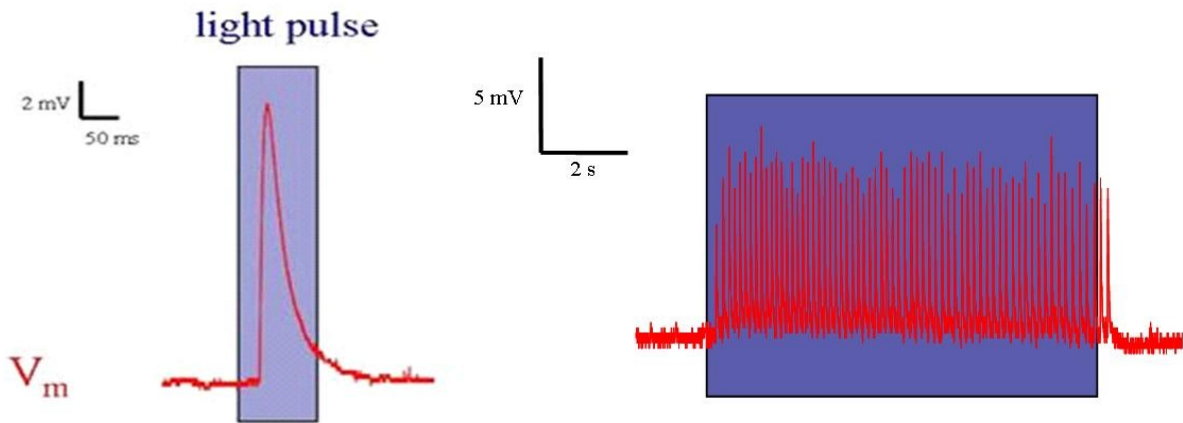


Figure 4-12. Short and long light exposures can elicit single responses or trains of EJPs when ChR2 is expressed at the *Drosophila* neuromuscular junction

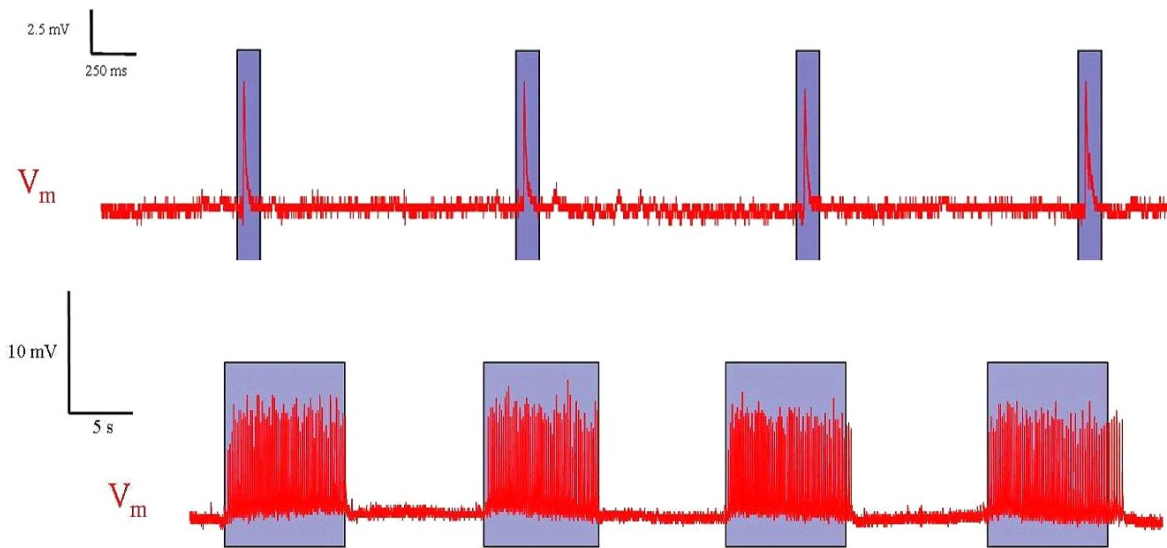


Figure 4-13. Short and long light pulses elicit reproducible responses in motor neurons expressing ChR2.

4.7 Photoactivated adenylate cyclase

Previous work at the *Drosophila* neuromuscular junction showed that mEJP frequency increased when intracellular cAMP levels were raised by stimulating adenylate cyclase with Forskolin or using the membrane permeable cAMP analog 4-chlorophenylthio-cAMP (Yoshihara et al., 2000) . We tested whether flies expressing PAC showed an increase in mEJP frequency after activating PAC with blue (480 nm) light. Voltage measurements were performed on flies which expressed PAC at the neuromuscular junction using the motor neuron specific driver line D-42 Gal-4 (Parkes et al., 1998).

Experiments were conducted as follows, one minute bins of resting membrane potential were taken before, during, and after stimulation with blue light. Traces were then analyzed for mean frequency before and after stimulation of PAC. Flies expressing PAC showed a significant increase in mEJP frequency after a 1 minute application of blue light (1.3 Hz before light application and 5.3 Hz after, $p < 0.001$, $n = 10$) compared to PAC without D-42 which showed no increase (figure 4-14 A & B).

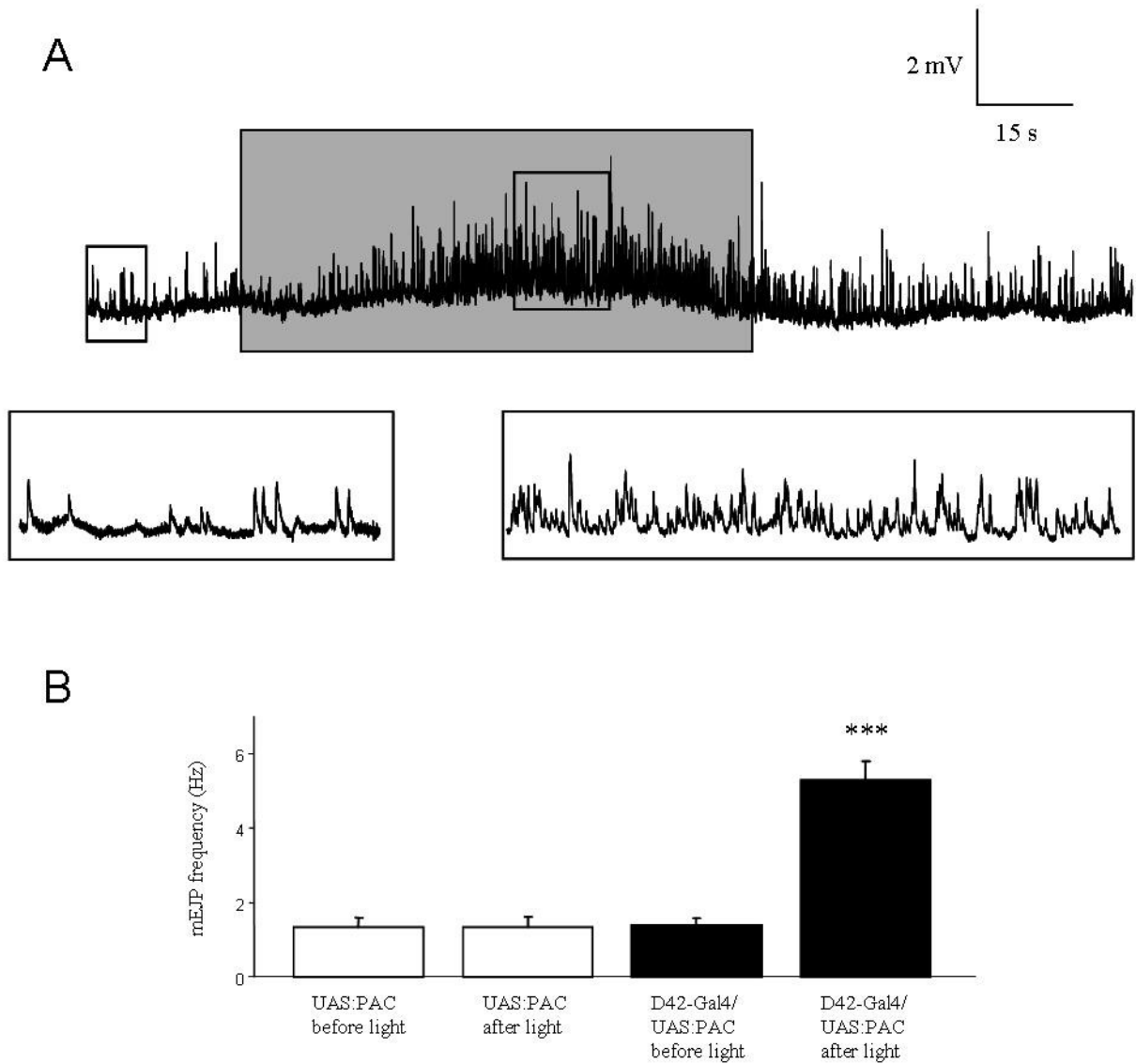


Figure 4-14. Stimulation of PAC with blue light (grey box) significantly increases mEJP frequency in cut motor neurons at the *Drosophila* larval neuromuscular junction in 1mM extracellular calcium ($p < 0.001$, $n = 10$) (A & B).

When experiments were performed in the absence of extracellular calcium, one minute stimulation of PAC with blue light also increased mEJP frequency (0.61 Hz before and 3.1 Hz after stimulation with blue light ($n = 5$, $p < 0.05$) (figure 4-15 A & B), albeit to a lesser extent than what was observed in 1 mM extracellular calcium. This calcium independent response is thought to act through a neuronal synaptobrevin (n-syb) dependent pathway (Yoshihara et al., 2000).

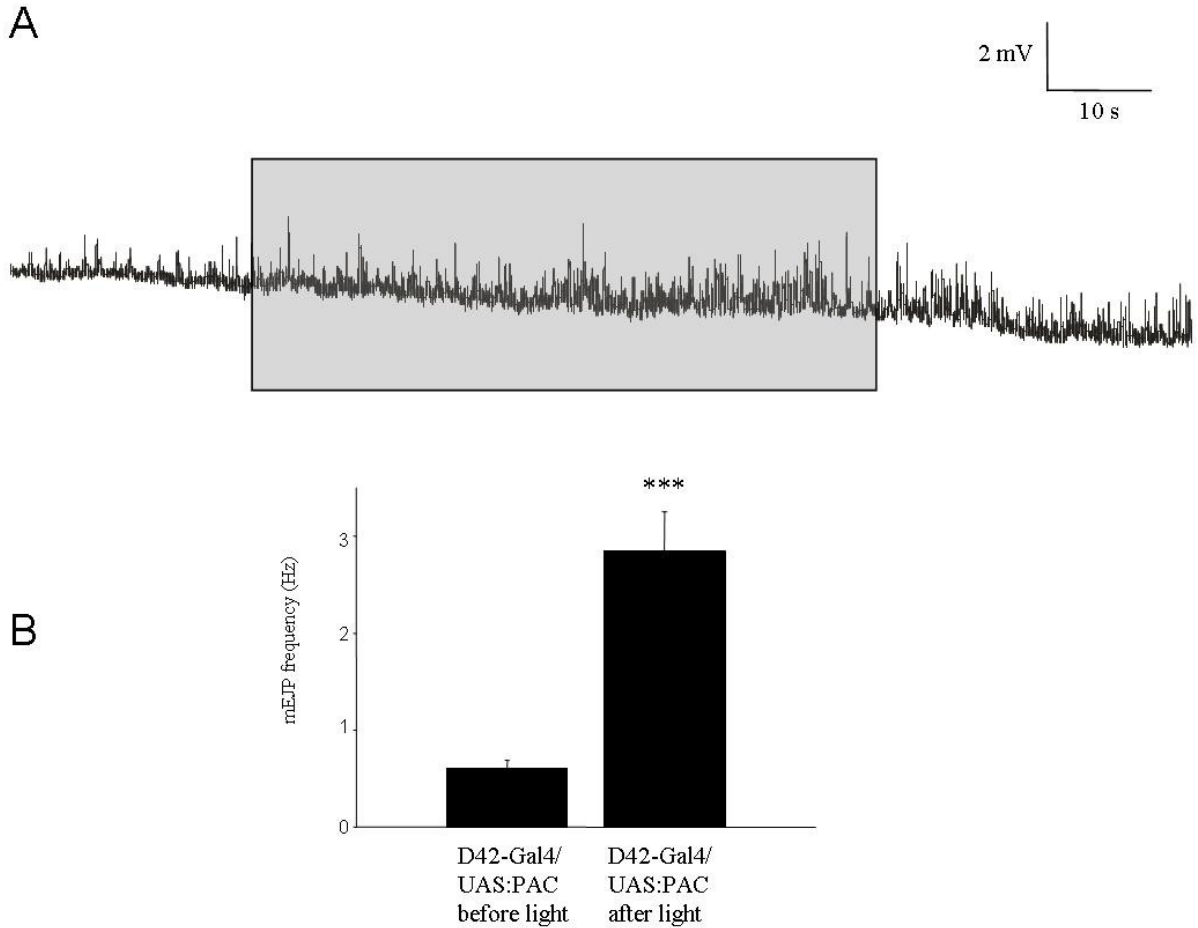


Figure 4-15. Stimulation of PAC (grey box) increases mEJP frequency in cut motor neurons in the absence of extracellular calcium ($p < 0.05$, $n = 5$) (A & B).

Increases in cAMP activate PKA which is thought to phosphorylate Synapsin (Ceccaldi et al., 1995). This results in a conformational change which allows reserve pool vesicles bound to the actin cytoskeleton to release and enter the cycling pool of vesicles. These reserve pool vesicles can be larger than normal synaptic vesicles (Steinert et al., 2006), therefore we compared mean mEJP amplitude before and after stimulation with blue light in 1 mM and also in the absence of extracellular calcium. No difference was observed in mean mEJP amplitude before and after stimulation of PAC under both conditions (Figure 4-16 A & B). There was also no change in the amplitude frequency distribution before and after PAC stimulation in the presence and absence of calcium (figure 4-16 C & D)

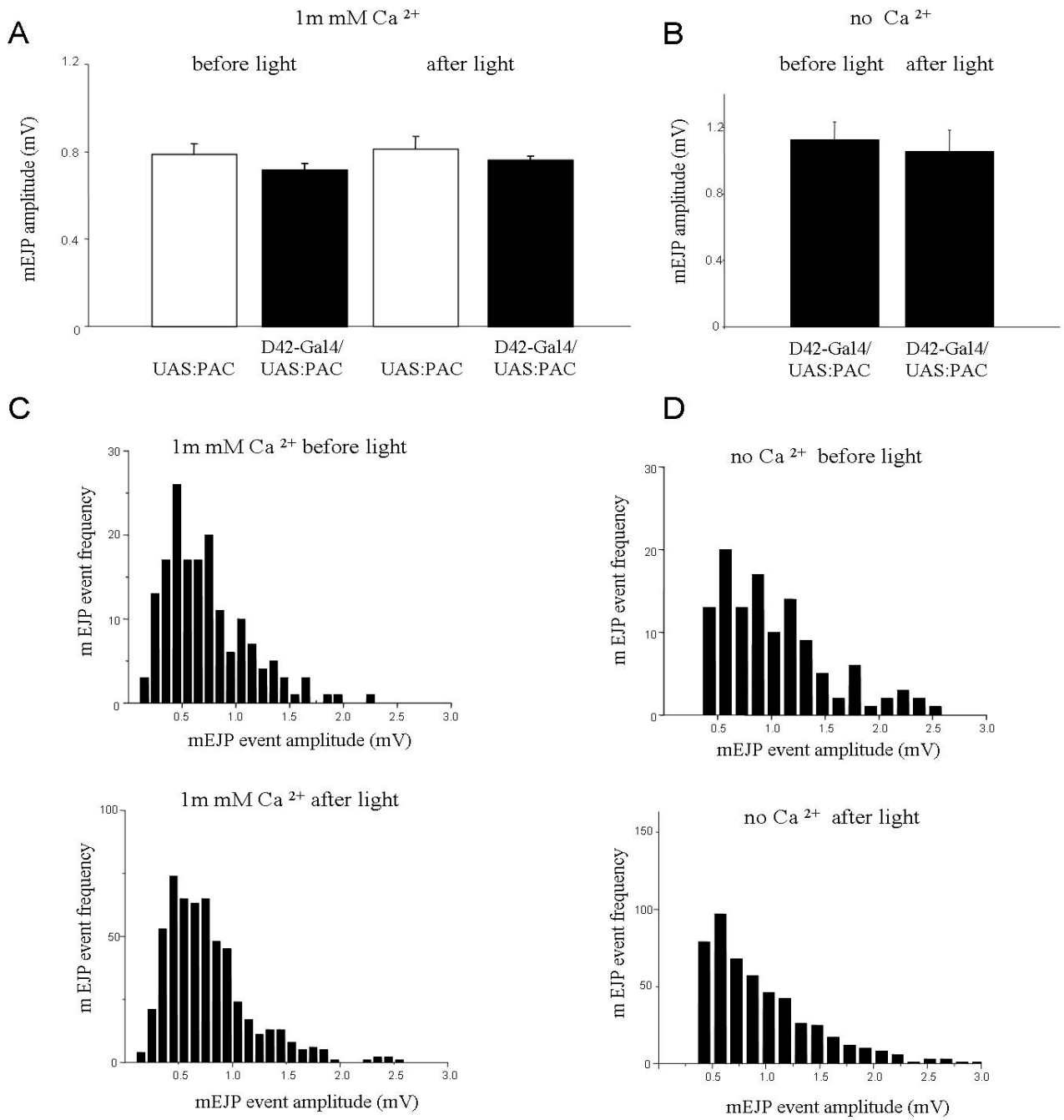


Figure 4-16. Mean mEJP amplitude (A & B) and frequency distribution (C & D) does not change after activation of PAC in 0 and 1 mM calcium (1mM calcium n = 10, no calcium n = 5, p > 0.05).

Further experiments to characterize PAC's effect on synaptic transmission were based directly on the previous electrophysiological characterization of *dunce* and *rutabaga* mutants (Zhong and Wu, 1991). They showed that under low release probability conditions (.2 mM extracellular Ca^{2+}) *rutabaga* flies (which should have low levels of cAMP) showed smaller EJC amplitudes compared to *dunce* mutants (which presumably have high levels of intracellular cAMP). EJPs were evoked at 8 Hz with a stimulating pipette in the absence and presence of blue light. Under these conditions, stimulation of PAC rapidly modifies synaptic transmission (figure 4-17).

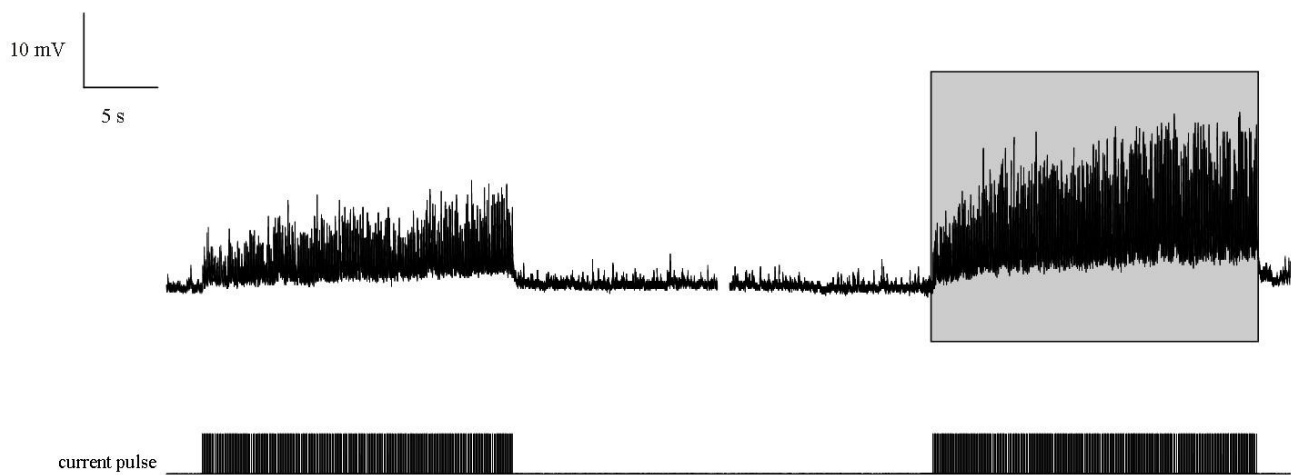


Figure 4-17. Stimulation of PAC can also acutely modify synaptic transmission under low release probability conditions.

Experiments were also performed with the motor neurons left intact and attached to the ventral ganglion and surprisingly, activation of PAC seems to result in motorneuron activity. We expressed a UAS-PAC constructs using two different motor nerve specific Gal-4 promoters, D-42 (Parkes et al., 1998) and Ok-6 (Petersen et al., 1997). Larva were dissected as described previously (Schroll et al., 2006) with motor nerves left intact and recordings were performed in muscles 6 and 7.

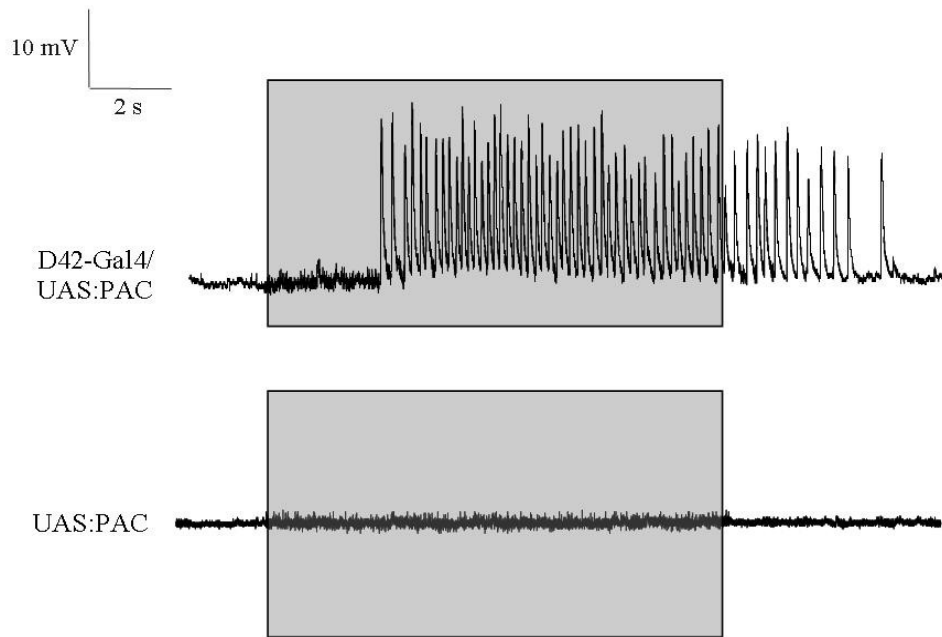


Figure 4-18. Application of blue light to intact motor neurons expressing PAC results in activity (grey box indicates light pulse).

Firing did not immediately follow onset of the 10 second light pulse (as seen previously with ChR2). Motor nerves expressing PAC with D-42 Gal-4 began to fire $3.2 \pm .9$ seconds after application of blue light with an average frequency of 12 ± 1.8 Hz and continued to fire 6.2 ± 2 seconds after cessation of the light stimulus ($n = 8$) (figure 4-18). Light evoked pulses had an average amplitude of 16.4 ± 4.6 mV suggesting that only one of the two motor nerves which innervate muscles 6 and 7 were firing.

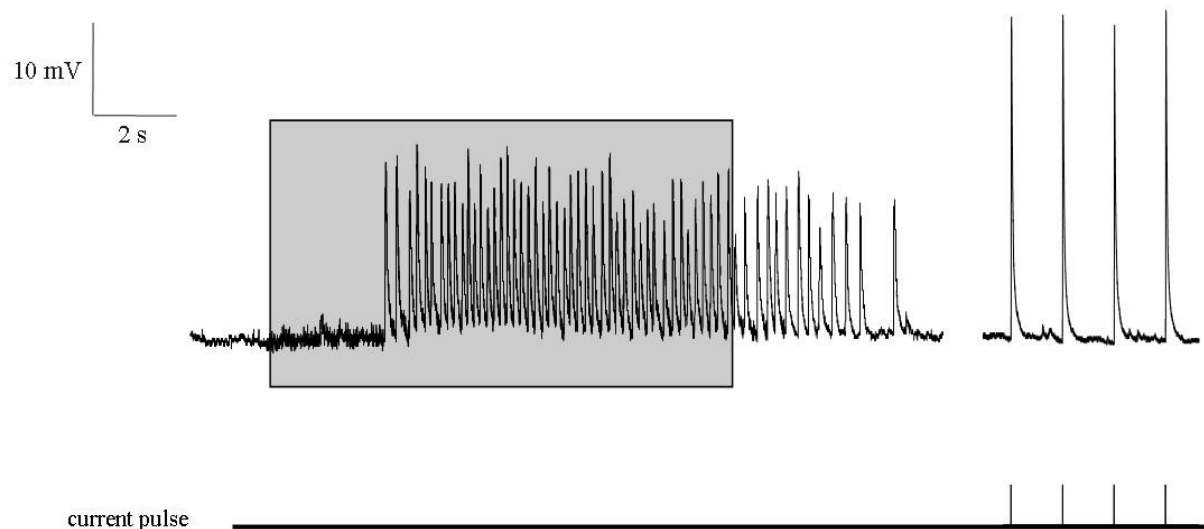


Figure 4-19. Stimulating PAC in intact motor neurons only stimulates one of the two motor neurons which innervate the muscle 6 and 7 synapse. Light stimulation is indicated by the grey box. The first four EJPs were evoked in the nerve motor unit, after the light induced response, with with a stimulating pipette. Given the amplitude of the evoked response, this suggests that only one of the two motor neurons are firing in response to PAC stimulation.

To confirm this, experiments were performed where first light evoked responses were recorded. Then motor nerves were cut from the ventral ganglion and responses were evoked in the same muscle fiber using a stimulating pipette (figure 4-19). Given the amplitude of the light evoked response, this suggests that only one of the two motor neurons which innervate muscles 6 and 7 (the MN 6/7-Ib and MSNb/d-Is motor neurons) is firing in response to increases in intracellular cAMP. When one compares this response, to the activity patterns of the MN 6/7-Ib and MSNb/d-Is motor neurons (Lnenicka and Keshishian, 2000) it appears that only the MN 6/7-Ib motor neuron is firing after stimulation of PAC (figure 4-20).

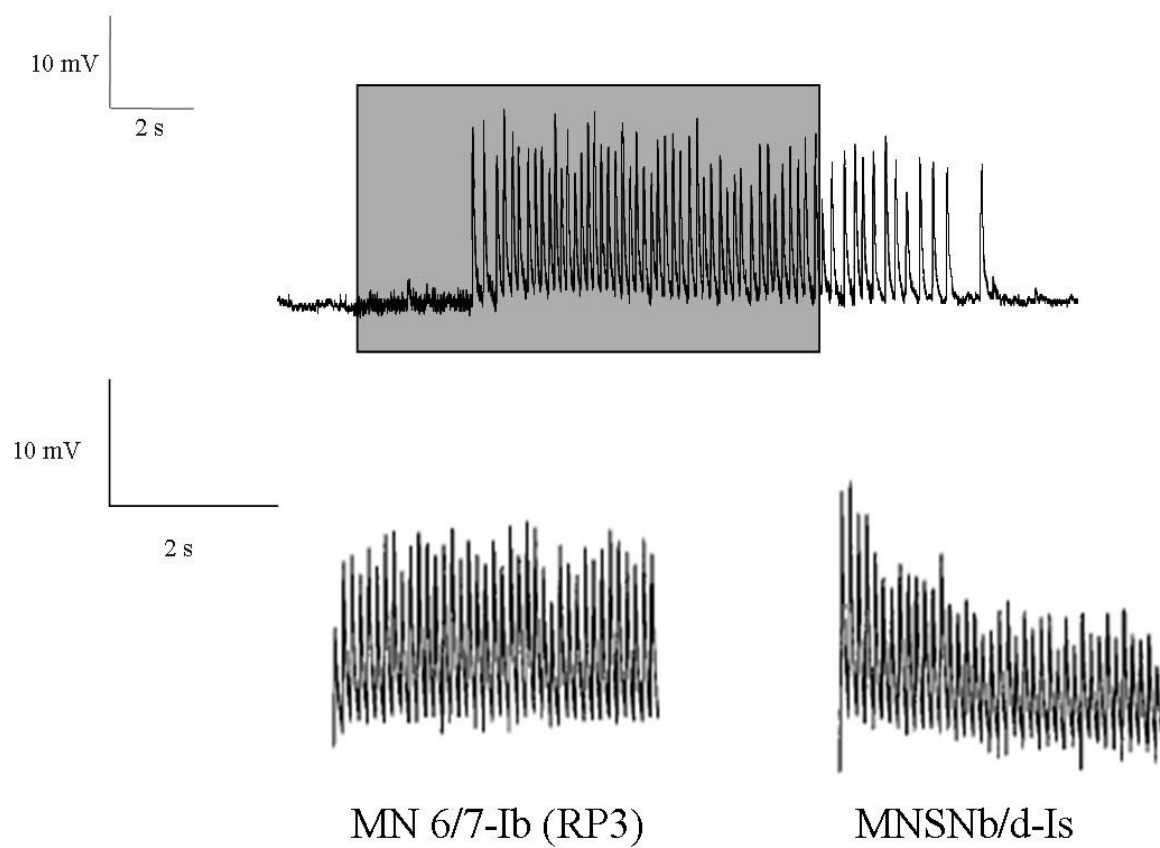


Figure 4-20. Light evoked responses in motor neurons expressing PAC appear to be due to activity in the MN6/7-Ib (RP3) motor neuron. Upper diagram is the same recording as in figure 4-19. Lower diagram: recordings showing the individual responses of the MN6/7-Ib and MNSNb/d-Is motor neurons to 10 Hz stimulation (Lnenicka and Keshishian, 2000).

5. Discussion

5.1 The potential Sap-47¹⁵⁶ phenotype

An inordinate amount of time and effort was spent attempting to determine if the *Sap-47*¹⁵⁶ null mutant EJP signal displayed a decreased decay time compared to wild type. With the observed decrease in associative olfactory learning it was tempting to speculate that a decrease in the duration of the synaptic signal would help explain this learning phenotype if one imagines associative learning to occur in an integrate and fire model. Consider the following example where the signals from two cells (which transmit the stimuli to be associated) overlap in the dendrites of the integrator cell. If *Sap-47*¹⁵⁶ null mutants because of a defect in synaptic transmission did display shorter evoked EJP (and also EPSP) decay times then the window of opportunity when the two signals could summate and initiate an action potential in the integrator cell would be shorter. This would have been a plausible cellular explanation for the observed decrease in olfactory associative learning observed in *Sap-47*¹⁵⁶ null mutant flies.

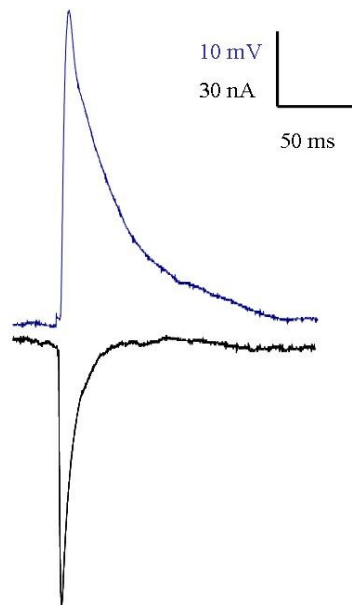


Figure 5-1. The time course of an EJP (blue) and an EJC (black). One can see that more than half of the duration of an EJP is due passive membrane properties (charging and discharging of the membrane capacitance).

With the advantage of hindsight, it is not surprising that no significant difference in the decay of evoked EJPs was observed between wild type and *Sap-47*¹⁵⁶ null mutant flies. Voltage decay measurements (TD₅₀) were highly variable from preparation to preparation because a voltage signal is heavily affected by passive membrane properties. An excitatory junctional current (EJC) typically lasts around 40 ms. The EJC is the amount of current which enters a muscle fiber through postsynaptic glutamate receptors. When one compares the time course of an EJC and an EJP (figure 5-1) it becomes apparent that the time course of the EJP signal is affected by other parameters.

The rise time can be represented by:

$$V(t) = V(1 - e^{-t/\tau})$$

The fall time can be represented by:

$$V(t) = V(e^{-t/\tau})$$

where $\tau = r_m c_m$

r_m = specific membrane resistance ($\Omega \text{ cm}^2$)

c_m = specific membrane capacitance ($\mu\text{F}/\text{cm}^2$)

The specific membrane capacitance for a lipid bilayer is approximately $1 \mu\text{F}/\text{cm}^2$ and is generally thought to remain constant, therefore, much of the variability in the voltage signal comes from the membrane resistance. Since R_m is simply the reciprocal of the conductance, the duration of the voltage signal is effected by the number of channels open on the cell surface and potentially by the size of the hole created by the recording electrode. Also, the number of voltage gated K channels present on the muscle fiber could effect the rate of EJP decay. It becomes apparent therefore that changes in EJP kinetics aren't necessarily a reliable parameter for comparison.

5.2 Null mutant data

A majority of the flies characterized in this thesis showed normal synaptic transmission at the neuromuscular junction, when specific synaptic proteins (SAP-47, Synapsin, SAP-47 Synapsin double mutant, and SRPK3) were deleted or overexpressed. If there was some disagreement in the different paired measurements this might have been grounds for concern however the data obtained is rather consistent. Mean mEJP amplitudes were measured for five different null mutant lines (plus wild type Canton-S and w^{1118}) and all mean values were all within one tenth of a millivolt. Mean evoked EJPs from the same seven lines were all within 2 mV. With such consistent responses it is likely that basic synaptic transmission was simply unaffected in these lines, however there are some explanations as to why no electrophysiological phenotype was observed.

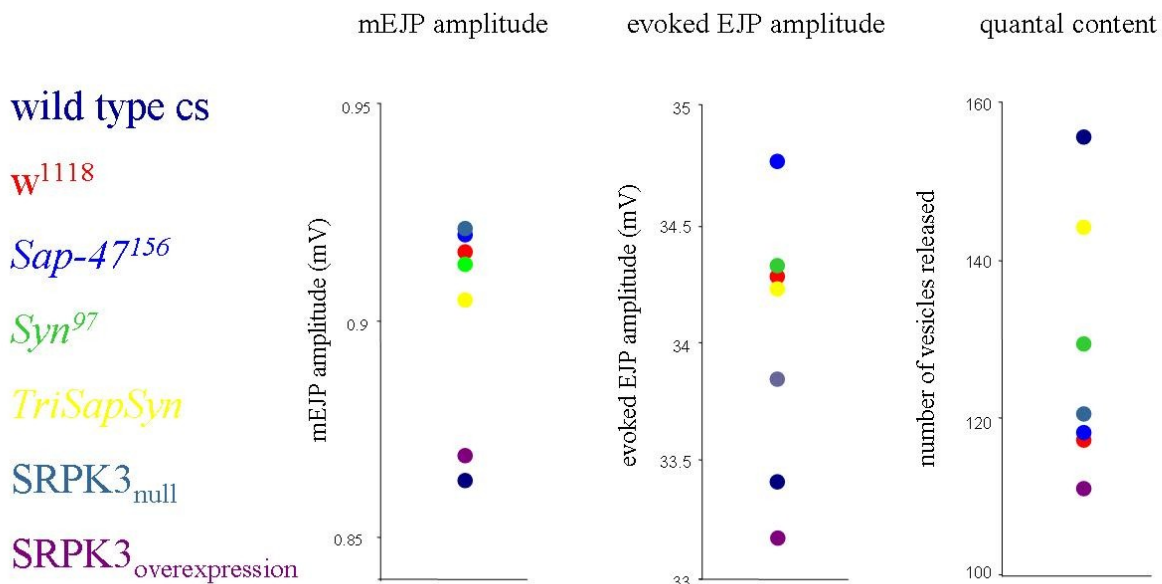


Figure 5-2. Mean mEJP, evoked EJP, and quantal content data for wild type-cs, w^{1118} , *Sap-47¹⁵⁶*, *Synapsin⁹⁷*, *Sap-47¹⁵⁶* *Synapsin⁹⁷* double mutant, *SRPK3_{null}*, and *SRPK3_{overexpression}*.

One explanation is that all the mutant lines which were characterized in this thesis were null mutants. This implies that the gene for the synaptic protein of interest was absent for the entire lifespan of the fly. In the course of development it is possible that compensatory changes could have taken place which offset any deficiencies which might have occurred because of the missing synaptic protein. Experiments using a heat shock RNAi line for the synaptic protein of interest which would acutely knock down expression of a gene could therefore control for any developmental compensation that might be taking place.

Another type of compensation which has been shown to occur at the *Drosophila* neuromuscular junction is a recently reported phenomenon known as synaptic homeostasis (Frank et al., 2006). Frank et al., showed that application of the glutamate receptor antagonist philanthotoxin-433 resulted in an increase in presynaptic neurotransmitter release, independent of protein synthesis and evoked transmission. This suggests that perhaps spontaneous release of synaptic vesicles may act like a cellular ping, checking to see that information transfer with the post synaptic receptive field is intact. It also shows that the magnitude of the presynaptic response can be modulated, presumably by altering the presynaptic calcium channel conductance or their proximity to active zones. If such a drastic modification of synaptic output occurs on the minute time scale in the absence of synaptic activity, this suggests that synapses are extremely dynamic structures. It is therefore not surprising that a presynaptic terminal can adapt in order to compensate for one or two missing synaptic proteins. Of course another possible explanation is that genetic safe guards have evolved to ensure that synapses can still function, even if certain synaptic proteins are missing. This type of physiologic redundancy is required when dealing with processes which are essential for the well being of the organism.

There is substantial evidence from behavioural experiments that deletion of Synapsin or SAP-47 proteins results in defects in associative learning in larvae and adult flies. Given Synapsin and SAP-47's close association to synaptic vesicles, these learning defects likely reflect impairment in some aspect of synaptic function or plasticity in neurons of the central brain. Another likely explanation for the lack of phenotypes at the neuromuscular junction is that neuromuscular synapses are very different from central synapses in *Drosophila*. Peripheral synapses are designed for synaptic transmission en masse, not cellular information processing, learning, and memory. The number of synaptic vesicles available for release is several orders of magnitude higher at the neuromuscular junction (around 80,000 vesicles) than at central synapses, which is thought to be around 20 to 30 vesicles per synapse

(Yasuyama et al., 2002). This is also the case for the number of active zones at central and peripheral synapses (ten or so compared to several thousand). If deletion of a synaptic protein did result in an alteration in some aspect of synaptic function, this difference might be more apparent at more refined central synapses whereas this difference would likely be obscured at the neuromuscular junction. Also, most central synapses in *Drosophila* are cholinergic (and GABAergic) however the neuromuscular junction is a glutamatergic synapse. It is not inconceivable that SAP-47 and Synapsin have different functions at glutamatergic and cholinergic presynaptic terminals. Synapsin for example has been shown to play different roles in vesicle cycling at excitatory and inhibitory synapses (Gitler et al., 2004).

5.3 A possible *Löchrig* phenotype

Of all the mutant lines characterized in this thesis, the most intriguing results came from *Löchrig* flies. *Loe* flies have a morphologic and physiologic phenotype at the neuromuscular junction that suggests that vesicle recycling is impaired in *Loe* flies. Evidence which supports this hypothesis comes from imaging data as well as electrophysiological measurements presented in this thesis.

Immunohistochemistry suggests that active zones (nc82) and various synaptic proteins (nc46, 3C11) appear normal in *Loe* flies, however, stainings of the presynaptic membrane are abnormal. Presynaptic boutons are typically round in wild type flies whereas *Löchrig* boutons have a more drawn out appearance. This is particularly interesting because experiments with the styryl dye FM1-43 suggest that the cycling pool of vesicles appears to be located at the bouton periphery at the neuromuscular junction (Kuromi and Kidokoro, 2000, 2003). Endocytosis at the neuromuscular junction is thought to occur at the periphery via clathrin lattice dependent bulk uptake of membrane at a rate of around 1,000 vesicles per second (Delgado et al., 2000). Mutations which disrupt different aspects of vesicle recycling generally result in larger quantal events (Verstreken et al., 2002, Koh et al., 2004). Since intravesicular glutamate concentration is thought to be homogenous in synaptic vesicles at the larval neuromuscular junction (Karunanithi et al., 2002) this suggests that the larger observed response is likely due to larger synaptic vesicles.

When *Löchrig* larva were characterized at the neuromuscular junction they also showed an increased mean mEJP amplitude. When an amplitude frequency distribution was plotted, mini events in *Loe* larvae showed a pronounced rightward shift compared to wild type, suggesting an increased frequency of large amplitude events. These results along with the morphology data are consistent with the hypothesis that *Loe* flies may have an impairment in synaptic vesicle recycling, however further characterization is necessary before an effect can be proven or discounted. EM experiments examining synaptic vesicle size must be performed to confirm that *Loe* larva do in fact have larger synaptic vesicles. Also, ideally real time vesicle cycling would be examined at the neuromuscular junction using FM1-43 (Kuromi and Kidokoro, 2000, 2003). *Loe* flies also need to be further characterized biochemically to see if circulating cholesterol levels in the brain were normal. Ideally “float assays” should also be performed to see if lipid rafts were disrupted in *Loe* flies. Further characterization of the *Löchrig* phenotype at the neuromuscular junction could provide interesting implications for the role of cholesterol (and possibly lipid rafts) in synaptic function and neurodegenerative disorders.

5.3 Heterologous expression of Channelrhodopsin-2 and PAC at the neuromuscular junction

The most interesting results obtained in this thesis came from the heterologous expression of light activated proteins at the neuromuscular junction. Light activated proteins are becoming a preferred method for noninvasive manipulation of activity in specific populations of neurons.

Channelrhodopsin-2 is especially well suited for precise temporal control of neuronal activity because of its unusually fast gating kinetics. Channelrhodopsin-2 can be easily expressed in different cell types and there is the possibility that one might be able to modify the channels photocycle (Bamann et al., 2007) so that ChR2 would open in response to light of a different wavelength. Already Channelrhodopsin-2 is being used to put to rest long standing disagreements as to how neurons encode, represent, and process information (Huber et al., 2008, Wang et al., 2007).

The PAC protein, in contrast to its ionotropic counter part ChR2, simulates activation of metabotropic pathways (specifically G α s). Stimulation of PAC at the *Drosophila* neuromuscular junction increases mEJP frequency in cut motor neurons. One minute pulses of blue light resulted in a significant increase in the number of mEJPs in 1 mM calcium. PAC also increase mEJP activity in the absence of extracellular calcium, presumably by acting through a synaptobrevin dependent pathway (Yoshihara et

al., 1999). The observed difference in mEJP frequency in the presence and absence of extracellular calcium is likely due to calcium entering the presynaptic terminal. This could occur via activation of presynaptic cyclic nucleotide gated ion channels (Cheung et al., 2006) which slightly depolarize the presynaptic terminal, thereby activating presynaptic voltage gated ion channels. Work by Steinert et al., 2006 suggested that sustained crawling activity causes an “experience-dependent formation and recruitment of large vesicles from the reserve pool”. We did not observe an increase in mEJP amplitude before and after stimulation of PAC which is consistent with what would be predicted with larva in lag phase however all experiments in this thesis were performed in the absence of crawling controls. Experiments looking at evoked activity in low calcium in the presence and absence of blue light showed similar results to previous work in *dunce* and *rutabaga* mutants (Zhong and Wu, 1991). Evoked response amplitude was increased when intracellular cAMP levels were raised (after stimulation of PAC or in *dunce* mutants). This is yet another instance where PAC stimulation gives a similar physiologic phenotype to previous genetic and pharmacologic interventions, further illustrating PAC's utility for determining the various functions cAMP has at the synapse.

Of course PAC's biggest advantages are the efficacy and specificity which comes from being a genetically encoded adenylate cyclase. Effects which take pharmacologic compounds almost a half an hour to evoke can be accomplished by stimulating PAC for a minute. Previous work with the adenylate cyclase agonist Forskolin, and the membrane permeable cAMP analogs dibutyryl cAMP and CPT cAMP, showed an increase in mEJP frequency at the *Drosophila* neuromuscular junction 20 to 30 minutes after application (Yoshihara et al., 1999) whereas this occurs after only one minute of PAC stimulation. PAC's ability to rapidly and specifically increase intracellular cAMP levels allows for unparalleled access for manipulating cAMP levels *in vivo*

As a closing comment, Craig Venters work sequencing the ocean metagenome has resulted in over 2000 proteins which contain rhodopsin like motifs (Yooseph et al., 2007), suggesting that more proteins which can be used for manipulating neuronal activity may be on the way. The *Drosophila* neuromuscular junction, because of its simplicity and accessibility, is an ideal model synapse for the characterization of proteins with optophysiologic potential.

6. References

Abbott L, Regehr W: Synaptic computation. *Nature* 2004, 14;431(7010):796-803.

Arnold C, Reisch N, Leibold C, Becker S, Prüfert K, Sautter K, Palm D, Jatzke S, Buchner S, Buchner E: Structure-function analysis of the cysteine string protein in *Drosophila*: cysteine string, linker and C terminus. *J Exp Biol* 2004, 207(8):1323-34.

Atwood HL, Karunanithi S: Diversification of synaptic strength: presynaptic elements. *Nat Rev Neurosci* 2002, 3(7): 497–516.

Ball R, Xing B, Bonner P, Shearer J, Cooper RL: Long-term *in vitro* maintenance of neuromuscular junction activity of *Drosophila* larvae. *Comp Biochem Physiol A Mol Integr Physiol* 2003, 134(2): 247-55.

Bamann C, Kirsch T, Nagel G, Bamberg E: Spectral characteristics of the photocycle of channelrhodopsin-2 and its implication for channel function. *J Mol Biol* 2008, 375(3):686-94.

Bekkers JM, Richerson GB, Stevens CF: Origin of variability in quantal size in cultured hippocampal neurons and hippocampal slices. *Proc Natl Acad* 1990, 87(14):5359-62.

Berke B, Wu CF: Regional calcium regulation within cultured *Drosophila* neurons: effects of altered cAMP metabolism by the learning mutations *dunce* and *rutabaga*. *J Neurosci* 2002, 1;22(11):4437-47.

Boyden ES, Zhang F, Bamberg E, Nagel G, Deisseroth K: Millisecond-timescale, genetically targeted optical control of neural activity. *Nat Neurosci* 2005, 8(9):1263-8.

Brand AH, Perrimon N: Targeted gene expression as a means of altering cell fates and generating dominant phenotypes. *Development* 1993, (118) 401-415.

Broadie K: Synapse scaffolding: intersection of endocytosis and growth. *Curr Biol* 2004, 5;14(19): 853-5.

Budnik V, Gramates L: Neuromuscular Junctions in *Drosophila*. *International Review of Neurobiology* 1999, Volume 43.

Budnik V, Zhong Y, Wu C: Morphological plasticity of motor axons in *Drosophila* mutants with altered excitability. *J Neurosci.* 1999, 10(11):3754-68.

Ceccaldi PE, Grohovaz F, Benfenati F, Chiergatti E, Greengard P, Valtorta F: Dephosphorylated synapsin I anchors synaptic vesicles to actin cytoskeleton: an analysis by videomicroscopy. *J Cell Biol.* 1995, 128(5):905-12.

Cheung U, Atwood HL, Zucker RS: Presynaptic effectors contributing to cAMP-induced synaptic potentiation in *Drosophila*. *J Neurobiol* 2006, 66(3):273-80.

Chi P, Greengard P, Ryan TA: Synaptic vesicle mobilization is regulated by distinct synapsin I phosphorylation pathways at different frequencies. *Neuron* 2003, 10;38(1):69-78.

Clements JD, Lester RA, Tong G, Jahr CE, Westbrook GL: The time course of glutamate in the synaptic cleft. *Science* 1992, 27;258(5087):1498-501.

Cohen S, Jurgens G: *Drosophila* headlines. *Trends Genet* 1991, 7(8):267-72.

Deák P, Omar MM, Saunders RD, Pál M, Komonyi O, Szidonya J, Maróy P, Zhang Y, Ashburner M, Benos P, Savakis C, Siden-Kiamos I, Louis C, Bolshakov VN, Kafatos FC, Madueno E, Modolell J, Glover DM: P-element insertion alleles of essential genes on the third chromosome of *Drosophila melanogaster*: correlation of physical and cytogenetic maps in chromosomal region 86E-87F. *Genetics*. 1997, 147(4):1697-722.

Del Castillo J, Katz B: Statistical factors involved in neuromuscular facilitation and depression. *J Physiol* 1954, 28;124(3):574-85.

Del Castillo J, Katz B: Quantal components of the end-plate potential. *J Physiol* 1954, 28;124(3): 560-73.

Delgado R, Maureira C, Oliva C, Kidokoro Y, Labarca P: Size of vesicle pools, rates of mobilization, and recycling at neuromuscular synapses of a *Drosophila* mutant, *shibire*. *Neuron* 2000, 28(3):941-53.

Dellinger B, Felling R, Ordway RW: Genetic modifiers of the *Drosophila* NSF mutant, *comatose*, include a temperature-sensitive paralytic allele of the calcium channel alpha1-subunit gene, *cacophony*. *Genetics* 2000, 155(1):203-11.

Diamond J, Jahr C: Transporters buffer synaptically released glutamate on a submillisecond time scale. *J Neurosci* 1997, 17(12):4672-87.

DiAntonio A, Petersen SA, Heckmann M, Goodman CS: Glutamate receptor expression regulates quantal size and quantal content at the *Drosophila* neuromuscular junction. *J Neurosci* 1999, 19(8): 3023-32.

Dickman DK, Horne JA, Meinertzhagen IA, Schwarz TL: A slowed classical pathway rather than kiss-and-run mediates endocytosis at synapses lacking synaptojanin and endophilin. *Cell* 2005, 4;123(3): 521-33.

Diegelmann S, Nieratschker V, Werner U, Hoppe J, Zars T, Buchner E: The conserved protein kinase-A target motif in synapsin of *Drosophila* is effectively modified by pre-mRNA editing. *BMC Neurosci* 2006, 14;7:76.

Dietschy JM, Turley SD: Cholesterol metabolism in the brain. *Curr Opin Lipidol* 2001, 12(2):105-12.

Doerks T, Huber S, Buchner E, Bork P: BSD: a novel domain in transcription factors and synapse-associated proteins. *Trends Biochem Sci* 2002, 27(4):168-70.

Dudel J, Kuffler S: The quantal nature of transmission and spontaneous miniature potentials at the crayfish neuromuscular junction. *J Physiol* 1961, 155:514-29.

Dudel J, Kuffler S: Presynaptic inhibition at the crayfish neuromuscular junction.

J Physiol, 1961, 155:543-62.

Dudel J, Kuffler S: Mechanism of facilitation at the crayfish neuromuscular junction. *J Physiol* 1961, 155:530-42.

Edwards. F: Anatomy and electrophysiology of fast central synapses lead to a structural model for long term potentiation. *Physiol. Rev* 1995, 64, 648-676.

Fatt P, Katz B: Spontaneous subthreshold activity at motor nerve endings. *J Physiol* 1952, 117, 109–128.

Feng J, Chi P, Blanpied TA, Xu Y, Magarinos AM, Ferreira A, Takahashi RH, Kao HT, McEwen BS, Ryan TA, Augustine GJ, Greengard P: Regulation of neurotransmitter release by synapsin III. *J Neurosci* 2002, 1;22(11):4372-80.

Flannery JG, Greenberg KP: Looking within for vision. *Neuron* 2006, 6;50(1):1-3.

Frank CA, Kennedy MJ, Goold CP, Marek KW, Davis GW: Mechanisms underlying the rapid induction and sustained expression of synaptic homeostasis. *Neuron* 2006, 22;52(4):663-77.

Funk N, Becker S, Huber S, Brunner M, Buchner E: Targeted mutagenesis of the Sap47 gene of *Drosophila*: flies lacking the synapse associated protein of 47 kDa are viable and fertile. *BMC Neurosci* 2004, 29;5(1):16.

Gitler D, Takagishi Y, Feng J, Ren Y, Rodriguiz RM, Wetsel WC, Greengard P, Augustine GJ: Different presynaptic roles of synapsins at excitatory and inhibitory synapses. *J Neurosci* 2004, 15;24(50):11368-80.

Godenschwege TA, Reisch D, Diegelmann S, Eberle K, Funk N, Heisenberg M, Hoppe V, Hoppe J, Klagges BR, Martin JR, Nikitina EA, Putz G, Reifegerste R, Reisch N, Rister J, Schaupp M, Scholz H, Schwarzel M, Werner U, Zars TD, Buchner S, Buchner E: Flies lacking all synapsins are unexpectedly healthy but are impaired in complex behaviour. *Eur J Neurosci* 2004, 20(3): 611-22.

Gorczyca M, Augart C, Budnik V: Insulin-like receptor and insulin-like peptide are localized at neuromuscular junctions in *Drosophila*. *J Neurosci* 1993, 13(9):3692-704.

Gray E, Guillery R: Synaptic morphology in the normal and degenerating nervous system. *Int Rev Cytol* 1966, 19:111-82.

Grigliatti T, Hall L, Rosenbluth R, Suzuki D: Temperature-sensitive mutations in *Drosophila melanogaster*. XIV. A selection of immobile adults. *Mol Gen Genet* 1973, 24;120(2):107-14.

Guerrero G, Reiff DF, Agarwal G, Ball RW, Borst A, Goodman CS, Isacoff EY: Heterogeneity in synaptic transmission along a *Drosophila* larval motor axon. *Nat Neurosci* 2005, 8(9):1188-96.

Halpern ME, Chiba A, Johansen J, Keshishian H: Growth cone behavior underlying the development of stereotypic synaptic connections in *Drosophila* embryos. *J Neurosci* 1991, 11(10):3227-38.

Heckmann M, Dudel J: Recordings of glutamate-gated ion channels in outside-out patches from *Drosophila* larval muscle. *Neurosci Lett* 1995, 196(1-2):53-6.

Heckmann M, Bufler J, Franke C, Dudel J: Kinetics of homomeric GluR6 glutamate receptor channels. *Biophys J* 1996, 71(4):1743-50.

Heckmann M, Parzefall F, Dudel J: Activation kinetics of glutamate receptor channels from wild-type *Drosophila* muscle. *Pflugers Arch* 1996, 432(6):1023-9.

Heckmann M, Dudel J: Desensitization and resensitization kinetics of glutamate receptor channels from *Drosophila* larval muscle. *Biophys J* 1997, 72(5):2160-9.

Heuser JE, Reese TS: Evidence for recycling of synaptic vesicle membrane during transmitter release at the frog neuromuscular junction. *J Cell Biol* 1973, 57(2): 315–344.

Heuser JE, Reese TS, Landis DM: Functional changes in frog neuromuscular junctions studied with freeze-fracture. *J Neurocytol* 1974, 3(1): 109–131, 1974.

Hoang B, Chiba A: Single-cell analysis of *Drosophila* larval neuromuscular synapses.

Dev Biol 2001, 1;229(1):55-70.

Hoeffler JP, Meyer TE, Yun Y, Jameson JL, Habener JF: Cyclic AMP-responsive DNA-binding protein: structure based on a cloned placental cDNA. Science, 1988, 9;242(4884):1430-3.

Hofbauer, A: Eine Bibliothek monoklonaler Antikörper gegen das Gehirn von *Drosophila melanogaster*. Habilitationsschrift 1991, Universität Würzburg.

Hou D, Suzuki K, Wolfgang WJ, Clay C, Forte M, Kidokoro Y. Presynaptic impairment of synaptic transmission in *Drosophila* embryos lacking Gs(alpha). J Neurosci 2003, 23(13):5897-905.

Huber D, Petreanu L, Ghitani N, Ranade S, Hromádka T, Mainen Z, Svoboda K. Sparse optical microstimulation in barrel cortex drives learned behaviour in freely moving mice. Nature 2008, 451(7174):61-4.

Hurd D, Saxton W: Kinesin mutations cause motor neuron disease phenotypes by disrupting fast axonal transport in *Drosophila*. Genetics 1996, 144: 1075-1085.

Iseki M, Matsunaga S, Murakami A, Ohno K, Shiga K, Yoshida K, Sugai M, Takahashi T, Hori T, Watanabe M: A blue-light-activated adenylyl cyclase mediates photoavoidance in *Euglena gracilis*.

Nature 2002, 415(6875):1047-51 .

Jan LY, Jan YN: L-glutamate as an excitatory transmitter at the *Drosophila* larval neuromuscular junction. J Physiol 1976, 262(1):215-36.

Jan LY, Jan YN: Properties of the larval neuromuscular junction in *Drosophila melanogaster*. J Physiol 1976, 262(1):189-214.

Jia X, Gorczyca M, Budnik V: Ultrastructure of neuromuscular junctions in *Drosophila*: comparison of wild type and mutants with increased excitability. J Neurobiol 1993, 24(8):1025-44.

Johansen J, Halpern M, Johansen K, Keshishian H: Stereotypic morphology of glutamatergic synapses on identified muscle cells of *Drosophila* larvae. J Neurosci 1989, 9(2): 710-725.

Karunanithi S, Marin L, Wong K, Atwood H: Quantal size and variation determined by vesicle size in normal and mutant *Drosophila* glutamatergic synapses. J Neurosci 2002, 22(23):10267-76.

Katz B, Miledi R: A study of spontaneous miniature potentials in spinal motoneurons. J Physiol 1963, 168:389-422.

Kawasaki F, Felling R, Ordway RW: A temperature-sensitive paralytic mutant defines a primary synaptic calcium channel in *Drosophila*. J Neurosci 2000, 20(13):4885-9.

Kennedy MB, McGuinness T, Greengard P: A calcium/calmodulin-dependent protein kinase from mammalian brain that phosphorylates Synapsin I: partial purification and characterization. J Neurosci 1983, 3(4):818-31.

Keshishian H, Broadie K, Chiba A, Bate M: The *Drosophila* neuromuscular junction: A model system for studying synaptic development and function. Annu Rev Neurosci 1996, 19: 545-75.

Kittel RJ, Wichmann C, Rasse TM, Fouquet W, Schmidt M, Schmid A, Wagh DA, Pawlu C, Kellner RR, Willig KI, Hell SW, Buchner E, Heckmann M, Sigrist SJ: Bruchpilot promotes active zone assembly, Ca²⁺ channel clustering, and vesicle release. Science 2006, 312(5776):1051-4.

Klagges BR, Heimbeck G, Godenschwege TA, Hofbauer A, Pflugfelder GO, Reifegerste R, Reisch D, Schaupp M, Buchner S, Buchner E: Invertebrate synapsins: a single gene codes for several isoforms in *Drosophila*. *J Neurosci* 1996, 15;16(10):3154-65.

Koh TW, Verstreken P, Bellen HJ: Dap160/intersectin acts as a stabilizing scaffold required for synaptic development and vesicle endocytosis. *Neuron* 2004, 43(2):193-205.

Kuramoto N, Wilkins ME, Fairfax BP, Revilla-Sanchez R, Terunuma M, Tamaki K, Iemata M, Warren N, Couve A, Calver A, Horvath Z, Freeman K, Carling D, Huang L, Gonzales C, Cooper E, Smart TG, Pangalos MN, Moss SJ: Phospho-dependent functional modulation of GABA(B) receptors by the metabolic sensor AMP-dependent protein kinase. *Neuron* 2007, 18;53(2):233-47.

Kurdyak P, Atwood H, Stewart, B, and Wu CF: Differential physiology and morphology of motor axons to ventral longitudinal muscles in larval *Drosophila*. *J Comp Neurol* 1994, 350: 463-472.

Kuromi H, Kidokoro Y: Tetanic stimulation recruits vesicles from reserve pool via a cAMP-mediated process in *Drosophila* synapses. *Neuron*. 2000, 27(1):133-43.

Kuromi H, Kidokoro Y: Selective replenishment of two vesicle pools depends on the source of Ca²⁺ at the *Drosophila* synapse. *Neuron* 2002, 18;35(2):333-43.

Kuromi H, Kidokoro Y: Two synaptic vesicle pools, vesicle recruitment and replenishment of pools at the *Drosophila* neuromuscular junction. *J Neurocytol* 2003, 32(5-8):551-65.

Lnenicka G, Keshishian H: Identified motor terminals in *Drosophila* larvae show distinct differences in morphology and physiology. *J Neurobiol* 2000, 43:186 -197.

Lnenicka G, Spencer G, Keshishian H: Effect of reduced impulse activity on the development of identified motor terminals in *Drosophila* larvae. *J Neurobiol* 2003, 5;54(2):337-45.

MacLean J, Zhang Y, Johnson B, Harris-Warrick R: Activity-independent homeostasis in rhythmically active neurons. *Neuron* 2003, (1):109-20.

Macleod G, Hegstrom-Wojtowicz M, Charlton M, Atwood H: Fast calcium signals in *Drosophila* motor neuron terminals. *J Neurophysiol* 2002, 88(5):2659-63.

Marrus S, Portman S, Allen M, Moffat K, DiAntonio A: Differential localization of glutamate receptor subunits at the *Drosophila* neuromuscular junction. *J Neurosci* 2004, 11;24(6):1406-15.

Martin AR: A further study of the statistical composition transmission of the end-plate potential. *J Physio* 1955, 130, 114–122.

Mastrogiacomo A, Parsons S, Zampighi G, Jenden D, Umbach J, Gundersen C: Cysteine string proteins: a potential link between synaptic vesicles and presynaptic Ca²⁺ channels. *Science* 1994, 18;263(5149):981-2.

Millar AG, Bradaes H, Charlton MP, Atwood HL: Inverse relationship between release probability and readily releasable vesicles in depressing and facilitating synapses. *J Neurosci* 2002 Nov 15;22(22) 9661-7.

Nagel G, Ollig D, Fuhrmann M, Kateriya S, Musti AM, Bamberg E, Hegemann P: Channelrhodopsin-1: a light-gated proton channel in green algae. *Science* 2002, Jun 28;296(5577): 2395-8.

Nagel G, Szellas T, Huhn W, Kateriya S, Adeishvili N, Berthold P, Ollig D, Hegemann P, Bamberg E: Channelrhodopsin-2, a directly light-gated cation-selective membrane channel. *Proc Natl Acad Sci* 2003, 100, 13940-13945.

Nieratschker V, Bloch A, Bock N, Bucher D, Eberle K, Asan E, Jauch M, Buchner S, and Buchner B: Genetic knock-out of SRPK3 causes *Bruchpilot* accumulation in larval motor nerves, behavioral defects, and early death in *Drosophila*. In submission.

Nusser Z, Cull-Candy S, Farrant M: Differences in synaptic GABA(A) receptor number underlie variation in GABA mini amplitude. *Neuron* 1997, 19(3):697-709.

Parkes TL, Elia AJ, Dickinson D, Hilliker AJ, Phillips JP, Boulianne GL: Extension of *Drosophila* lifespan by overexpression of human SOD1 in motoneurons. *Nat Genet* 1998, 19, 171-174.

Pawlu C, DiAntonio A, Heckmann M: Postfusional control of quantal current shape. *Neuron* 2004, 27;42(4):607-18.

Petersen S, Fetter R, Noordermeer J, Goodman C, DiAntonio A: Genetic analysis of glutamate receptors in *Drosophila* reveals a retrograde signal regulating presynaptic transmitter release. *Neuron* 1997, 19(6):1237-48.

Polymeropoulos MH, Lavedan C, Leroy E, Ide SE, Dehejia A, Dutra A, Pike B, Root H, Rubenstein J, Boyer R, Stenroos ES, Chandrasekharappa S, Athanassiadou A, Papapetropoulos T, Johnson WG, Lazzarini AM, Duvoisin RC, Di Iorio G, Golbe LI, Nussbaum RL: Mutation in the alpha-synuclein gene identified in families with Parkinson's disease. *Science* 1997, 27;276(5321):2045-7.

Poodry C, Edgar L: Reversible alteration in the neuromuscular junctions of *Drosophila melanogaster* bearing a temperature-sensitive mutation, *shibire*. *J Cell Biol* 1979, 81(3):520-7.

Prinz A, Bucher D, Marder E: Similar network activity from disparate circuit parameters. *Nat Neurosci* 2004, 7(12):1345-52.

Qin G, Schwarz T, Kittel R, Schmid A, Rasse T, Kappei D, Ponimaskin E, Heckmann M, Sigrist S: Four different subunits are essential for expressing the synaptic glutamate receptor at neuromuscular junctions of *Drosophila*. *J Neurosci* 2005, 23;25(12):3209-18.

Reichmuth C, Becker S, Benz M, Debel K, Reisch D, Heimbeck G, Hofbauer A, Klagges B, Pflugfelder G, Buchner E: The Sap47 gene of *Drosophila melanogaster* codes for a novel conserved neuronal protein associated with synaptic terminals. *Brain Res Mol Brain Res* 1995, 32(1):45-54.

Renden RB, Broadie K: Mutation and activation of Galpha s similarly alters pre- and postsynaptic mechanisms modulating neurotransmission. *J Neurophysiol* 2003, 89(5):2620-38.

Richmond J, Broadie K: The synaptic vesicle cycle: exocytosis and endocytosis in *Drosophila* and *C. elegans*. *Curr Opin Neurobiol* 2002, 12(5): 499–507

Rizzoli SO, Betz WJ: Synaptic vesicle pools. *Nat Rev Neurosci* 2005, 6(1): 57-69.

Rohrbough J, Broadie K: Lipid regulation of the synaptic vesicle cycle. *Nat Rev Neuro* 2005, 6:139-150.

Rosahl TW, Spillane D, Missler M, Herz J, Selig DK, Wolff JR, Hammer RE, Malenka RC, Südhof TC: Essential functions of synapsins I and II in synaptic vesicle regulation. *Nature* 1995, 8;375(6531): 488-93.

Rosenmund C, Stevens CF: Definition of the readily releasable pool of vesicles at hippocampal synapses. *Neuron* 1996, 16(6): 1197–201.

Ryan TA, Li L, Chin LS, Greengard P, Smith SJ: Synaptic vesicle recycling in synapsin I knock-out mice. *J Cell Biol* 1996, 134(5):1219-27.

Schroll C, Riemensperger T, Bucher D, Ehmer J, Voller T, Erbguth K, Gerber B, Hendel T, Nagel G, Buchner E, Fiala A: Light-induced activation of distinct modulatory neurons triggers appetitive or aversive learning in *Drosophila* larvae. *Curr Biol* 2006, 16(17):1741-7.

Schuster C, Ultsch A, Schloss P, Cox J, Schmitt B, Betz H: Molecular cloning of an invertebrate glutamate receptor subunit expressed in *Drosophila* muscle. *Science* 1991, 254(5028):112-4.

Schwartz JH, Greenberg SM: Molecular mechanism for memory: second messenger-induced modifications of protein kinases in nerve cells. *Ann Rev Neurosci* 1987, 10:459–476.

Shayan A, Atwood H: Synaptic ultrastructure in nerve terminals of *Drosophila* larvae overexpressing the learning gene *dunce*. *J Neurobiol* 2000, 43: 89-97.

Sigrist S, Thiel P, Reiff D, Lachance P, Lasko P, Schuster C: Postsynaptic translation affects the efficacy and morphology of neuromuscular junctions. *Nature* 2000, 405:1062-1065.

Sigrist S, Reiff D, Thiel P, Steinert J, Schuster C: Experience-dependent strengthening of *Drosophila* neuromuscular junctions. *J Neurosci* 2003, 23(16):6546-6556.

Simons K, Ikonen E: Functional rafts in cell membranes. *Nature* 1997, 387(6633):569-72.

Stewart B, Atwood H, Renger J, Wang, J, Wu C: Improved stability of *Drosophila* larval neuromuscular preparations in haemolymph-like physiological solutions. *J Comp Physiol* 1994, 175: 179-191.

Stewart B, Schuster CM, Goodman CS, Atwood HL: Homeostasis of synaptic transmission in *Drosophila* with genetically altered nerve terminal morphology. *J Neurosci* 1996, 16 (12), 3877-3886.

Südhof T: The synaptic vesicle cycle revisited. *Neuron* 2000, 28(2): 317–20.

Südhof T: The synaptic vesicle cycle. *Annu Rev Neurosci* 2004, 27:509-47.

Suzuki K, Okamoto T, Kidokoro Y: Biphasic modulation of synaptic transmission by hypertonicity at the embryonic *Drosophila* neuromuscular junction. *J Physiol* 2002, 545(Pt 1):119-31.

Suzuki K, Grinnell AD, Kidokoro Y: Hypertonicity-induced transmitter release at *Drosophila* neuromuscular junctions is partly mediated by integrins and cAMP/protein kinase A. *J Physiol*. 2002, 538(Pt 1):103-19.

Takamori S, Holt M, Stenius K, Lemke EA, Grønborg M, Riedel D, Urlaub H, Schenck S, Brügger B, Ringler P, Müller SA, Rammner B, Gräter F, Hub JS, De Groot BL, Mieskes G, Moriyama Y, Klingauf J, Grubmüller H, Heuser J, Wieland F, Jahn R: Molecular anatomy of a trafficking organelle.

Cell. 2006, 127(4):831-46.

Trussell L, Fischbach G: Glutamate receptor desensitization and its role in synaptic transmission. *Neuron* 1989, 3(2):209-18.

Ueda A, Wu CF: Distinct frequency-dependent regulation of nerve terminal excitability and synaptic transmission by IA and IK potassium channels revealed by *Drosophila* Shaker and Shab mutations.

J Neurosci 2006, 7;26(23):6238-48.

Umbach J, Zinsmaier K, Eberle K, Buchner E, Benzer S, Gunderson CB: Presynaptic dysfunction in *Drosophila* csp mutants. Neuron 1994, 13 (4), 899-907.

Verstreken P, Kjaerulff O, Lloyd T, Atkinson R, Zhou Y, Meinertzhagen I, Bellen H: Endophilin mutations block clathrin-mediated endocytosis but not neurotransmitter release. Cell 2002, 5;109(1): 101-12.

Verstreken P, Bellen H: Neuroscience. The meaning of a mini. Science 2001, 20;293(5529):443-4.

Wagh D, Rasse T, Asan E, Hofbauer A, Schwenkert I, Dürbeck H, Buchner S, Dabauvalle M, Schmidt M, Qin G, Wichmann C, Kittel R, Sigrist S, Buchner E: Bruchpilot, a protein with homology to ELKS/CAST, is required for structural integrity and function of synaptic active zones in *Drosophila*. Neuron 2006, 49(6):833-44.

Wang H, Peca J, Matsuzaki M, Matsuzaki K, Noguchi J, Qiu L, Wang D, Zhang F, Boyden E, Deisseroth K, Kasai H, Hall WC, Feng G, Augustine GJ: High-speed mapping of synaptic connectivity using photostimulation in Channelrhodopsin-2 transgenic mice. Proc Natl Acad Sci 2007, 104(19): 8143-8.

Wolfgang WJ, Roberts IJ, Quan F, O'Kane C, Forte M: Activation of protein kinase A-independent pathways by Gs alpha in *Drosophila*. Proc Natl Acad Sci 1996, 10;93(25):14542-7.

Wong K, Karunanithi S, Atwood HL: Quantal unit populations at the *Drosophila* larval neuromuscular junction. J Neurophysiol 1999, 82(3):1497-511.

Yasuyama K, Meinertzhagen IA, Schürmann FW: Synaptic organization of the mushroom body calyx in *Drosophila melanogaster*. J Comp Neurol 2002, 445(3):211-26.

Yooseph S, Sutton G, Rusch DB, Halpern AL, Williamson SJ, Remington K, Eisen JA, Heidelberg KB, Manning G, Li W, Jaroszewski L, Cieplak P, Miller CS, Li H, Mashiyama ST, Joachimiak MP, van Belle C, Chandonia JM, Soergel DA, Zhai Y, Natarajan K, Lee S, Raphael BJ, Bafna V, Friedman R, Brenner SE, Godzik A, Eisenberg D, Dixon JE, Taylor SS, Strausberg RL, Frazier M, Venter JC: The Sorcerer II Global Ocean Sampling expedition: expanding the universe of protein families. PLoS Biol. 2007, (3):e16.

Zhang D, Kuromi H, Kidokoro Y: Activation of metabotropic glutamate receptors enhances synaptic transmission at the *Drosophila* neuromuscular junction. Neuropharmacology 1999, 38(5):645-57.

Zhong Y, Wu CF: Altered synaptic plasticity in *Drosophila* memory mutants with a defective cyclic AMP cascade. Science 1991, 11;251(4990):198-201.

Zinsmaier K, Hofbauer A, Heimbeck G, Pflugfelder G, Buchner S, Buchner E: A cysteine-string protein is expressed in retina and brain of *Drosophila*. J Neurogenet 1990, 7(1):15-29.

Zinsmaier K, Eberle K, Buchner E, Walter N, Benzer S: Paralysis and early death in cysteine string protein mutants of *Drosophila*. Science 1994, 18;263(5149):977-80.

Appendix A: Fortran code for analysis of eEJP amplitude and decay

```
parameter( leninp=20000, lendkt=5000 )
c
character filinp*64, filout*64, hdrstr*64
character timein(leninp)*13, timprs*13
real*4 voltin(leninp),
1 timdkt(lendkt), voldkt(lendkt),
2 volsig(lendkt), volfit(lendkt),
3 smucof(32)
c
common /xxxxxx/ lunout
c
data volsig/lendkt*0.00/
c
5000 format( a )
c5010 format( a13, f12.4 ) ! use if timein is character variable
5010 format( a13, 1x, f7.4 ) ! use if delimiter not replaced
with spaces
c5020 format( 3(i2,1x), i4, f12.4 ) ! use if timein is integer variable
c5020 format( 3(i2,1x), i4, 1x, f7.4 ) ! use if delimiter not replaced
with spaces
c
6000 format( ' #', i2.2, '!', 2x, a64 )
6110 format( i5, 2x, a13, f8.4, a8 )
6120 format( i5, 2x, 2(i2.2, '!'), i2.2, '!', i4.4, f8.4 )
c6120 format( i5, 2x, 3i3.2, i5.4, f8.4 )
6122 format( i5, 2x, 3(i2.2,2x), i4.4, 4x, f7.4 )
6130 format( i5, a15, f8.4, f10.6, a8 )
6140 format( i5, a15, 3f9.4, a8 )
6150 format( a10, f10.5, a5, f10.5 )
6190 format( '====', i4, a15, 4f10.5, 1x, 2f7.3, a8 )
6990 format( ' - ', a8, i5, a7 )
6992 format( ' - ', a8, f7.1, a4 )
6993 format( ' - ', a8, f7.3, a4 )
6994 format( ' - ', a8, f11.5, a4 )
6998 format( ' - ', a8, a15 )
c
write( *, '( "=== Start Data Analysis" )' )
c
c Open analysis messages and results file
c
lunout = 7
```

```

filout = 'a.f.out'
open( unit = lunout, file = filout, status = 'unknown' )
write( lunout, '( "== Open Output Data File: ", a64 )' ) filout
c
c Define data and analysis parameters (see ! comment statements)
c
write( lunout, '( "== Set Data and Analysis Parameters" )' )
resrat = 1    ! response rate (hertz, 1/sec)
samrat = 2000 ! sampling rate (hertz, 1/sec)
write( lunout, 6992 ) 'resrat =', resrat, 'hz'
write( lunout, 6992 ) 'samrat =', samrat, 'hz'
c
numhdr = 8    ! number of header records in data file
write( lunout, 6990 ) 'numhdr =', numhdr, 'rec'
c
timlbc = 5    ! look-back time in peak-rise search (ms)
nptlbc = samrat * timlbc / 1000
write( lunout, 6992 ) 'timlbc =', timlbc, 'ms'
write( lunout, 6990 ) 'nptlbc =', nptlbc, 'pts'
c
timbas = 10   ! amount of time of baseline average (ms)
nptbas = samrat * timbas / 1000
write( lunout, 6992 ) 'timbas =', timbas, 'ms'
write( lunout, 6990 ) 'nptbas =', nptbas, 'pts'
c
timxtr = 5    ! amount of extra time not skipped (ms)
nptxtr = samrat * timxtr / 1000
write( lunout, 6992 ) 'timxtr =', timxtr, 'ms'
write( lunout, 6990 ) 'nptxtr =', nptxtr, 'pts'
c
volrso = 0.0025 ! estimated voltage resolution (volts)
volinc = 3 * volrso
write( lunout, 6994 ) 'volrso =', volrso, 'v '
write( lunout, 6994 ) 'volinc =', volinc, 'v '
c
dkpbeg = 0.80 ! decay time const, begin (frac peak)
c  dkpbeg = 0.90 ! decay time const, begin (frac peak)
dkpend = 0.40 ! decay time const, end (frac peak)
c  dkpend = 0.30 ! decay time const, end (frac peak)
write( lunout, 6993 ) 'dkpbeg =', dkpbeg
write( lunout, 6993 ) 'dkpend =', dkpend
c
c Generate second order smoothing coefficients
c
numcof = 7

```

```

c  numcof = 35
   call gencof( numcof, numccc, smucof )
   write( lunout, 6990 ) 'numcof =', numcof
   write( lunout, 6990 ) 'numccc =', numccc
c
c  Open time-voltage recordings data file
c
c  NOTE: must use dos2unix on file to convert end of line
c  ----> dos2unix File_From_Dan File_For_Input_Interim
c
c  NOTE: may use sed on file to convert delimiter to spaces
c  ----> sed 's/delimiter/ /g' File_For_Input_Interim > File_For_Input
c
   luninp = 5
c  filinp = 'aau.in' ! dos2unix only applied to short file from Dan
c  filinp = 'aas.in' ! dos2unix and sed applied to short file from Dan
c  filinp = 'aauss.in' ! dos2unix and sed applied to selected (to
c          ! every fifth point) to short file from Dan
c  filinp = 'auss.in' ! dos2unix and sed applied to selected to file
from Dan
c  filinp = '052806_WT.in'
c  filinp = '052806_LOE.in'
   filinp = '042006_B1_M6_A4.3_raw.ASC'
c  filinp = '042006_B1_M6_A43.in'
c  filinp = '042006_B1_M6_A44.in'
c  filinp = '042606_A_M6_A5_LONG2.in'
c  filinp = '042606_B_M6_A53.in'
   filinp = 'playu2.in'
   open( unit = luninp, file = filinp, status = 'old',
1  err = 9900, iostat = ierflg, form = 'formatted' )
   write( lunout, '( " = Open Input Data File: ", a64 ) ' ) filinp
c -- Locate leading edge of peak
c
   write( lunout, '( " - at locate leading edge of peak" ) ' )
   ir = 0
2000 ir = ir + 1
   read( luninp, 5010, err = 9910, end = 9920, iostat = ierflg )
1  timein(ir), voltin(ir)
   if( ir .le. nptlbc ) go to 2000
   if( ( voltin(ir) - voltin(ir-nptlbc) ) .lt. volinc ) go to 2000
   write( lunout, 6110 ) ir, timein(ir), voltin(ir), 'locedg'
   timprs = timein(ir)
   write( lunout, 6998 ) 'timprs =', timprs
c
c -- Save baseline data before peak

```



```

c
write( lunout, ' " - at save baseline data before peak" ' )
nptcop = nptblk + nptbas
write( lunout, 6990 ) 'nptcop =', nptcop, 'pts'
do ic = 1, nptcop
  timein(ic) = timein(ir-nptcop+ic)
  voltin(ic) = voltin(ir-nptcop+ic)
  write( lunout, 6110 ) ic, timein(ic), voltin(ic), 'savbas'
enddo
c -- Estimate baseline voltage, using averaging
write( lunout, ' " - at estimate baseline voltage" ' )
call getavg( voltin(1), nptbas, basest, basunc )
write( lunout, 6994 ) 'basest =', basest, 'v '
write( lunout, 6994 ) 'basunc =', basunc, 'v '
c -- Estimate peak voltage, using smoothing
c
write( lunout, ' " - at estimate peak voltage" ' )
volmax = voltin(nptcop)
pekest = volmax - basest
do ic = nptcop, nptset
  volsmu = smucof(0) * voltin(ic)
  do is = 1, numccc
    volsmu = volsmu + smucof(is) *
1    ( voltin(ic-is) + voltin(ic+is) )
  enddo
  write( lunout, 6130 ) ic, timein(ic), voltin(ic), volsmu,
1 'pekest'
  if( volsmu .gt. volmax ) then
    volmax = volsmu
    pekest = volmax - basest
  else
    if( ( volsmu - basest ) / pekest .lt. dkpbeg ) go to 2200
  endif
enddo
2200 continue
write( lunout, 6994 ) 'volmax =', volmax, 'v '
write( lunout, 6994 ) 'pekest =', pekest, 'v '
c
c -- Estimate decay time constant, using fit to log of decay voltage
c
write( lunout, ' " - at estimate decay time constant" ' )
idkbeg = ic
idkend = nptset
nptdkt = idkend - idkbeg + 1
timref = redtim( timein(idkbeg) )

```

```

volref = voltin(idkbeg) - basest
do id = idkbeg, idkend
  timdkt(id) = redtim( timein(id) ) - timref
  voldkt(id) = log( ( voltin(id) - basest ) / volref )
  write( lunout, 6140 ) id, timein(id), timdkt(id), voltin(id),
1  voldkt(id), 'dktcon'
enddo
c
mwt = 0
call fit( timdkt(idkbeg), voldkt(idkbeg), nptdkt,
1  volsig(1), mwt, a, b, siga, sigb, chi2, q )
write( lunout, 6150 ) ' - const =', a, ' +/-', siga
write( lunout, 6150 ) ' - slope =', b, ' +/-', sigb
dktcon = -1000.0 / b
dktunc = abs( dktcon * sigb / b )
write( lunout, 6993 ) 'dktcon =', dktcon, 'ms'
write( lunout, 6993 ) 'dktunc =', dktunc, 'ms'
c
c -- Evaluate adequacy of decay fit
c
write( lunout, ' " - at evaluate adequacy of decay fit" ' )
c
do id = idkbeg, idkend
  volffit(id) = a + b * timdkt(id)
  write( lunout, 6140 ) id, timein(id), voldkt(id), volffit(id),
1  voldkt(id) - volffit(id), 'dktfit'
enddo
c
call anlres( nptdkt, timdkt(idkbeg), voldkt(idkbeg),
1  volffit(idkbeg) )
c
-- Skip data to next peak
c
nptskp = samrat / resrat - nptset - nptxtr
write( lunout, 6990 ) 'nptskp =', nptskp, 'pts'
do ic = 1, nptskp
  if( ( ic .lt. 5 ) .or. ( ic .gt. nptskp-4 ) ) then
    read( luninp, 5010, err = 9910, end = 9920, iostat = ierflg )
1  timein(ic), voltin(ic)
    write( lunout, 6110 ) ic, timein(ic), voltin(ic), 'skpdat'
  else
    read( luninp, 5010, err = 9910, end = 9920, iostat = ierflg )
c
end

```

Appendix B: *Curriculum Vitae*

Daniel B. Bucher

Hochbergstrasse 6
97450 Arnstein
Germany

Lab: (0931) 888-4480
Cell: (0176) 2038-4090
danindeutschland@gmail.com



Education

Diploma and Ph.D. (2004 – present)
Electrophysiologic analysis of synaptic function *Drosophila* neuromuscular junction
Julius-Maximilians-Universität, Würzburg, Germany

Graduate student (2001 – 2003) synaptic physiology
Vollum Institute, Oregon Health & Science University, Portland, OR, USA

Pregraduate (1997 – 2001) neuroscience and neurophysiology
University of Iowa Hospitals & Clinics, Iowa City, IA, USA

Bachelor of Science (1993 – 1997) molecular biology and genetics
University of Iowa, Iowa City, IA, USA

Research Experience

December 2004 - present
Graduate Student
Lehrstuhl für Genetik und Neurobiologie
Theodor-Boveri-Institut für Biowissenschaften, Universität Würzburg
Erich Buchner and Martin Heisenberg, Advisors

- Electrophysiological recordings at the *Drosophila* neuromuscular junction
 - Computational simulation of neuromuscular junction active zones
 - Open source electrophysiology acquisition and analysis platform

June 2001 - July 2003
Graduate Student
Vollum Institute, Oregon Health & Science University
Mike Kavanaugh, Gary Thomas, Larry Trussell, Gary Westbrook, Advisors

- Electrophysiological recordings from slices
 - Patch recordings from hippocampal, cerebellar, and brainstem slices
 - Patch recordings from cultured cells and neurons
 - Transporter (EAAT) structure & function analysis in oocytes

August 1995 - May 2001

Research Assistant

Department of Internal Medicine, University of Iowa Hospitals and Clinics

Michael Welsh and Peter Snyder, Advisors

- Analysis of ion channel structure & function
 - Molecular biology (site directed mutagenesis)
 - *Xenopus laevis* laparotomy and oöcyte culture
 - Heterologous expression of channel constructs in oöcytes
 - TEVC and patch clamp (inside out, outside out, macro) recordings

September 1993 - August 1995

Student Assistant

University of Iowa Department of Pharmacology

Gerald Gebhart and Rich Traub, Advisors

- Mechanisms of peripheral and visceral hyperalgesia
 - *Rattus norvegicus* spinal laminectomy
 - Cryosections of rat dorsal root ganglia
 - Immunohistochemistry to quantify c-fos expression
 - Solution chemistry and general lab maintenance

Teaching Experience

Inlingua certified English instructor

Genetics Practical (2005, 2006, 2007, 2008)

Neurobiology Practical (2005, 2006, 2007, 2008)

Genetic and Microbiology Practical (2008)

Genetic Methods Practical (2007)

Cellular Neurophysiology, Vollum Institute (2002 & 2003)

Medical Neuroanatomy, University of Iowa (2000)

Fundamentals of Genetics, University of Iowa (1996, 1997, 1998)

Publications

Bucher D, Schwärtzel M, Fiala A, Buchner E. A photo-activated adenylyl cyclase cloned from *Eulgena gracilis* can be used to modulate synaptic transmission at the *Drosophila* neuromuscular junction. In preparation.

Nieratschker V, Bloch A, Bock N, Bucher D, Eberle K, Asan E, Jauch M, Buchner S, Buchner E. Genetic knock-out of SRPK3 causes Bruchpilot accumulation in larval motor nerves, behavioral defects, and early death in *Drosophila*. In preparation

Saumweber T, Michels B, Bucher D, Funk N, Reisch D, Krohne G, Wegener S, Buchner E, Gerber B. Associative learning is impaired upon lack of the presynaptic protein SAP47. In submission.

Schroll C, Riemensperger T, Bucher D, Ehmer J, Voller T, Erbguth K, Gerber B, Hendel T, Nagel G, Buchner E, Fiala A. Light-induced activation of distinct modulatory neurons triggers appetitive or aversive learning in *Drosophila* larvae. *Curr Biol*, 2006. 16(17): 1741-7.

Snyder, P, Olson D, McDonald F, Bucher D. Multiple WW domains, but not the C2 domain, are required for inhibition of the epithelial Na⁺ channel by human Nedd4. *J Biol Chem*, 2001. 276(30): 28321-6.

Snyder, P, Bucher D, Olson D. Gating induces a conformational change in the outer vestibule of ENaC. *J Gen Physiol*, 2000. 116(6): 781-90.

Snyder, P, Olson D, Bucher D. A pore segment in DEG/ENaC Na(+) channels. *J Biol Chem*, 1999. 274(40): 28484-90.

Posters and Talks

Cold Spring Harbor Neurobiology of *Drosophila* 2007

11th European *Drosophila* Neurobiology conference

7th meeting of the German Society for Neuroscience

30th, 31st, 32nd meetings of the Society for Neuroscience

44th and 45th meeting of the Biophysical Society

Molecular Mechanisms of Disease 1997

Awards and Fellowships

Graduiertenkolleg GK-1156 Fellowship (September 2005 - July 2007)

Ruth L. Kirschstein National Research Service Award (August 2001 - August 2003)

University of Iowa Staff Tuition Scholarship (spring 1999, fall 2000)

Computer skills:

Microsoft (Powerpoint, Excel, etc.)

Macintosh (OS-X, etc)

Linux (Knoppix, Ubuntu, Susie)

Image processing software (Image J, Metamorph, Corel Draw, Photoshop)

Extensive knowledge of electrophysiology acquisition and analysis software platforms

Neuron simulation programs (Neuron, Genesis)

LaTeX

Languages:

English (native)

German (fluent)

Spanish (basic)

Mandarin Chinese (very basic)

Interests:

Alpinism (snowboarding/skiing, rock/mountain climbing), chess, computational modeling of neuronal activity, guitar (outlaw country), open source electrophysiology acquisition and analysis platform development, teaching English as a second language, reading, and travel.

Appendix C: Publications

Bucher D, Schwärzkel M, Fiala A, Buchner E. A photo-activated adenylyl cyclase cloned from *Eulgena gracilis* can be used to modulate synaptic transmission at the *Drosophila* neuromuscular junction. In preparation.

Nieratschker V, Bloch A, Bock N, Bucher D, Eberle K, Asan E, Jauch M, Buchner S, Buchner E. Genetic knock-out of SRPK3 causes Bruchpilot accumulation in larval motor nerves, behavioral defects, and early death in *Drosophila*. In preparation

Saumweber T, Michels B, Bucher D, Funk N, Reisch D, Krohne G, Wegener S, Buchner E, Gerber B. Associative learning is impaired upon lack of the presynaptic protein SAP47. In submission.

Schroll C, Riemensperger T, Bucher D, Ehmer J, Voller T, Erbguth K, Gerber B, Hendel T, Nagel G, Buchner E, Fiala A. Light-induced activation of distinct modulatory neurons triggers appetitive or aversive learning in *Drosophila* larvae. *Curr Biol*, 2006. 16(17): 1741-7.

Snyder, P, Olson D, McDonald F, Bucher D. Multiple WW domains, but not the C2 domain, are required for inhibition of the epithelial Na⁺ channel by human Nedd4. *J Biol Chem*, 2001. 276(30): 28321-6.

Snyder, P, Bucher D, Olson D. Gating induces a conformational change in the outer vestibule of ENaC. *J Gen Physiol*, 2000. 116(6): 781-90.

Snyder, P, Olson D, Bucher D. A pore segment in DEG/ENaC Na⁽⁺⁾ channels. *J Biol Chem*, 1999. 274(40): 28484-90.

Erklärung gemäß § 4 Absatz 3 der Promotionsordnung der Fakultät für Biologie der Bayerischen Julius-Maximilians-Universität Würzburg vom 15. März 1999.

Hiermit erkläre ich, die vorgelegte Dissertation selbständig angefertigt zu haben und keine anderen als die von mir angegebenen Quellen und Hilfsmittel benutzt zu haben. Alle aus der Literatur entnommenen Stellen sind als solche kenntlich gemacht. Des Weiteren erkläre ich, dass die vorliegende Arbeit weder in gleicher noch in ähnlicher Form bereits in einem anderen Prüfungsverfahren vorgelegen hat. Zuvor habe ich keine akademischen Grade erworben oder zu erwerben versucht.

Würzburg, den 19.03.2008

Dange

Dr. Erich Buchner for allowing me to finish my thesis work in his lab...

Dr. Doris Kretzschmar for her role in setting all this up...

Dr. Heisenberg for setting up such a unique and pleasant work environment...

Dr.'s Andre Fiala and Henrike Scholz for helpful discussion...

Dr. Georg Nagel for reviewing this thesis and interesting lunch time conversations...

Konrad Oechsner for excellent technical assistance, integrated circuit assembly basics, and a little more perspective on all things electronic...

Andreas Eckart for excellent technical support

Dr's Arnim Jenett and Johannes Schindelin for introducing me to life beyond the GUI, information theory fundamentals, and general good times...

Dr. Dhananjay Wagh for helping me find my way around the department when I first arrived and for introducing me to Sir Edmund Blackadder...

Vanessa Nieratschker for her invaluable contribution to my appreciation of the German language...

The folks at Open Office for providing an open source office application suit...

The people who I am currently forgetting to include but whose assistance was invaluable...